Activation of the ISR mediates the behavioral and neurophysiological abnormalities in Down syndrome

Ping Jun Zhu[1,2], Sanjeev Khatiwada[1,2,3], Ya Cui[4,5], Lucas C. Reineke[1,2], Sean W. Dooling[2,6], Jean J. Kim[4,7], Wei Li[4,5], Peter Walter[8,9*], Mauro Costa-Mattioli[1,2*]

[1]Department of Neuroscience,

[2]Memory and Brain Research Center,

[3]Verna and Marrs McLean Department of Biochemistry and Molecular Biology,

[4]Division of Biostatistics, Dan L Duncan Cancer Center and Department of Molecular and Cellular Biology,

Baylor College of Medicine, Houston, Texas.

[5]Department of Biological Chemistry, University of California, Irvine, Irvine, CA.

[6]Department of Molecular and Human Genetics,

[7]Stem Cells and Regenerative Medicine Center,

Baylor College of Medicine, Houston, Texas, USA.

[8]Howard Hughes Medical Institute,

[9]Department of Biochemistry and Biophysics,

University of California at San Francisco, San Francisco, California, USA.

*Correspondence to: Mauro Costa-Mattioli (costamat@bcm.edu), Peter Walter (peter@walterlab.ucsf.edu)

Key words: learning and memory, protein homeostasis networks, synaptic plasticity.

Abstract

Down syndrome (DS) is the most common genetic cause of intellectual disability. Protein homeostasis is essential for normal brain function, but little is known about its role in DS pathophysiology. Here, we find that the integrated stress response (ISR)—a signaling network that maintains proteostasis—is activated in the brains of DS mice and individuals with DS, reprogramming translation. Genetic and pharmacological suppression of the ISR, by inhibiting the ISR-inducing kinase PKR or boosting the function of the eIF2•eIF2B complex, reverses the changes in translation and inhibitory synaptic transmission, and rescues the synaptic plasticity and long-term memory deficits in DS mice. Our findings unveil a crucial role for the ISR in DS and suggest tuning of the ISR as a promising therapeutic intervention.

Intellectual disability (ID) affects approximately 2-3% of the human population (*1*). Recent array-based comparative genomic studies have identified a large number of chromosomal aberrations in individuals with ID (*2, 3*). Down syndrome (DS), a chromosomal condition and the most common genetic cause of ID, is a substantial biomedical and socio-economic problem (*4*), for which there is no effective treatment. Thus, the identification of novel neuronal targets for the development of pharmacotherapies to treat the memory decline associated with DS is an important goal.

DS results from the presence of an extra copy of human chromosome 21 (CH21, also known as *Homo sapiens* autosome 21, HSA21) leading to genetic imbalance. Gene expression studies showed that the overall genome-wide differences between individuals with DS and euploid controls map not only to CH21, but also to other chromosomes (*5, 6*). These observations indicate that the DS phenotype could be due to wide-spread pleiotropic dysregulation of gene expression (*7*). Consequently, most of the focus in the field has been to understand how alterations in the expression of specific genes in CH21 trisomic cells lead to neurodevelopmental dysfunction (*8*). However, the degree to which defects in the protein homeostasis (proteostasis) might contribute to the cognitive deficits associated with DS has remained largely unexplored.

The brain must adapt to stress conditions that occur as a result of numerous environmental and/or genetic factors. The integrated stress response (ISR) is one of the circuits that responds to stress conditions aiming to restore proteostasis by regulating protein synthesis rates (*9*). The central regulatory hub of the ISR is the eukaryotic translation initiation factor eIF2, the target of four kinases that are activated in response to different stresses. In its GTP-bound state, eIF2 assembles into the eIF2•GTP•Met-

$tRNA_i$ ternary complex (TC) that delivers the $_i$Met-tRNA to the small ribosomal subunit (40S), priming translation initiation (*10*). After recognition of an AUG codon, GTP is hydrolyzed and the resulting eIF2•GDP leaves the ribosome. It is recycled to the GTP-bound state by eIF2B, which serves as eIF2's dedicated guanine nucleotide exchange factor (GEF).

Translational control by the ISR is exerted by phosphorylation of the α-subunit of eIF2 on a single serine (Serine51), which converts eIF2 from a substrate into an inhibitor of eIF2B: eIF2-P binds more tightly to eIF2B and blocks its GEF activity. Thus, reducing TC formation inhibits general translation (*10*).

Activation of the ISR in the brains of Ts65Dn mice and individuals with DS. To determine whether protein homeostasis is altered in DS, we first measured protein synthesis rates in a mouse model of DS (Ts65Dn) that recapitulates the learning and memory deficits of the human syndrome (*11, 12*). Ts65Dn mice are trisomic for approximately two-thirds of the genes orthologous to human CH21. We measured translation in the hippocampus of wild type (WT) euploid mice and Ts65Dn mice by comparing polysome sedimentation in sucrose gradients and then assessing ribosome/mRNA engagement. In this assay, the position of a given mRNA in the sucrose gradient is determined by the number of associated ribosomes. mRNAs that are poorly or not translated accumulate near the top, whereas translationally active mRNAs are associated with multiple ribosomes (polysomes) and sediment to the bottom of the gradient (**Fig. 1A**). Compared to WT mice, mRNA translation in the hippocampus of Ts65Dn mice is reduced, as indicated by a 32 ± 8 % decrease in polysomes/sub-

polysome ratio (**Fig. 1B-C**). An independent translation assay measuring puromycin incorporation into nascent polypeptide chains confirms that protein synthesis was markedly reduced (39 ± 7%) in the hippocampus of Ts65Dn mice (**Fig. 1D-E**).

To determine the mechanism(s) underlying the reduced translation in Ts65Dn mice, we first asked whether the ISR, a major pathway that regulates translation initiation (*9*), is activated in the brain of Ts65Dn mice. Consistent with the decrease in overall protein synthesis (**Fig. 1B-E**), we found that the ISR is activated in the hippocampus of Ts65Dn mice, as determined by the increased eIF2-P levels (**Fig. 1F**). To assess whether these changes are also observed in the human condition, we measured eIF2-P levels in post-mortem brain samples from human individuals with DS. Indeed, we found increased eIF2-P levels in brain samples from human individuals with DS compared to non-DS euploid controls (**Fig. 1G** and **Table S1**). Moreover, when we reprogrammed a fibroblast line derived from an individual with DS (CCL-54™ from ATCC) into induced pluripotent stem cells (iPSCs), we identified one clone that is CH21-trisomic (DS) and another clone from the same individual that is fortuitously euploid (control) (**Fig. S1**). Microsatellite and karyotyping analysis demonstrated that the euploid iPSC clone was isogenic (**Fig. S1** and see Materials and Methods), likely because the individual had mosaic DS, or the extra chromosome was lost during cell line propagation. While extensive serial passaging (> 70 passages) of trisomic-21 iPSCs may have caused cells to become euploid (*13*), we find this unlikely since karyotyping was performed on passage 9 (**Fig. S1**). Regardless of its etiology, the euploid isogenic line offers the rare opportunity of an ideal isogenic control for our studies. Importantly, we found that the ISR is activated in the CH21-trisomic iPSCs, but not in the isogenic euploid iPSCs, as indicated by increased eIF2-P levels (**Fig. 1H**).

Similarly, we found that the ISR is also activated in a previously reported CH21-trisomic iPSC line (DS1) (*14*) compared to its respective isogenic control (DS2U) (**Fig. S2**). As expected from the increased eIF2-P levels (**Fig. 1H**), protein synthesis is reduced in the DS iPSC line compared to the euploid isogenic control (**Fig. 1I-J**). Taken together, activation of the ISR in the brains of Ts65Dn mice and human individuals with DS emerges as a common molecular signature of the condition.

We next examined whether changes in the activity of mTORC1 (the mammalian target of rapamycin complex 1), which regulates translation initiation rates by a pathway that is distinct and independent from the ISR (*15*), could also contribute to the decreased translation in the brain of Ts65Dn mice. mTORC1 regulates translation rates by phosphorylating its downstream targets, the ribosomal protein S6 and the translational repressor cap-binding protein eIF4E binding protein 1 (4E-BP1) (**Fig. S3A**). We found that in the hippocampus of WT and Ts65Dn mice, the phosphorylation states of these mTORC1 targets, as well as that of the cap-binding protein eIF4E [a key translation initiation factor (*10*)], are indistinguishable (**Fig. S3B-G**), underscoring that the translation repression in DS mice is likely exerted by ISR activation.

The PKR-branch of the ISR is activated in the brain of Ts65Dn mice. In the brain, eIF2 has been shown to be phosphorylated by three kinases: PKR (double-stranded RNA-dependent kinase), GCN2 (general control non-derepressible 2), and PERK (PKR-like endoplasmic reticulum kinase) (**Fig. S4A**). The fourth ISR kinase HRI (heme-regulated inhibitor) has been extensively studied in erythroid cells, and little is known about its function in the brain. To examine which eIF2 kinase is responsible for the

increase in eIF2-P in Ts65Dn mice, we measured their degree of auto-phosphorylation, indicative of their activation (*16*). Phosphorylation of PKR, but not of GCN2 or PERK, is increased in the hippocampus of Ts65Dn mice (**Fig. S4B-G**). The unfolded protein response (UPR), which in addition to PERK includes, the ER stress sensors IRE1 (inositol requiring enzyme 1) and ATF6 (activating transcription factor 6), has was recently implicated in DS (*17, 18*). We do not observe changes in the activity of IRE1 and ATF6 in the brains of Ts65Dn mice (**Fig. S5**). Taken together with the fact that PERK was not activated in Ts65Dn mice, our data indicate that the ISR (but not the UPR) is selectively activated in the hippocampus of Ts65Dn mice.

Importantly, in the hippocampus (**Fig. 2A-B**) and cortex (**Fig. S6**) of Ts65Dn mice lacking PKR (Ts65Dn-*Pkr*$^{-/-}$ mice), eIF2-P levels are reduced compared to Ts65Dn mice. Moreover, genetic inhibition of PKR in Ts65Dn mice (Ts65Dn-*Pkr*$^{-/-}$ mice) is sufficient to de-repress translation in the brains of Ts65Dn mice (**Fig. 2C-D**). Hence, the results suggest that the increased levels of eIF2-P and resulting in sustained translational repression in the brain of Ts65Dn mice is mediated, at least in part, by activation of the PKR branch of the ISR.

Inhibition of the PKR-branch of the ISR rescues the deficits in long-term memory and synaptic plasticity in Ts65Dn mice. Individuals with DS exhibit learning and memory deficits, specifically in hippocampus-dependent tasks (*4, 19*). To investigate whether activation of the ISR contributes to long-term memory deficits in DS mice, we first examined hippocampus-dependent contextual fear memory. In this task, we paired a context (conditioned stimulus; CS) with a foot shock (the unconditioned stimulus; US).

Twenty-four hours after training, we exposed mice to the CS and measured their fear responses ("freezing behavior") as an index of the strength of their long-term memory (**Fig. 2E**). While freezing prior to training is similar in Ts65Dn mice and naïve WT mice, Ts65Dn mice exhibit a significant reduction in freezing behavior 24 hours after a normal training paradigm (two foot-shocks at 0.7 mA for 2 sec), indicating that their long-term contextual fear memory is impaired (**Fig. 2F**), in agreement with previous work (*20, 21*). Genetic ablation of PKR in Ts65Dn mice (Ts65Dn-*Pkr*$^{-/-}$ mice) significantly improves their long-term memory (**Fig. 2F**). We have previously shown that a weak training protocol (one foot-shock at 0.35 mA for 1 sec) induced a better long-term fear memory in *Pkr*$^{-/-}$ mice compared to their WT littermates (*22*). However, in response to a normal and more conventional training protocol (two foot-shocks at 0.7 mA for 2 sec), the one we used to reveal that Ts65Dn mice exhibit impaired memory, *Pkr*$^{-/-}$ mice and WT littermates show normal long-term memory (**Fig. S7A**). Thus, genetic deletion of PKR selectively improves long-term memory in Ts65Dn mice. Consistent with these results, treatment with an inhibitor of PKR, PKRi (*22*), reversed the long-term memory deficits in Ts65Dn mice (**Fig. 2G**), but has no effect on WT mice (**Fig. S7B**).

To corroborate these findings, we assessed long-term object recognition memory, which is also dependent on the hippocampus (*23*). In this task, animals need to differentiate between a familiar and a novel object. During acquisition, two identical objects are placed in a box and mice are allowed to explore them (**Fig. 2H**). Ts65Dn and WT mice spend on average an equal amount of time investigating the identical objects (**Fig. S8A-B**). Twenty-four hours later when one object is replaced by a novel one, relying on their memory for the old object, WT mice preferentially explore the novel object.

In contrast, Ts65Dn mice show markedly reduced object discrimination, indicating that their long-term object recognition memory is impaired (**Fig. 2I**), in agreement with previous results (*19, 24*). Again, these deficits in long-term memory are ameliorated by genetic (**Fig. 2I**) or pharmacological inhibition of PKR in Ts65Dn mice (**Fig. 2J, Fig. S8C-E**). Finally, both genetic and pharmacological inhibition of the PKR restores behavioral flexibility in Ts65Dn mice in a spontaneous alternation T-maze task (**Fig. S9**).

We next investigated whether the inhibition of PKR improves the long-term deficits in synaptic plasticity in Ts65Dn mice. To this end, we recorded protein synthesis-dependent late-long-term potentiation (L-LTP), which is thought to underlie long-term memory (*25*), in hippocampal slices. As expected, L-LTP is impaired in slices from Ts65Dn mice and genetic ablation of PKR rescues the impaired L-LTP in Ts65Dn mice (**Fig. 2K**). Consistent with these data, treatment with PKRi improves L-LTP in slices from Ts65Dn mice (**Fig. 2L**). We previously showed that genetic or pharmacological inhibition of PKR did not further enhance L-LTP induced by 4 tetanic trains in WT slices (*22*); hence, the effects of these manipulations were specific to Ts65Dn mice. Collectively, our data support the notion that in Ts65Dn mice, the cognitive impairment at both the behavioral and synaptic levels is due, at least in part, to activation of the PKR branch of the ISR.

Inhibition of the ISR rescues the dysregulated translational program in Ts65Dn mice. To decipher the translational landscape in the brain of Ts65Dn mice in an unbiased manner, we next compared genome-wide transcriptional changes by RNA sequencing (RNA-seq) to translational changes, as determined by the sequencing of polysome-

associated mRNA in the brain of WT and Ts65Dn mice (**Fig. 3A**). As expected, in Ts65Dn mice, we found numerous genes that are transcriptionally and/or translationally dysregulated (**Fig. 3B-C**). GO-term enrichment analysis reveals categories of genes involved in mRNA metabolism, and signaling pathways involved in LTP regulation and memory storage (**Fig. 3D**). To identify the mRNAs whose translation is altered in Ts65Dn mice, we focused on mRNAs that are not significantly altered at the transcriptional level but are translationally increased or decreased (> 1.5-fold) in Ts65Dn mice. This analysis reveals 662 differences in the brain of Ts65Dn mice (**Fig. 3E**, **Table S2**). Of note, the expression of over 80 % of the mRNAs whose association with ribosomes is reduced in Ts65Dn mice is selectively corrected in Ts65Dn-*Pkr*$^{-/-}$ mice (**Fig. 3E**, **Table S2** and **Fig. S10**). Moreover, as an expected outcome of ISR induction, a subset of mRNAs shows increased association with the polysome fraction in Ts65Dn mice, but not in Ts65Dn-*Pkr*$^{-/-}$ mice (**Fig. 3E** and **Table S2**). Thus, inhibition of the PKR branch of the ISR partially corrects the dysregulated translational program in Ts65Dn mice.

Inhibition of the ISR rescues the deficits in protein synthesis, long-term memory and synaptic plasticity in Ts65Dn mice. Because i) eIF2 is the central hub of the ISR and its phosphorylation reduces general protein synthesis rates by inhibiting eIF2B (*10*), ii) the ISR is activated in the brains of Ts65Dn mice, and iii) protein synthesis is a primary node of proteostatic control, and its regulation is crucial for synaptic plasticity and long-term memory formation (*26*), we reasoned that either direct inhibition of the ISR by reducing eIF2-P levels or promoting the activity of eIF2B should similarly reverse the cognitive deficits in Ts65Dn mice. To test these predictions, we first crossed Ts65Dn mice

with heterozygous *Eif2s1*$^{S/A}$ mice, in which in one of the alleles the phosphorylation site at serine51 of eIF2α was replaced by non-phosphorylatable alanine. We found that in the brain of Ts65Dn-*Eif2s1*$^{S/A}$ mice, eIF2–P levels are reduced compared to Ts65Dn mice (**Fig. 4A-B**). As expected, direct reduction of eIF2–P levels in Ts65Dn mice (Ts65Dn-*Eif2s1*$^{S/A}$ mice) restores the aberrant translation (**Fig. 4C-D**). More importantly, reduction of eIF2–P levels corrects the deficits in long-term memory (**Fig. 4E** and **Fig. S11**) and L-LTP in Ts65Dn mice (**Fig. 4F**) but has no effect on WT mice (**Fig. S12**). Hence, direct reduction of eIF2-P levels and thus, correction of the aberrant translation in Ts65Dn mice rescues their deficits in L-LTP and long-term memory.

To further support these findings, we treated Ts65Dn mice with the small-molecule, drug-like ISR inhibitor ISRIB. ISRIB is a potent eIF2B activator that enhances GEF activity by facilitating eIF2B assembly into its decameric holo-enzyme, resulting in the reversal of eIF2–P-mediated translational events (*27-29*). Treatment with ISRIB parallels the effects of reducing eIF2–P levels genetically: ISRIB rescues the impairment in long-term memory (**Fig. 4G**) and L-LTP (**Fig. 4H**) in Ts65Dn mice, while it does not further enhance L-LTP (**Fig. S13A**) or long-term fear memory (**Fig. S13B**) in WT mice. Taken together, direct genetic or pharmacological manipulation of the efficacy of the central ISR effector eIF2-P rescues the core deficits in long-term memory and synaptic plasticity in Ts65Dn mice.

Inhibition of the ISR reverses the enhanced inhibitory synaptic transmission in Ts65Dn mice. According to previous reports, the deficits in L-LTP and long-term memory in Ts65Dn mice can be attributed to enhanced inhibitory synaptic transmission (*24, 30, 31*). Thus, we first wondered whether reversal of the PKR-mediated increase in eIF2-P

also corrects the abnormally high inhibitory synaptic transmission observed in Ts65Dn mice. As expected, whole-cell recordings show that inhibitory synaptic transmission is enhanced in Ts65Dn mice (**Fig. 5A-B**). Specifically, we observe significant enhancement of the frequency (but not the amplitude) of miniature inhibitory postsynaptic currents (mIPSCs) in hippocampal slices from Ts65Dn mice (**Fig. 5A-B, Fig. S14A**). The enhanced synaptic inhibition is reduced in hippocampal slices from Ts65Dn-*Pkr*$^{-/-}$ mice (**Fig. 5A-B**), as well as in slices from Ts65Dn mice treated with PKRi (**Fig. 5C-D, Fig. S14B**). Of note, excitatory synaptic transmission (determined by measuring mEPSCs frequency and amplitude) is not altered in the hippocampus of Ts65Dn mice (**Fig. S15**). Accordingly, genetically reduction of eIF2-P levels (**Fig. 5E-F** and **Fig. S14C**) or promoting the activity of eIF2B with ISRIB (**Fig. 5G-H** and **Fig. S14D**) reduce the enhanced synaptic inhibition in Ts65Dn mice. Thus, inhibition of the ISR at the level of the initiating kinase PKR or at its central eIF2•eIF2B regulatory hub reverses the enhanced synaptic inhibitory tone in Ts65Dn mice.

Discussion

It is widely accepted that *de novo* protein synthesis is required for the formation of long-term memory (*32, 33*). Research in different species and animal models over the last decade showed that the ISR is a central proteostasis network causally controlling long-term memory formation. This conclusion is supported by three types of observations. First, genetic or pharmacological suppression of the ISR, by inhibiting the eIF2 kinases or boosting the function of the eIF2•eIF2B complex, facilitates long-term memory formation (*26*). Second, activation of the ISR by inhibiting the eIF2 phosphatases or

activating PKR in the hippocampus impairs long-term memory (*26*). Finally, mutations in key components ISR that induce the ISR have been associated with intellectual disability (*35-37*), underscoring the importance of the ISR in mnemonic processes.

Here we found that activation of the ISR can account, at least in part, for the core behavioral and neurophysiological abnormalities in Ts65Dn mice, a model system of DS. The potential significance of our findings is highlighted by the observation that the activation of the ISR in the brains of Ts65Dn mice is recapitulated in the brains of individuals with DS, as well as in human CH21-trisomic iPSCs derived from individuals with DS. Thus, ISR-mediated maladapted regulation of protein synthesis may emerge as a central molecular mechanism underlying the cognitive decline associated with DS.

Given the heterogeneity of the genetic perturbations in DS, it seems unlikely that aberrant levels of a single protein are the sole cause of the long-term memory deficits associated with DS. Instead of repairing the expression of individual genes, we correct the overall translational program controlled by the ISR by restoring the function of eIF2•eIF2B, where the ISR exerts its central control. Briefly, we find that inhibition of the activated ISR either upstream at the level of the ISR-inducing kinase PKR or downstream by manipulating the central ISR signaling hub (eIF2•eIF2B) rescues the cognitive deficits and neurophysiological abnormalities in Ts65Dn mice. By correcting the translational program controlled by the ISR, we overcame a central limitation of the field: it is just not feasible to determine *in vivo* the causal role of all of the individually dysregulated proteins in long-term memory formation by overexpressing or knocking them down, which would require hundreds of experiments, and given the current technology, it is certainly not possible to test all combinatorial possibilities. Beyond these limitations, it may prove not

useful to target specific genes if the ultimate cause of the disorder lies in global proteostasis defects that are sensed as a generic stress condition in the brain by the ISR.

Excessive synaptic inhibition is thought to cause the deficits in hippocampal L-LTP and long-term memory in Ts65Dn mice (*24, 30, 31*). We provide genetic and pharmacological evidence that inhibition of the ISR reverses the excessive synaptic inhibition and, in turn, the deficits in L-LTP and long-term memory that likely result from it. Thus, our findings present a model that links these two axes of dysfunction—increased synaptic inhibition and impaired L-LTP, and long-term memory formation—through a single proteostasis network, the ISR.

In addition to reducing enhanced synaptic inhibition, other manipulations and pathways [serotonin, sonic hedgehog (Shh), minocycline, lithium, exercise, BDNF] have been shown to improve the memory and/or L-LTP deficits in Ts65Dn mice. It is interesting to note that these manipulations modulate the ISR: minocycline, which has been reported to improve memory in Ts65Dn mice (*38*), inhibits the ISR by reducing eIF2-P levels (*39*). Treatment with fluoxetine, a serotonin reuptake inhibitor, improved long-term memory in Ts65Dn mice (*40*) and was shown to inhibit the PKR-branch of the ISR (*41*). The synthetic activator of the Shh pathway SAG 1.1 rescued memory in Ts65Dn mice (*42*). While it is currently unknown whether SAG 1.1 inhibits the ISR, another pharmacological activator of the Shh blocked the PERK-branch of the ISR resulting in decreased eIF2-P levels (*43*). Lithium improved LTP and memory in Ts65Dn mice (*44*) and inhibited the ISR by promoting eIF2B activity (*45*). Exercise, which has been reported to improve cognitive function in Ts65Dn mice (*46*), was recently shown to block the ISR in the hippocampus of an Alzheimer's Disease (AD) mouse model (*47*). Finally, pharmacological induction of

BDNF, with the recently developed BDNF-mimetic drug 7,8-dihydroxyflavone (DHF) reversed the deficits in LTP and long-term memory in Ts65Dn mice (*48*) and BDNF inhibited the ISR in neurons, by promoting eIF2B activity and reducing eIF2-P levels (*49*). These observations raise the intriguing possibility that the manipulations reported to reverse the memory deficits in Ts65Dn may do so, either directly or indirectly, by modulating the ISR, which might lie at the crossroad of the different pathways implicated in DS.

Finally, DS is characterized by a high incidence of early onset AD and activation of the ISR has been implicated in a variety of neurodegenerative disorders, including AD (*50*), traumatic brain injury (*51*), prion disease (*52*) and myelination disorders (*53, 54*). Thus, genetic or pharmacological modulation of the ISR may emerge as a promising avenue to alleviate a wide range of cognitive disorders resulting from a disruption in protein homeostasis.

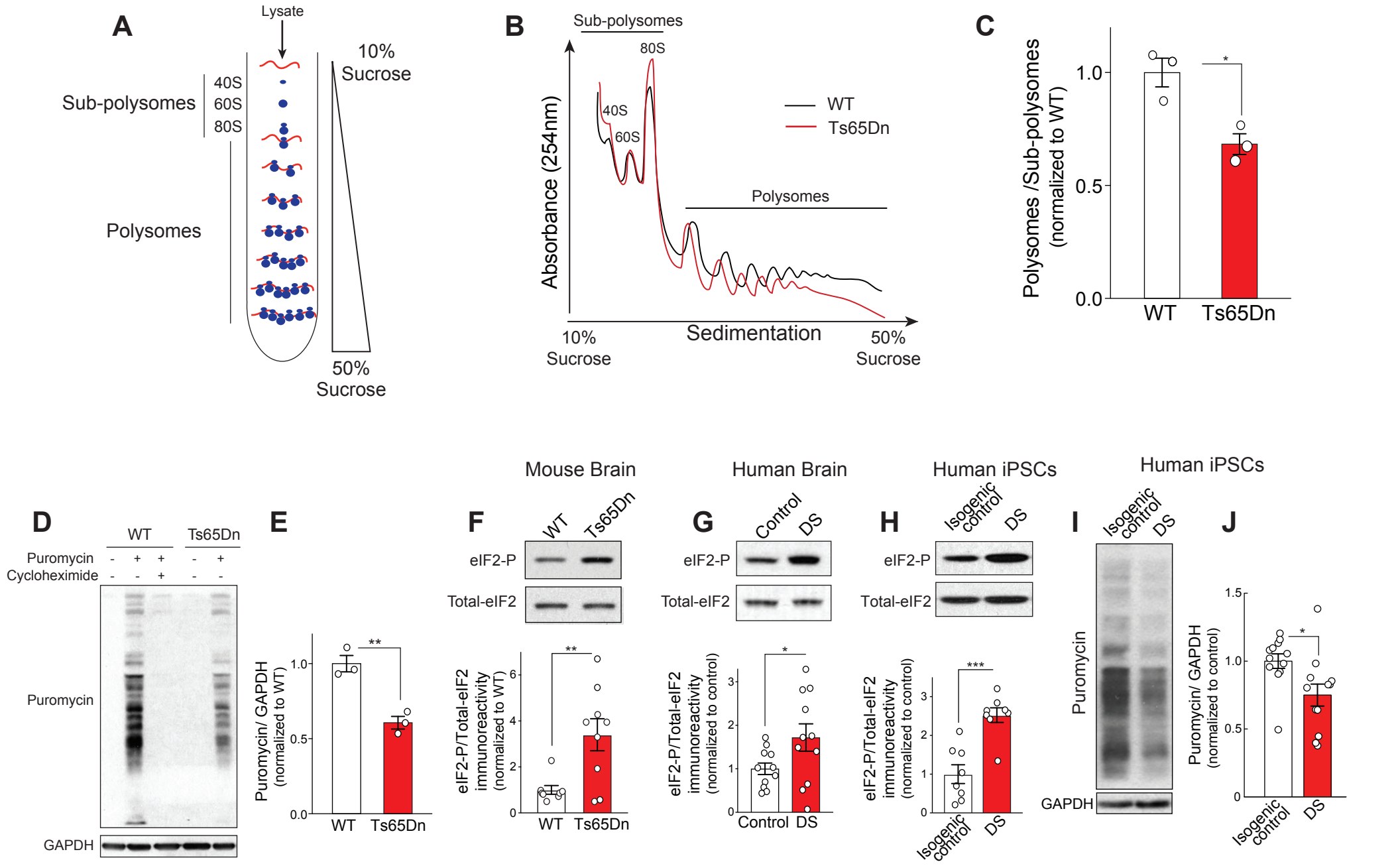

Fig. 1. Zhu et al.

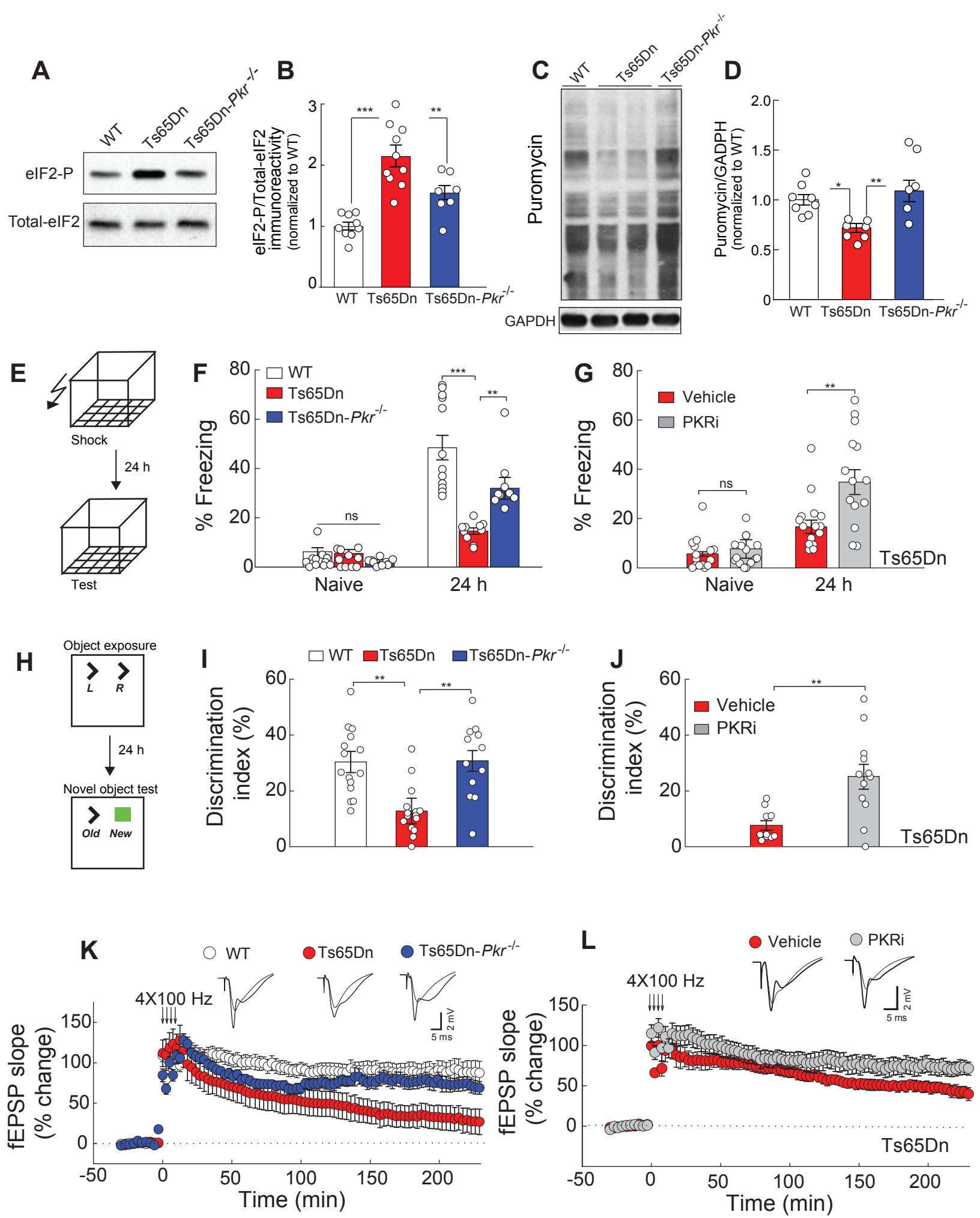

Fig. 2. Zhu et al.

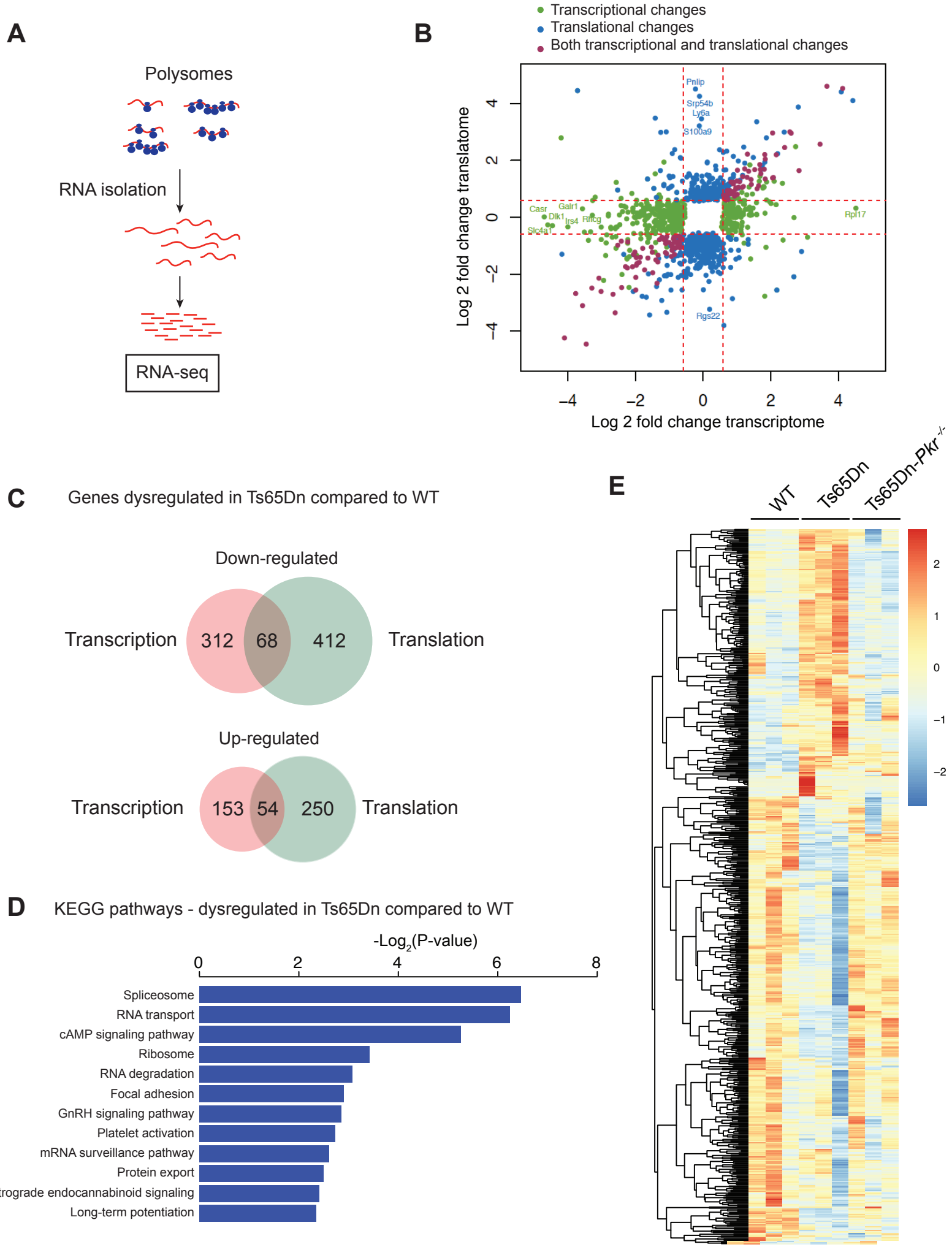

Fig. 3. Zhu et al.

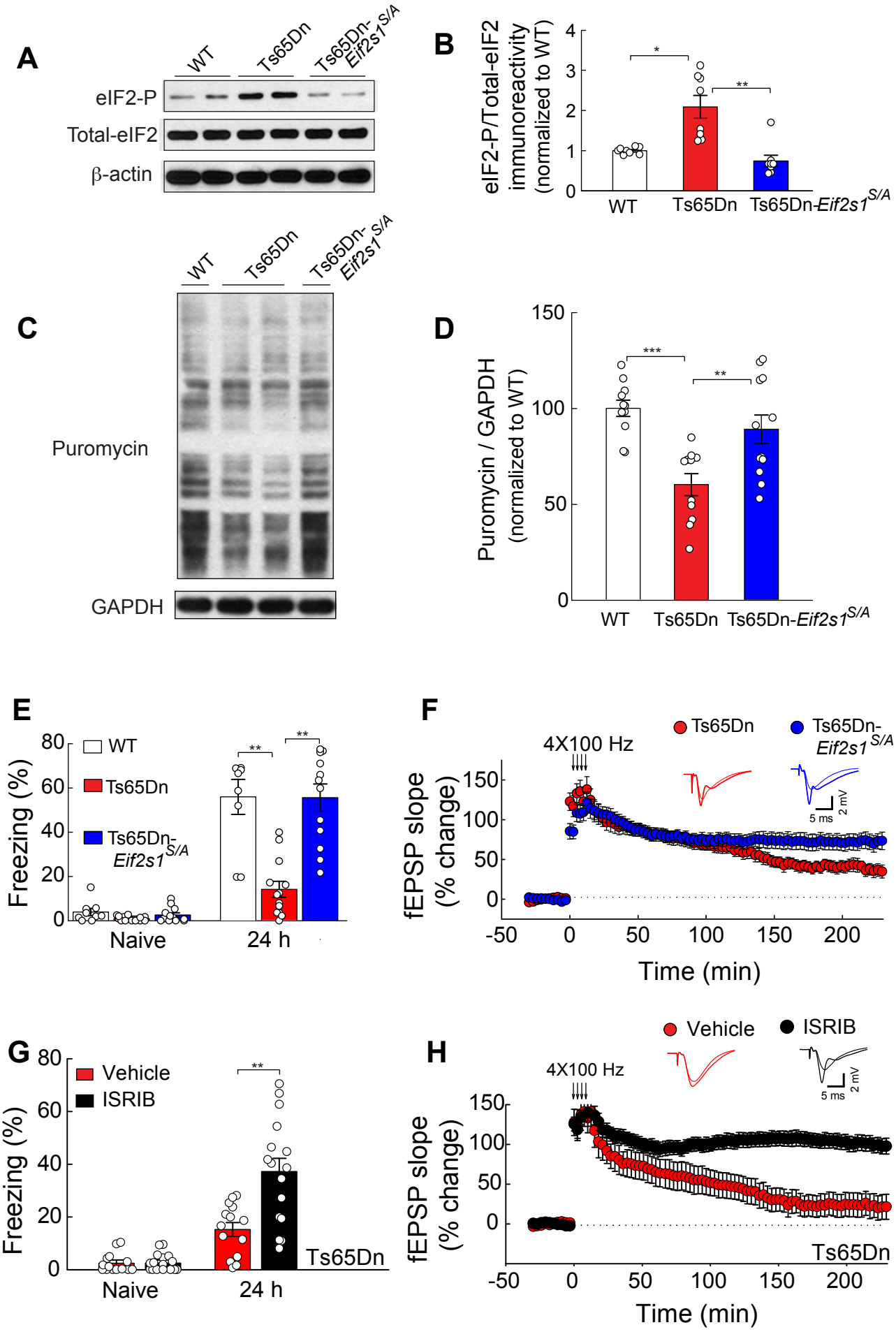

Fig. 4. Zhu et al.

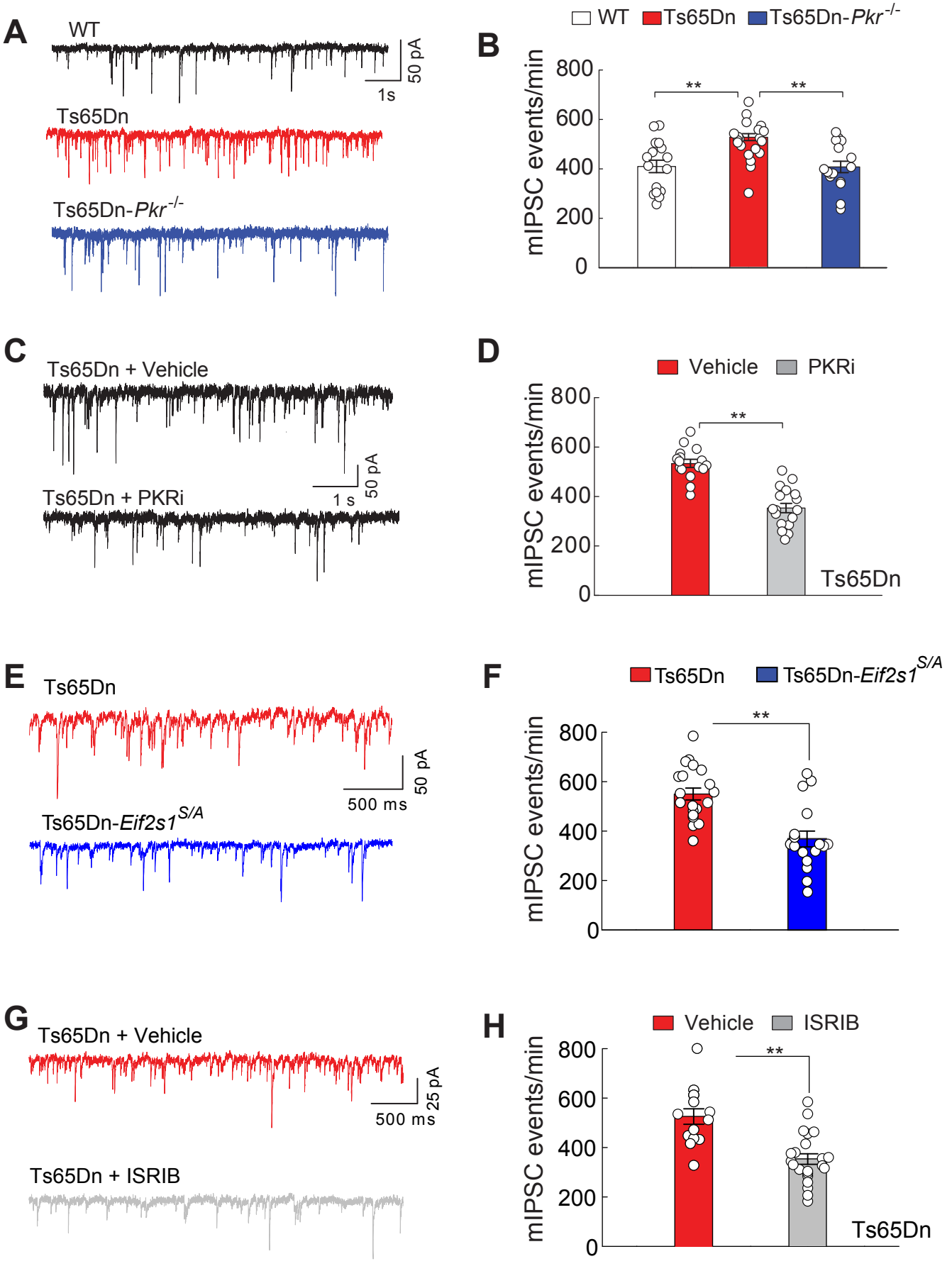

Fig. 5. Zhu et al.

Figure Legends

Fig. 1. The ISR is activated in the brains of DS mice (Ts65Dn) and individuals with DS. (**A**) Schematic of polysome profiling sedimentation. Following ultracentrifugation, sub-polysomes (40S, 60S, and 80S) and polysomes are separated based on size. (**B-C**) Representative polysome profile traces (**B**) and quantification (**C**) of polysomes/sub-polysomes ratio in the hippocampus of WT and Ts65Dn mice (n = 3 per group, t_4 = 4.05, two-tailed Student's t-test). (**D-E**) Incorporation of puromycin into nascent peptides was detected using an anti-puromycin antibody. A representative Western blot (**D**) and quantification (**E**) in hippocampal extract from WT and Ts65Dn mice (n = 3 per group, t_4 = 5.69). Treatment with the protein synthesis inhibitor cycloheximide was included as control. (**F-H**) Representative Western blot and quantification of eIF2-P levels in (**F**) hippocampal extracts from WT and Ts65Dn mice (n = 8-9 per group, t_{15} = 3.14), (**G**) post-mortem human brain extracts from controls and individuals with DS (n = 11 per group, t_{20} = 2.10), and (**H**) human iPSC extracts from an individual with DS (CH21-trisomic, n = 8 per group, t_{14} = 4.95) compared to its isogenic control. (**I-J**) Incorporation of puromycin into nascent peptides in iPSCs was detected using an anti-puromycin antibody. A representative Western blot (**I**) and quantification (**J**) in the DS CH21-trisomic iPSCs compared to the isogenic control line (n = 12 per group, t_{22} = 2.51). "Isogenic control" indicates iPSCs that are diploid for CH21, whereas "DS" indicates iPSCs that are CH21-trisomic. Both lines were derived from the same individual with DS and the experiment was replicated in 8-12 wells per genotype. Data are mean ± s.e.m. *P < 0.05, **P < 0.01, ***P < 0.001.

Fig. 2. Inhibition of PKR rescues the deficits in long-term memory and synaptic plasticity in Ts65Dn mice. (**A**-**B**) Representative Western blot (**A**) and quantification (**B**) of eIF2-P levels in hippocampal extracts from WT (n = 9), Ts65Dn (n = 10), and Ts65Dn-*Pkr*$^{-/-}$ mice (n = 7, $F_{2,23}$ = 4.12, One-way ANOVA). (**C-D**) Incorporation of puromycin into nascent peptides was detected using an anti-puromycin antibody. A representative Western blot (**C**) and quantification (**D**) in hippocampal extracts from WT (n = 8), Ts65Dn (n = 7) and Ts65Dn-*Pkr*$^{-/-}$ mice (n = 6, $F_{18,2}$ = 25.16). (**E**) Schematic of the fear conditioning paradigm. (**F**) Genetic inhibition of PKR: freezing behavior before (naïve) and 24 hours post-training in WT (n = 12), Ts65Dn (n = 10), and Ts65Dn-*Pkr*$^{-/-}$ mice (n = 9, H = 22.74, One-way ANOVA on Ranks). (**G**) Pharmacological inhibition of PKR: freezing behavior before (naïve) and 24 hours post-training in vehicle-treated (n =15) and PKRi-treated Ts65Dn mice (n = 14, t_{27} = 3.21). (**H**) Schematic of the object recognition task. (**I**) Genetic inhibition of PKR: novel object discrimination index 24 hours post-training in WT (n = 15), Ts65Dn (n = 15) and Ts65Dn-*Pkr*$^{-/-}$ mice (n = 12, $F_{2,39}$ = 11.56). (**J**) Pharmacological inhibition of PKR: novel object discrimination index 24 hours post-training in vehicle-treated (n = 10) and PKRi-treated Ts65Dn mice (n = 12, t_{20} = 3.48). (**K**) Genetic inhibition of PKR: L-LTP induced by four trains of high frequency stimulation (HFS, 4 X 100 Hz) in WT (n = 10), Ts65Dn (n = 14) and Ts65Dn-*Pkr*$^{-/-}$ mice (n = 14, H = 15.72, P < 0.05). (**L**) Pharmacological inhibition of PKR: L-LTP induced by 4 X 100 Hz of HFS in vehicle-treated (n = 7) and PKRi-treated Ts65Dn mice (n = 13, t_{18} = 2.32, P < 0.05, Mann-Whitney U test). Data are mean ± s.e.m. *P < 0.05, **P < 0.01, ***P < 0.001.

Fig 3. Inhibition of the ISR rescues the dysregulated translational program in the brain of Ts65Dn mice. (**A**) Schematic of the polysome profiling followed by RNA-seq protocol. (**B**) Scatterplot showing the genes significantly up- or down-regulated (>1.5 fold) at the transcriptional and/or translational levels in the brain of Ts65Dn mice. mRNAs whose expression was not altered between genotypes were removed from the analysis (white square). (**C**) Venn diagram depicting transcriptionally and translationally up- or down-regulated genes in Ts65Dn mice. (**D**) KEGG pathway enrichment analysis of the genes downregulated in Ts65Dn mice compared to WT. (**E**) Heat map showing genes that are significantly up- or down-regulated only at the translational level in Ts65Dn mice and rescued in Ts65Dn-*Pkr*$^{-/-}$ mice (n = 3 per group).

Fig. 4. Genetic or pharmacological inhibition of the ISR rescues the deficits in memory and synaptic plasticity in Ts65Dn mice. (**A-B**) Representative Western blot (**A**) and quantification (**B**) of eIF2-P levels in hippocampal extracts from WT (n = 8), Ts65Dn (n = 8), and Ts65Dn-*Eif2s1*$^{S/A}$ mice (n = 8, H = 15.92). (**C-D**) Incorporation of puromycin into nascent peptides was detected using an anti-puromycin antibody. A representative Western blot (**C**) and quantification (**D**) in hippocampal extracts from WT (n = 11), Ts65Dn (n = 11) and Ts65Dn-*Eif2s1*$^{S/A}$ mice (n = 12, $F_{31,2}$ = 11.23). (**E**) Genetic inhibition of the ISR: freezing behavior before (naïve) and 24 hours post-training in WT (n = 9), Ts65Dn (n = 13) and Ts65Dn-*Eif2s1*$^{S/A}$ mice (n = 12, $F_{2,31}$ = 20.25). (**F**) Genetic inhibition of the ISR: L-LTP induced by 4 X 100 Hz of HFS in Ts65Dn (n = 10) and Ts65Dn-*Eif2s1*$^{S/A}$ mice (n = 9, t_{17} = 3.1, P < 0.01). (**G**) Pharmacological inhibition of the ISR: freezing behavior before (naïve) and 24 hours post-training in vehicle-treated (n =

14) and ISRIB-treated (n = 16) Ts65Dn mice (t_{28} = 4.35, Mann-Whitney U test). (**H**) Pharmacological inhibition of the ISR: L-LTP induced by 4 X 100 Hz of HFS in vehicle-treated (n = 8) and ISRIB-treated (n = 9) Ts65Dn mice (t_{15} = 4.84, P < 0.001). Data are mean ± s.e.m. *P < 0.05, **P < 0.01.

Fig. 5. Genetic or pharmacological inhibition of the ISR suppresses the increased inhibitory synaptic responses in Ts65Dn mice. (**A-B**) Sample traces (**A**) and summary data (**B**) show frequency of mIPSCs in CA1 neurons from WT (n = 16), Ts65Dn (n = 20) and Ts65Dn-*Pkr*$^{-/-}$ (n = 16) mice ($F_{2,49}$ = 7.76). (**C-D**) Sample traces (**C**) and summary data (**D**) show frequency of mIPSCs in CA1 neurons from vehicle-treated (n = 16) and PKRi-treated (n = 17) Ts65Dn mice (t_{31} = 7.09). (**E-F**) Sample traces (**E**) and summary data (**F**) show frequency of mIPSCs in CA1 neurons from Ts65Dn (n = 20) and Ts65Dn-*Eif2s1*$^{S/A}$ mice (n = 17, t_{35} = 4.58). (**G-H**) Sample traces (**G**) and summary data (**H**) show frequency of mIPSCs in CA1 neurons from vehicle-treated (n = 13) and ISRIB-treated Ts65Dn mice (n = 22, t_{33} = 6.18). Data are mean ± s.e.m. **P < 0.01.

Material and Methods

Mouse husbandry. All experiments were conducted on 3-5 months old animals. Ts65Dn mice were purchased from Jackson laboratory. *Pkr*$^{-/-}$ mice (*22*) and *Eif2s1*$^{S/A}$ mice (*55*) have been previously described. Double mutant mice were generated by crossing Ts65Dn mice to either *Pkr*$^{-/-}$ mice or *Eif2s1*$^{S/A}$ mice. It is not possible to obtain Ts65Dn mice in a pure genetic background because repeated backcrossing of the Ts65Dn chromosome onto an inbreed genetic background for several generations fails to recover trisomic progeny. Thus, investigators in the field are required to use the Ts65Dn mice in a hybrid background. We used littermate controls for our experiments. Briefly, to generate Ts65Dn-*Pkr*$^{-/-}$ mice, we first crossed Ts65Dn female (B6EiC3H) with *Pkr*$^{-/-}$ males (129Svev). The resulting F1 Ts65Dn-*Pkr*$^{+/-}$ females were crossed with *Pkr*$^{+/-}$ males. Finally, we compared side-by-side Ts65Dn mice withTs65Dn-*Pkr*$^{-/-}$ mice from the same F2 litter. Thus, littermate controls have the same hybrid background as our experimental mice (Ts65Dn mice). Similarly, when we crossed Ts65Dn females (B6EiC3H) with *Eif2*$^{S/A}$ males (C57Bl6), we compared Ts65Dn-*Eif2s1*$^{S/S}$ with Ts65Dn-*Eif2s1*$^{S/A}$ littermate controls. Ts65Dn mice were genotyped as recommended by Jackson laboratory. PKRi (*56*) was freshly dissolved in saline and Ts65Dn mice and WT littermates were administered either PKRi (0.1 mg/kg) or vehicle (0.02 % DMSO) intraperitoneal (i.p.) for 6 days, as we previously described (*22*). Ts65Dn mice were injected with ISRIB (2.5 mg/kg) or vehicle once every two days for a week, as previously described (*27*). Mice were weaned at the third postnatal week, genotyped and kept on a 12h / 12h light/dark cycle (lights on at 7:00 am) and had access to food and water ad libitum. Animal care and

experimental procedures were approved by the institutional animal care and use committee (IACUC) at Baylor College of Medicine, according to NIH Guidelines.

Electrophysiology. Electrophysiological recordings were performed as previously described (*22*). Field recording were performed from CA1 horizontal hippocampal slices (320 μm thick), which were cut from the brain of adult mice (3-6 months old) with a vibratome (Leica VT 1000S, Leica Microsystems, Buffalo Grove, IL) at 4°C in artificial cerebrospinal fluid solution (ACSF; 95% O_2 and 5% CO_2) containing in mM: 124 NaCl, 2.0 KCl, 1.3 $MgSO_4$, 2.5 $CaCl_2$, 1.2 KH_2PO_4, 25 $NaHCO_3$, and 10 glucose (2-3 ml/min). Slices were incubated for at least 60 min prior to recording in an interface chamber and continuously perfused with artificial cerebrospinal fluid (ACSF) at 28 - 29°C at a flow rate of 2 - 3 ml/min. The recording electrodes were placed in the stratum radiatum. Field excitatory postsynaptic potentials (fEPSPs) were recorded with ACSF-filled micropipettes and were elicited by bipolar stimulating electrodes placed in the CA1 stratum radiatum to excite Schaffer collateral and commissural fibers. The intensity of the 0.1-ms pulses was adjusted to evoke 30 - 35% of maximal response. A stable baseline of responses at 0.033 Hz was established for at least 30 min. L-LTP was induced by applying four tetanic trains of high-frequency stimulation (100 Hz, 1 s) separated by 5-min intervals.

Whole-cell recordings were performed using a MultiClamp 700B amplifier (Molecular Devices, Union City, CA) in a submerged chamber (2 - 3 ml/min) at 31 - 32°C using conventional patch-clamp techniques. CA1 neurons were visually identified by infrared differential interference contrast video microscopy on the stage of an upright microscope (Axioskope FS2, Carl Zeiss, Oberkochen, Germany). Patch pipettes (resistances 2 - 5

MΩ) were filled with (in mM): 140 CsCl, 10 HEPES, 10 Na_2-phosphocreatine, 0.2 BAPTA, 2 Mg_3-ATP, 0.2 Na_3-GTP; pH was adjusted to 7.2 and osmolarity to 295~300 mOsm using a Wescor 5500 vapor pressure osmometer (Wescor, Logan, UT). Miniature inhibitory postsynaptic currents (mIPSCs) were recorded at -60 mV in the presence of NBQX (5 μM, 2,3-dihydroxy-6-nitro-7-sulfamoyl-benzo[f]quinoxaline disodium salt), AP5 (25 μM, DL-2-Amino-5-phosphonopentanoic acid) and TTX (1 μM, tetrodotoxin). For recording excitatory currents, CsCl was replaced with 130 mM K-gluconate and 10 mM KCl. Excitatory postsynaptic currents (EPSCs) were recorded at -70 mV in the presence of 100 μM picrotoxin. All drugs were obtained from Tocris (Ellisville, MO).

Western Blotting. Hippocampus and cortex from mice were isolated, homogenized in cold homogenizing buffer [200 mM HEPES, 50 mM NaCl, 10% Glycerol, 1% Triton X-100, 1 mM EDTA, 50 mM NaF, 2 mM Na_3VO_4, 25 mM β-glycerophosphate, and EDTA-free complete ULTRA tablets (Roche, Indianapolis, IN)], and centrifuged at 14,000 *rpm* for 15 min at 4° C. Human tissue was obtained from University of Maryland Brain and Tissue Bank, a brain and tissue repository of the NIH Neurobiobank. Post-mortem human brain samples from Down syndrome patients and those from age- and sex-matched unaffected controls (see Supplementary Table I) were homogenized as described above. The supernatants (30 μg of protein/sample) were resolved on SDS–PAGE (15%) and transferred onto nitrocellulose membranes (Pall, Port Washington, NY). Antibodies against p-eIF2α (catalog # 3398, 1:1000), total eIF2α (catalog # 9722, 1:1000), total PERK (catalog # 3192, 1:1000), p-4E-BP1 (catalog # 9459, 1:1000), total 4E-BP1 (catalog # 9452, 1:1000), p-S6 (catalog # 4856, 1:1000), total S6 (catalog # 2217, 1:1000), p-eIF4E (catalog # 9741, 1:1000), GAPDH (catalog # 2118, 1:5000) were purchased from

Cell Signaling Technology (Danvers, MA), β-actin (1:5000) from Novus Biologicals (Centennial, CO), p-PKR (catalog # ab32036, 1:500), p-GCN2 (catalog # ab75836, 1:1000), and total-GCN2 (catalog # ab137543, 1:1000) from Abcam (Cambridge, MA), total-PKR (catalog # 18244-1-AP, 1:1000) from Proteintech (Rosemont, IL), p-PERK (catalog # 649401, 1:1000) from Biolegend (San Diego, CA), ATF6 (catalog # 24169, 1:2000) from Proteintech, and total-eIF4E (catalog # 610269, 1:1000) from BD Transduction Laboratories.

Measuring Ire1 activity by RT-PCR and qPCR. For RT-PCR, RNA was isolated from the hippocampus from WT and Ts65Dn mice and reverse transcribed with the VILO superscript kit (Thermo Fisher Scientific). cDNA for *XBP1* was then amplified with specific primers (Fw: AAACAGAGTAGCAGCGCAGACTGC and Rev: TCCTTCTGGGTAGACCT CTGGGAG). The PCR products were digested with the Pst1 restriction enzyme (New England Biolabs) and the products were subjected to agarose gel electrophoresis. For qPCR, PowerUp SYBR green master mix was used on a step-one plus qPCR machine (Applied Biosystems) using cDNA prepared as described above. Primers specific for spliced (Fw: CTGAGTCCGAATCAGGTGCAG and Rev: GTCCATGGGAAGATGTTCTG G) and unspliced *XBP1* (CAGCACTCAGACTATGTGCA and Rev: GTCCATGGGAAGAT GTTCTGG) were previously described (*57*).

Generation of Down Syndrome (DS) iPS cells. To determine whether the ISR response was activated in cells from DS patients, we reprogramed Detroit 532 foreskin fibroblasts (ATCC® CCL-54™, Lot # 58237511) by infecting them with a non-integrating Sendai

viruses (*58*) expressing OCT4, SOX2, KLF4, and C-MYC (*59*) (Thermo Fisher Scientific, CytoTune™-iPS 2.0 Sendai Reprogramming Kit) using manufacturer's recommendations. Clonal human induced pluripotent cell (hiPSC) colonies were manually picked and expanded under feeder-free conditions using hESC-qualified Matrigel (Corning) and TeSR-E8 medium (STEMCELL Technologies). The cell line was designated as HSCC-046iPS-S and abbreviated as "DS" followed by the clone number. As expected, a clonal line (DSc1) was shown to have a trisomy 21 male karyotype by G-banding at Passage 9 (Fig. S1A). Surprisingly, a second clonal line (DSc2) was found to have a normal male karyotype (Fig. S1B), which was used as an "isogenic control". The authenticity of the euploid (DSc2) clone was confirmed by short-tandem repeats (STRs) profile using the ATCC's STR Profiling Cell Authentication Service. Briefly, the euploid DSc2 iPSCs clone, which was discovered serendipitously, perfectly matched the original CCL-54™ line (Figure S1C) and was the perfect isogenic control for our experimental DSc1 line. iPSCs were cultured on Matrigel® hESC-Qualified Matrix (Corning) and in mTeSR™1 medium (Stemcell Technologies) and passaged using ReLeSR™ (Stemcell Technologies) every 4 - 5 days with daily medium changes.

Novel Object Recognition. The experimenters were blind to the genotype for all of the behavioral experiments. For object recognition, mice were handled for 5 days (5-10 min for each day) and then habituated to a black Plexiglas rectangular chamber (31 x 24 cm, height 27 cm) for 10 min under dim ambient light for 5 days. Two identical objects were presented to mice to explore for 5 min, after which, mice were returned to the home cage. Twenty-four hours later, one object was replaced by one novel object and the mouse was

again placed in the chamber 5 min. The novel object has the same height and volume but different shape and appearance. Exploration of the objects was defined as sniffing of the objects (with nose contact or head directed to the object) within at 2 cm radius of the objects. Sitting or standing on the objects was not scored as exploration. Behavior was recorded from cameras positioned above the training chamber. Discrimination Index (DI) was computed as DI = (Novel Object Exploration Time – Familiar Object Exploration Time/Total Exploration Time) X 100. To control for odor cues, the open field arena and the objects were thoroughly cleaned with ethanol, dried, and ventilated between mice.

Contextual fear conditioning. Experiments were performed as previously described (*55*), with some modifications. Briefly, mice were first handled for 5 min per day for 5 days and then habituated to the conditioning chamber for 20 min for another 2 days. On the training day, mice were placed in the conditioning chamber for 2 min (naïve) and then received two-foot shocks (0.75 mA, 2 sec, 90 sec apart), after which the mice remained in the chamber for an additional minute before being returned to their home cages. Twenty-four hours later, mice were re-exposed to the same context (training chamber) for 5 min and "freezing" (immobility with the exception of respiration) responses were recorded using real-time video and analyzed by FreezeView. The fear condition training was always the last behavioral test performed.

T-maze spontaneous alternation task. The apparatus was a black wooden T-maze with 25 cm high walls and each arm was 30 cm long and 9 cm wide. A removable central partition was used during the sample phase but not the test phase of each trial. Guillotine

doors were positioned at the entrance to each goal arm. At the beginning of the sample phase, both doors were raised, and the mouse was placed at the end of the start arm facing away from the goal arms. Each mouse was allowed to make a free choice between the two goal arms; after its tail had cleared the door of the chosen arm, the door was closed, and the mouse was allowed to explore the arm for 30 sec. The mouse was then returned to the end of the start arm, with the central partition removed and both guillotine doors raised, signaling the beginning of the test phase. This sequence (trial) was repeated 20 times. Trials that were not completed within 120 seconds were terminated and disregarded during analysis. Correct alteration between trails was expressed as % alteration = (number of correct alteration) / 20 x 100%.

Polysome profiling and RNA isolation. Polysome profiling followed by RNA sequencing was carried out as we previously described (*60*), with some modifications. Briefly, we prepared fresh 12 ml of 10 – 50% sucrose density gradients [10 mM HEPES-KOH (pH 7.6), 5 mM $MgCl_2$, 150 mM KCl, 200 U/ml RNasin Rnase inhibitor (Promega, Madison, WI)]. Gradients were kept at 4^o C for at least 2 h before use. Mouse brain tissue was dissected in a cutting solution [1X HBSS, 2.5 mM HEPES-KOH (pH 7.6), 35 mM glucose, 4 mM $NaHCO_3$, 100 μg/ml cycloheximide (Sigma-Aldrich, St. Louis, MO)] and washed in ice-cold PBS containing 100 μg/ml cycloheximide by centrifugation at 3000 rpm for 10 min at 4^{o}C. The tissue was then lysed in polysome lysis buffer [10 mM HEPES-KOH (pH 7.4), 5 mM $MgCl_2$, 150 mM KCl, 0.5 mM DTT, 100 U/ml RNasin Rnase inhibitor (Promega, Madison, WI), 100 μg/ml cycloheximide, and EDTA-free protease inhibitors (Roche Indianapolis, IN)] and centrifuged at 2000 x g for 10 min at 4^{o}C. The supernatant was

then transferred to a pre-chilled tube, supplemented with 0.5% NP-40, and kept on ice for 10 min. Samples were centrifuged at 14,000 rpm for 10 min at 4^{o}C. The supernatant was either layered onto sucrose gradient or reserved for total RNA isolation. Gradients were centrifuged in a SW-40Ti rotor at 35,000 rpm at 4^{o} C for 2 h and then analyzed by piercing the tube with a Brandel tube piercer, passing 70% sucrose through the bottom of the tube and monitoring the absorbance of the material eluting from the tube using an ISCO UA-6 UV detector. Fractions were collected throughout and RNA was extracted with TRIzol following manufacturer's instructions (Life Technologies, Carlsbad, CA).

Experiments were performed in three biological replicates for each group. Polysomal (light and heavy) mRNA was isolated from WT, Ts65Dn, and Ts65Dn-*Pkr*$^{-/-}$ mice. To identify the mRNAs translationally dysregulated in the brain of Ts65Dn mice compared to WT mice, we focused on mRNAs with no significant change in total mRNA levels, but either increased or decreased in their association with polysomes (> 1.5 fold) by comparing the ratio between the translational RNAseq (light and heavy polysmes) and transcriptional RNAseq (total RNA).

RNA-Seq and data analysis. RNA-seq library was generated using RNA isolated from polysomal fractions (light and heavy) and total RNA using the KAPA RNA HyperPrep Kits with RiboErase protocol for Total RNASeq. The library was then sequenced using Illumina NS500 Single-End 75bp (SE75), which generated 20-35 million reads per sample. For analysis of RNA-seq data, we removed adapters and low-quality bases by Trimmomatic (v0.38) (*61*) using default parameters. We then aligned clean reads to the mm10 mouse reference genome by HISAT2(v2.1.0) (*62*) and converted these aligned bam files into

bigwig format using RSeQC (v2.6.5) (*63*) and wigToBigWig from UCSC (*64*). Cufflinks (v2.2.1) (*65*) was used to assess differentially expressed genes (DEGs) (GENCODE vM18 as the genes reference annotation file) between groups [*q* (*p*-value corrected for false discovery rate, FDR) < 0.05 and fold change > 1.5). Default thresholds of Cufflinks were used to identify DEGs. In order to improve the robustness of transcript abundance estimates, we also used "-M" parameter of Cufflinks to mask rRNA regions (build mm10) retrieved from UCSC Table Browser. Only protein-coding genes (defined in GENCODE vM18 GTF file) whose significant differential expression status were labeled "yes" by Cufflinks were used in subsequent analyses. DEGs in light and heavy polysomes are combined and expressed as DEGs at the translational level. Because of low sequence depth, one of the heavy-polysome replicates in the Ts65Dn-*Pkr*$^{-/-}$ group was excluded from the analysis. For DEGs identified only in light or heavy polysomes, we used the expression values (RPKM) from the corresponding group (Fig. 3E). However, for genes that were found expressed in both light and heavy polysomes, we only used the RPKM value from the light polysomes to avoid combining different RPKM values. KEGG pathway enrichment analysis for genes down-regulated at only the translational level in Ts65Dn mice compared to WT was performed on the DAVID 6.8 website (*66*). In order to obtain the gene expression value matrix for all samples (including the low sequence depth), we used two R packages, Rsubread and edgeR, to count the reads number and convert the count number to RPKM value. Multi-mapping reads were also counted. A multi-mapping read will carry a count of 1/x, instead of 1, where x is the total number of alignments reported for the same read. We then used package pheatmap of R to generate the heatmap based on this RPKM matrix.

Surface Sensing of Translation (SUnSET). Protein synthesis was measured using SUnSET, a non-radioactive labeling method to monitor protein synthesis, as previously described (*67*). Briefly, hippocampal slices were cut (300 μm) with a McIlwain Tissue Chopper (Mickle, UK) and incubated for 1 hour at room temperature in oxygenated (95% O_2, 5% CO_2) ACSF followed by incubation at 32°C for 1 hour in oxygenated (95% O_2, 5% CO_2) ACSF prior to treatment as we previously described (*68*). Puromycin (10 μg/μl, dissolved in oxygenated ACSF) was bath applied to the slices for 20 min followed by a wash with untreated oxygenated ACSF. The slices were then snap-frozen on dry ice and stored at -80 C until use. Frozen slices were lysed in homogenization buffer (in mM: 40 Tris HCl, pH 8.0, 150 NaCl, 25 β-glycerophosphate, 50 NaF, 2 Na_3VO_3, 1X protease inhibitor cocktail, 10% glycerol, 1% Triton X-100). Puromycin incorporation was detected by Western blot using the 12D10 antibody to puromycin (Catalog # MABE343, 1:5000, EMD Millipore Corp, Darmstadt, Germany) as we previously described (*60*). The density of the resulting bands was quantified using ImageJ and statistical significance assessed by Student's *t*-test.

Statistical analyses. Data are presented as means ± SEM. Statistics were based on two-tailed Student's *t*-test or Mann-Whitney Rank Sum test for two-group comparisons. One-way ANOVA followed by Bonferroni post hoc analysis was performed for multiple comparisons, unless otherwise indicated. $P < 0.05$ was considered significant (*$P < 0.05$, **$P < 0.01$, ***$P < 0.001$, ****$P < 0.0001$).

References and Notes

1. K. Gardiner *et al.*, Down syndrome: from understanding the neurobiology to therapy. *The Journal of neuroscience : the official journal of the Society for Neuroscience* **30**, 14943-14945 (2010).
2. C. Rosenberg *et al.*, Array-CGH detection of micro rearrangements in mentally retarded individuals: clinical significance of imbalances present both in affected children and normal parents. *Journal of medical genetics* **43**, 180-186 (2006).
3. H. van Bokhoven, Genetic and epigenetic networks in intellectual disabilities. *Annual review of genetics* **45**, 81-104 (2011).
4. M. Dierssen, Down syndrome: the brain in trisomic mode. *Nature reviews. Neuroscience* **13**, 844-858 (2012).
5. A. Letourneau *et al.*, Domains of genome-wide gene expression dysregulation in Down's syndrome. *Nature* **508**, 345-350 (2014).
6. J. L. Olmos-Serrano *et al.*, Down Syndrome Developmental Brain Transcriptome Reveals Defective Oligodendrocyte Differentiation and Myelination. *Neuron* **89**, 1208-1222 (2016).
7. S. E. Antonarakis, Down syndrome and the complexity of genome dosage imbalance. *Nature reviews. Genetics* **18**, 147-163 (2017).
8. T. F. Haydar, R. H. Reeves, Trisomy 21 and early brain development. *Trends in neurosciences* **35**, 81-91 (2012).
9. H. P. Harding *et al.*, An integrated stress response regulates amino acid metabolism and resistance to oxidative stress. *Molecular cell* **11**, 619-633 (2003).
10. A. G. Hinnebusch, I. P. Ivanov, N. Sonenberg, Translational control by 5'-untranslated regions of eukaryotic mRNAs. *Science* **352**, 1413-1416 (2016).
11. R. H. Reeves *et al.*, A mouse model for Down syndrome exhibits learning and behaviour deficits. *Nature genetics* **11**, 177-184 (1995).
12. I. Das, R. H. Reeves, The use of mouse models to understand and improve cognitive deficits in Down syndrome. *Disease models & mechanisms* **4**, 596-606 (2011).
13. M. Inoue *et al.*, Autonomous trisomic rescue of Down syndrome cells. *Lab Invest* **99**, 885-897 (2019).
14. J. P. Weick *et al.*, Deficits in human trisomy 21 iPSCs and neurons. *Proceedings of the National Academy of Sciences of the United States of America* **110**, 9962-9967 (2013).
15. N. Sonenberg, A. G. Hinnebusch, Regulation of translation initiation in eukaryotes: mechanisms and biological targets. *Cell* **136**, 731-745 (2009).
16. H. Lavoie, J. J. Li, N. Thevakumaran, M. Therrien, F. Sicheri, Dimerization-induced allostery in protein kinase regulation. *Trends Biochem Sci* **39**, 475-486 (2014).
17. C. Lanzillotta *et al.*, Early and Selective Activation and Subsequent Alterations to the Unfolded Protein Response in Down Syndrome Mouse Models. *J Alzheimers Dis* **62**, 347-359 (2018).
18. S. Aivazidis *et al.*, The burden of trisomy 21 disrupts the proteostasis network in Down syndrome. *PloS one* **12**, e0176307 (2017).

19. F. Fernandez, C. C. Garner, Episodic-like memory in Ts65Dn, a mouse model of Down syndrome. *Behavioural brain research* **188**, 233-237 (2008).
20. A. C. Costa, J. J. Scott-McKean, M. R. Stasko, Acute injections of the NMDA receptor antagonist memantine rescue performance deficits of the Ts65Dn mouse model of Down syndrome on a fear conditioning test. *Neuropsychopharmacology : official publication of the American College of Neuropsychopharmacology* **33**, 1624-1632 (2008).
21. G. Deidda *et al.*, Reversing excitatory GABAAR signaling restores synaptic plasticity and memory in a mouse model of Down syndrome. *Nature medicine* **21**, 318-326 (2015).
22. P. J. Zhu *et al.*, Suppression of PKR promotes network excitability and enhanced cognition by interferon-gamma-mediated disinhibition. *Cell* **147**, 1384-1396 (2011).
23. S. D. Vann, M. M. Albasser, Hippocampus and neocortex: recognition and spatial memory. *Current opinion in neurobiology* **21**, 440-445 (2011).
24. F. Fernandez *et al.*, Pharmacotherapy for cognitive impairment in a mouse model of Down syndrome. *Nature neuroscience* **10**, 411-413 (2007).
25. G. Neves, S. F. Cooke, T. V. Bliss, Synaptic plasticity, memory and the hippocampus: a neural network approach to causality. *Nature reviews. Neuroscience* **9**, 65-75 (2008).
26. S. A. Buffington, W. Huang, M. Costa-Mattioli, Translational control in synaptic plasticity and cognitive dysfunction. *Annual review of neuroscience* **37**, 17-38 (2014).
27. C. Sidrauski *et al.*, Pharmacological brake-release of mRNA translation enhances cognitive memory. *eLife* **2**, e00498 (2013).
28. C. Sidrauski *et al.*, Pharmacological dimerization and activation of the exchange factor eIF2B antagonizes the integrated stress response. *eLife* **4**, (2015).
29. Y. Sekine *et al.*, Stress responses. Mutations in a translation initiation factor identify the target of a memory-enhancing compound. *Science* **348**, 1027-1030 (2015).
30. A. M. Kleschevnikov *et al.*, Hippocampal long-term potentiation suppressed by increased inhibition in the Ts65Dn mouse, a genetic model of Down syndrome. *The Journal of neuroscience : the official journal of the Society for Neuroscience* **24**, 8153-8160 (2004).
31. A. M. Kleschevnikov *et al.*, Increased efficiency of the GABAA and GABAB receptor-mediated neurotransmission in the Ts65Dn mouse model of Down syndrome. *Neurobiology of disease* **45**, 683-691 (2012).
32. E. R. Kandel, The molecular biology of memory storage: a dialogue between genes and synapses. *Science* **294**, 1030-1038 (2001).
33. M. Costa-Mattioli, W. S. Sossin, E. Klann, N. Sonenberg, Translational Control of Long-Lasting Synaptic Plasticity and Memory. *Neuron* **61**, 10-26 (2009).
34. W. S. Sossin, M. Costa-Mattioli, Translational Control in the Brain in Health and Disease. *Cold Spring Harbor perspectives in biology*, (2018).
35. B. Abdulkarim *et al.*, A Missense Mutation in PPP1R15B Causes a Syndrome Including Diabetes, Short Stature, and Microcephaly. *Diabetes* **64**, 3951-3962 (2015).

36. G. Borck *et al.*, eIF2gamma mutation that disrupts eIF2 complex integrity links intellectual disability to impaired translation initiation. *Molecular cell* **48**, 641-646 (2012).
37. K. D. Kernohan *et al.*, Homozygous mutation in the eukaryotic translation initiation factor 2alpha phosphatase gene, PPP1R15B, is associated with severe microcephaly, short stature and intellectual disability. *Human molecular genetics* **24**, 6293-6300 (2015).
38. C. L. Hunter, D. Bachman, A. C. Granholm, Minocycline prevents cholinergic loss in a mouse model of Down's syndrome. *Ann Neurol* **56**, 675-688 (2004).
39. Y. Choi *et al.*, Minocycline attenuates neuronal cell death and improves cognitive impairment in Alzheimer's disease models. *Neuropsychopharmacology : official publication of the American College of Neuropsychopharmacology* **32**, 2393-2404 (2007).
40. P. Bianchi *et al.*, Early pharmacotherapy restores neurogenesis and cognitive performance in the Ts65Dn mouse model for Down syndrome. *The Journal of neuroscience : the official journal of the Society for Neuroscience* **30**, 8769-8779 (2010).
41. R. H. Du *et al.*, Fluoxetine Inhibits NLRP3 Inflammasome Activation: Implication in Depression. *The international journal of neuropsychopharmacology / official scientific journal of the Collegium Internationale Neuropsychopharmacologicum* **19**, (2016).
42. I. Das *et al.*, Hedgehog agonist therapy corrects structural and cognitive deficits in a Down syndrome mouse model. *Science translational medicine* **5**, 201ra120 (2013).
43. M. Jimenez-Sanchez *et al.*, The Hedgehog signalling pathway regulates autophagy. *Nature communications* **3**, 1200 (2012).
44. A. Contestabile *et al.*, Lithium rescues synaptic plasticity and memory in Down syndrome mice. *The Journal of clinical investigation* **123**, 348-361 (2013).
45. S. Bertsch, C. H. Lang, T. C. Vary, Inhibition of glycogen synthase kinase 3[beta] activity with lithium in vitro attenuates sepsis-induced changes in muscle protein turnover. *Shock* **35**, 266-274 (2011).
46. E. Kida, A. Rabe, M. Walus, G. Albertini, A. A. Golabek, Long-term running alleviates some behavioral and molecular abnormalities in Down syndrome mouse model Ts65Dn. *Experimental neurology* **240**, 178-189 (2013).
47. J. Xia *et al.*, Treadmill exercise decreases beta-amyloid burden in APP/PS1 transgenic mice involving regulation of the unfolded protein response. *Neuroscience letters* **703**, 125-131 (2019).
48. M. Parrini *et al.*, Aerobic exercise and a BDNF-mimetic therapy rescue learning and memory in a mouse model of Down syndrome. *Scientific reports* **7**, 16825 (2017).
49. N. Takei, M. Kawamura, K. Hara, K. Yonezawa, H. Nawa, Brain-derived neurotrophic factor enhances neuronal translation by activating multiple initiation processes: comparison with the effects of insulin. *The Journal of biological chemistry* **276**, 42818-42825 (2001).

50. R. C. Chang, A. K. Wong, H. K. Ng, J. Hugon, Phosphorylation of eukaryotic initiation factor-2alpha (eIF2alpha) is associated with neuronal degeneration in Alzheimer's disease. *Neuroreport* **13**, 2429-2432 (2002).
51. A. Chou *et al.*, Inhibition of the integrated stress response reverses cognitive deficits after traumatic brain injury. *Proceedings of the National Academy of Sciences of the United States of America* **114**, E6420-E6426 (2017).
52. J. A. Moreno *et al.*, Sustained translational repression by eIF2alpha-P mediates prion neurodegeneration. *Nature* **485**, 507-511 (2012).
53. H. J. Kim *et al.*, Therapeutic modulation of eIF2alpha phosphorylation rescues TDP-43 toxicity in amyotrophic lateral sclerosis disease models. *Nature genetics* **46**, 152-160 (2014).
54. S. W. Way, B. Popko, Harnessing the integrated stress response for the treatment of multiple sclerosis. *Lancet Neurol* **15**, 434-443 (2016).
55. M. Costa-Mattioli *et al.*, eIF2alpha phosphorylation bidirectionally regulates the switch from short- to long-term synaptic plasticity and memory. *Cell* **129**, 195-206 (2007).
56. N. V. Jammi, L. R. Whitby, P. A. Beal, Small molecule inhibitors of the RNA-dependent protein kinase. *Biochem Biophys Res Commun* **308**, 50-57 (2003).
57. C. M. Oslowski, F. Urano, Measuring ER stress and the unfolded protein response using mammalian tissue culture system. *Methods in enzymology* **490**, 71-92 (2011).
58. N. Fusaki, H. Ban, A. Nishiyama, K. Saeki, M. Hasegawa, Efficient induction of transgene-free human pluripotent stem cells using a vector based on Sendai virus, an RNA virus that does not integrate into the host genome. *Proc Jpn Acad Ser B Phys Biol Sci* **85**, 348-362 (2009).
59. K. Takahashi, S. Yamanaka, Induction of pluripotent stem cells from mouse embryonic and adult fibroblast cultures by defined factors. *Cell* **126**, 663-676 (2006).
60. G. V. Di Prisco *et al.*, Translational control of mGluR-dependent long-term depression and object-place learning by eIF2alpha. *Nature neuroscience* **17**, 1073-1082 (2014).
61. A. M. Bolger, M. Lohse, B. Usadel, Trimmomatic: a flexible trimmer for Illumina sequence data. *Bioinformatics* **30**, 2114-2120 (2014).
62. D. Kim, B. Langmead, S. L. Salzberg, HISAT: a fast spliced aligner with low memory requirements. *Nature methods* **12**, 357-360 (2015).
63. L. Wang, S. Wang, W. Li, RSeQC: quality control of RNA-seq experiments. *Bioinformatics* **28**, 2184-2185 (2012).
64. W. J. Kent *et al.*, The human genome browser at UCSC. *Genome Res* **12**, 996-1006 (2002).
65. C. Trapnell *et al.*, Differential gene and transcript expression analysis of RNA-seq experiments with TopHat and Cufflinks. *Nature protocols* **7**, 562-578 (2012).
66. W. Huang da, B. T. Sherman, R. A. Lempicki, Bioinformatics enrichment tools: paths toward the comprehensive functional analysis of large gene lists. *Nucleic acids research* **37**, 1-13 (2009).
67. E. K. Schmidt, G. Clavarino, M. Ceppi, P. Pierre, SUnSET, a nonradioactive method to monitor protein synthesis. *Nature methods* **6**, 275-277 (2009).

68. W. Huang *et al.*, mTORC2 controls actin polymerization required for consolidation of long-term memory. *Nature neuroscience* **16**, 441-448 (2013).

Acknowledgments

We thank Marina Grasso and Christine Genero for administrative support, Hongyi Zhou for technical support, Andon Placzek and members of Costa-Mattioli laboratory for comments on the manuscript. We also thank Ping Zhang and Anel LaGrone of the Human Stem Cell Core at Baylor College of Medicine for their technical support. Human tissue was obtained from the NIH Neurobiobank at University of Maryland, Baltimore, MD. **Funding:** This work was supported by funding from the NIH (R01 NS076708) and the generous support from Sammons Enterprises to M.C.M and NIH (R01HG007538, R01CA193466 and R01 CA228140) to W. L. P.W. is an Investigator of the Howard Hughes Medical Institute.

Author contributions: Conceptualization and design; P.J.Z., S.K., P.W., and M.C.-M. Acquisition of data; P.J.Z., S.K., Y.C., L.C.R, S.W.D., J.J.K and W.L. Writing (Reviewing and Editing); P.J.Z., S.K., P.W., M.C.-M.

Competing Interest: The authors declare no competing interest. P.W. is an inventor on U.S. Patent 9708247 held by the Regents of the University of California that describes ISRIB and its analogs. Rights to the invention have been licensed by UCSF to Calico. W. L. is a consultant for the Chosen Med.

Data and material availability: All data needed to evaluate the conclusions in the paper are present in the paper and/or the supplementary materials, and the RNA-sequencing data were deposited in public data databases. Accession number of the RNAseq data is NCBI GEO: GSE138371.

Supplementary Material for

Activation of the ISR mediates the behavioral and neurophysiological abnormalities in Down syndrome

Ping Jun Zhu, Sanjeev Khatiwada, Ya Cui, Lucas C. Reineke, Sean W. Dooling, Jean J. Kim, Wei Li, Peter Walter*, Mauro Costa-Mattioli*

*Corresponding authors: Mauro Costa-Mattioli (costamat@bcm.edu), Peter Walter (peter@walterlab.ucsf.edu)

This PDF includes

Material and Methods

Mouse husbandry. All experiments were conducted on 3-5 months old animals. Ts65Dn mice were purchased from Jackson laboratory. *Pkr*$^{-/-}$ mice (*22*) and *Eif2s1*$^{S/A}$ mice (*55*) have been previously described. Double mutant mice were generated by crossing Ts65Dn mice to either *Pkr*$^{-/-}$ mice or *Eif2s1*$^{S/A}$ mice. It is not possible to obtain Ts65Dn mice in a pure genetic background because repeated backcrossing of the Ts65Dn chromosome onto an inbreed genetic background for several generations fails to recover trisomic progeny. Thus, investigators in the field are required to use the Ts65Dn mice in a hybrid background. We used littermate controls for our experiments. Briefly, to generate Ts65Dn-*Pkr*$^{-/-}$ mice, we first crossed Ts65Dn female (B6EiC3H) with *Pkr*$^{-/-}$ males (129Svev). The resulting F1 Ts65Dn-*Pkr*$^{+/-}$ females were crossed with *Pkr*$^{+/-}$ males. Finally, we compared side-by-side Ts65Dn mice withTs65Dn-*Pkr*$^{-/-}$ mice from the same F2 litter. Thus, littermate controls have the same hybrid background as our experimental mice (Ts65Dn mice). Similarly, when we crossed Ts65Dn females (B6EiC3H) with *Eif2*$^{S/A}$ males (C57Bl6), we compared Ts65Dn-*Eif2s1*$^{S/S}$ with Ts65Dn-*Eif2s1*$^{S/A}$ littermate controls. Ts65Dn mice were genotyped as recommended by Jackson laboratory. PKRi (*56*) was freshly dissolved in saline and Ts65Dn mice and WT littermates were administered either PKRi (0.1 mg/kg) or vehicle (0.02 % DMSO) intraperitoneal (i.p.) for 6 days, as we previously described (*22*). Ts65Dn mice were injected with ISRIB (2.5 mg/kg) or vehicle once every two days for a week, as previously described (*27*). Mice were weaned at the third postnatal week, genotyped and kept on a 12h / 12h light/dark cycle (lights on at 7:00 am) and had access to food and water *ad libitum.* Animal care and

experimental procedures were approved by the institutional animal care and use committee (IACUC) at Baylor College of Medicine, according to NIH Guidelines.

Electrophysiology. Electrophysiological recordings were performed as previously described (*22*). Field recording were performed from CA1 horizontal hippocampal slices (320 μm thick), which were cut from the brain of adult mice (3-6 months old) with a vibratome (Leica VT 1000S, Leica Microsystems, Buffalo Grove, IL) at 4°C in artificial cerebrospinal fluid solution (ACSF; 95% O_2 and 5% CO_2) containing in mM: 124 NaCl, 2.0 KCl, 1.3 $MgSO_4$, 2.5 $CaCl_2$, 1.2 KH_2PO_4, 25 $NaHCO_3$, and 10 glucose (2-3 ml/min). Slices were incubated for at least 60 min prior to recording in an interface chamber and continuously perfused with artificial cerebrospinal fluid (ACSF) at 28 - 29°C at a flow rate of 2 - 3 ml/min. The recording electrodes were placed in the stratum radiatum. Field excitatory postsynaptic potentials (fEPSPs) were recorded with ACSF-filled micropipettes and were elicited by bipolar stimulating electrodes placed in the CA1 stratum radiatum to excite Schaffer collateral and commissural fibers. The intensity of the 0.1-ms pulses was adjusted to evoke 30 - 35% of maximal response. A stable baseline of responses at 0.033 Hz was established for at least 30 min. L-LTP was induced by applying four tetanic trains of high-frequency stimulation (100 Hz, 1 s) separated by 5-min intervals.

Whole-cell recordings were performed using a MultiClamp 700B amplifier (Molecular Devices, Union City, CA) in a submerged chamber (2 - 3 ml/min) at 31 - 32°C using conventional patch-clamp techniques. CA1 neurons were visually identified by infrared differential interference contrast video microscopy on the stage of an upright microscope (Axioskope FS2, Carl Zeiss, Oberkochen, Germany). Patch pipettes

(resistances 2 - 5 MΩ) were filled with (in mM): 140 CsCl, 10 HEPES, 10 Na_2-phosphocreatine, 0.2 BAPTA, 2 Mg_3-ATP, 0.2 Na_3-GTP; pH was adjusted to 7.2 and osmolarity to 295~300 mOsm using a Wescor 5500 vapor pressure osmometer (Wescor, Logan, UT). Miniature inhibitory postsynaptic currents (mIPSCs) were recorded at -60 mV in the presence of NBQX (5 μM, 2,3-dihydroxy-6-nitro-7-sulfamoyl-benzo[f]quinoxaline disodium salt), AP5 (25 μM, DL-2-Amino-5-phosphonopentanoic acid) and TTX (1 μM, tetrodotoxin). For recording excitatory currents, CsCl was replaced with 130 mM K-gluconate and 10 mM KCl. Excitatory postsynaptic currents (EPSCs) were recorded at -70 mV in the presence of 100 μM picrotoxin. All drugs were obtained from Tocris (Ellisville, MO).

Western Blotting. Hippocampus and cortex from mice were isolated, homogenized in cold homogenizing buffer [200 mM HEPES, 50 mM NaCl, 10% Glycerol, 1% Triton X-100, 1 mM EDTA, 50 mM NaF, 2 mM Na_3VO_4, 25 mM β-glycerophosphate, and EDTA-free complete ULTRA tablets (Roche, Indianapolis, IN)], and centrifuged at 14,000 *rpm* for 15 min at 4° C. Human tissue was obtained from University of Maryland Brain and Tissue Bank, a brain and tissue repository of the NIH Neurobiobank. Post-mortem human brain samples from Down syndrome patients and those from age- and sex-matched unaffected controls (see Supplementary Table I) were homogenized as described above. The supernatants (30 μg of protein/sample) were resolved on SDS–PAGE (15%) and transferred onto nitrocellulose membranes (Pall, Port Washington, NY). Antibodies against p-eIF2α (catalog # 3398, 1:1000), total eIF2α (catalog # 9722, 1:1000), total PERK (catalog # 3192, 1:1000), p-4E-BP1 (catalog # 9459, 1:1000), total 4E-BP1

(catalog # 9452, 1:1000), p-S6 (catalog # 4856, 1:1000), total S6 (catalog # 2217, 1:1000), p-eIF4E (catalog # 9741, 1:1000), GAPDH (catalog # 2118, 1:5000) were purchased from Cell Signaling Technology (Danvers, MA), β-actin (1:5000) from Novus Biologicals (Centennial, CO), p-PKR (catalog # ab32036, 1:500), p-GCN2 (catalog # ab75836, 1:1000), and total-GCN2 (catalog # ab137543, 1:1000) from Abcam (Cambridge, MA), total-PKR (catalog # 18244-1-AP, 1:1000) from Proteintech (Rosemont, IL), p-PERK (catalog # 649401, 1:1000) from Biolegend (San Diego, CA), ATF6 (catalog # 24169, 1:2000) from Proteintech, and total-eIF4E (catalog # 610269, 1:1000) from BD Transduction Laboratories.

Measuring Ire1 activity by RT-PCR and qPCR. For RT-PCR, RNA was isolated from the hippocampus from WT and Ts65Dn mice and reverse transcribed with the VILO superscript kit (Thermo Fisher Scientific). cDNA for *XBP1* was then amplified with specific primers (Fw: AAACAGAGTAGCAGCGCAGACTGC and Rev: TCCTTCTGGGTAGACCT CTGGGAG). The PCR products were digested with the Pst1 restriction enzyme (New England Biolabs) and the products were subjected to agarose gel electrophoresis. For qPCR, PowerUp SYBR green master mix was used on a step-one plus qPCR machine (Applied Biosystems) using cDNA prepared as described above. Primers specific for spliced (Fw: CTGAGTCCGAATCAGGTGCAG and Rev: GTCCATGGGAAGATGTTCTG G) and unspliced *XBP1* (CAGCACTCAGACTATGTGCA and Rev: GTCCATGGGAAGAT GTTCTGG) were previously described (*57*).

Generation of Down Syndrome (DS) iPS cells. To determine whether the ISR response was activated in cells from DS patients, we reprogramed Detroit 532 foreskin fibroblasts (ATCC® CCL-54™, Lot # 58237511) by infecting them with a non-integrating Sendai viruses (*58*) expressing OCT4, SOX2, KLF4, and C-MYC (*59*) (Thermo Fisher Scientific, CytoTune™-iPS 2.0 Sendai Reprogramming Kit) using manufacturer's recommendations. Clonal human induced pluripotent cell (hiPSC) colonies were manually picked and expanded under feeder-free conditions using hESC-qualified Matrigel (Corning) and TeSR-E8 medium (STEMCELL Technologies). The cell line was designated as HSCC-046iPS-S and abbreviated as "DS" followed by the clone number. As expected, a clonal line (DSc1) was shown to have a trisomy 21 male karyotype by G-banding at Passage 9 (Fig. S1A). Surprisingly, a second clonal line (DSc2) was found to have a normal male karyotype (Fig. S1B), which was used as an "isogenic control". The authenticity of the euploid (DSc2) clone was confirmed by short-tandem repeats (STRs) profile using the ATCC's STR Profiling Cell Authentication Service. Briefly, the euploid DSc2 iPSCs clone, which was discovered serendipitously, perfectly matched the original CCL-54™ line (Figure S1C) and was the perfect isogenic control for our experimental DSc1 line. iPSCs were cultured on Matrigel® hESC-Qualified Matrix (Corning) and in mTeSR™1 medium (Stemcell Technologies) and passaged using ReLeSR™ (Stemcell Technologies) every 4 - 5 days with daily medium changes.

Novel Object Recognition. The experimenters were blind to the genotype for all of the behavioral experiments. For object recognition, mice were handled for 5 days (5-10 min for each day) and then habituated to a black Plexiglas rectangular chamber (31 x 24 cm,

height 27 cm) for 10 min under dim ambient light for 5 days. Two identical objects were presented to mice to explore for 5 min, after which, mice were returned to the home cage. Twenty-four hours later, one object was replaced by one novel object and the mouse was again placed in the chamber 5 min. The novel object has the same height and volume but different shape and appearance. Exploration of the objects was defined as sniffing of the objects (with nose contact or head directed to the object) within at 2 cm radius of the objects. Sitting or standing on the objects was not scored as exploration. Behavior was recorded from cameras positioned above the training chamber. Discrimination Index (DI) was computed as DI = (Novel Object Exploration Time – Familiar Object Exploration Time/Total Exploration Time) X 100. To control for odor cues, the open field arena and the objects were thoroughly cleaned with ethanol, dried, and ventilated between mice.

Contextual fear conditioning. Experiments were performed as previously described (*55*), with some modifications. Briefly, mice were first handled for 5 min per day for 5 days and then habituated to the conditioning chamber for 20 min for another 2 days. On the training day, mice were placed in the conditioning chamber for 2 min (naïve) and then received two-foot shocks (0.75 mA, 2 sec, 90 sec apart), after which the mice remained in the chamber for an additional minute before being returned to their home cages. Twenty-four hours later, mice were re-exposed to the same context (training chamber) for 5 min and "freezing" (immobility with the exception of respiration) responses were recorded using real-time video and analyzed by FreezeView. The fear condition training was always the last behavioral test performed.

T-maze spontaneous alternation task. The apparatus was a black wooden T-maze with 25 cm high walls and each arm was 30 cm long and 9 cm wide. A removable central partition was used during the sample phase but not the test phase of each trial. Guillotine doors were positioned at the entrance to each goal arm. At the beginning of the sample phase, both doors were raised, and the mouse was placed at the end of the start arm facing away from the goal arms. Each mouse was allowed to make a free choice between the two goal arms; after its tail had cleared the door of the chosen arm, the door was closed, and the mouse was allowed to explore the arm for 30 sec. The mouse was then returned to the end of the start arm, with the central partition removed and both guillotine doors raised, signaling the beginning of the test phase. This sequence (trial) was repeated 20 times. Trials that were not completed within 120 seconds were terminated and disregarded during analysis. Correct alteration between trails was expressed as % alteration = (number of correct alteration) / 20 x 100%

Polysome profiling and RNA isolation. Polysome profiling followed by RNA sequencing was carried out as we previously described (*60*), with some modifications. Briefly, we prepared fresh 12 ml of 10 – 50% sucrose density gradients [10 mM HEPES-KOH (pH 7.6), 5 mM $MgCl_2$, 150 mM KCl, 200 U/ml RNasin Rnase inhibitor (Promega, Madison, WI)]. Gradients were kept at 4^o C for at least 2 h before use. Mouse brain tissue was dissected in a cutting solution [1X HBSS, 2.5 mM HEPES-KOH (pH 7.6), 35 mM glucose, 4 mM $NaHCO_3$, 100 μg/ml cycloheximide (Sigma-Aldrich, St. Louis, MO)] and washed in ice-cold PBS containing 100 μg/ml cycloheximide by centrifugation at 3000 rpm for 10 min at 4^{o}C. The tissue was then lysed in polysome lysis buffer [10 mM HEPES-KOH (pH

7.4), 5 mM $MgCl_2$, 150 mM KCl, 0.5 mM DTT, 100 U/ml RNasin Rnase inhibitor (Promega, Madison, WI), 100 μg/ml cycloheximide, and EDTA-free protease inhibitors (Roche Indianapolis, IN)] and centrifuged at 2000 x g for 10 min at 4°C. The supernatant was then transferred to a pre-chilled tube, supplemented with 0.5% NP-40, and kept on ice for 10 min. Samples were centrifuged at 14,000 rpm for 10 min at 4°C. The supernatant was either layered onto sucrose gradient or reserved for total RNA isolation. Gradients were centrifuged in a SW-40Ti rotor at 35,000 rpm at 4° C for 2 h and then analyzed by piercing the tube with a Brandel tube piercer, passing 70% sucrose through the bottom of the tube and monitoring the absorbance of the material eluting from the tube using an ISCO UA-6 UV detector. Fractions were collected throughout and RNA was extracted with TRIzol following manufacturer's instructions (Life Technologies, Carlsbad, CA).

Experiments were performed in three biological replicates for each group. Polysomal (light and heavy) mRNA was isolated from WT, Ts65Dn, and Ts65Dn-*Pkr*$^{-/-}$ mice. To identify the mRNAs translationally dysregulated in the brain of Ts65Dn mice compared to WT mice, we focused on mRNAs with no significant change in total mRNA levels, but either increased or decreased in their association with polysomes (> 1.5 fold) by comparing the ratio between the translational RNAseq (light and heavy polysmes) and transcriptional RNAseq (total RNA).

RNA-Seq and data analysis. RNA-seq library was generated using RNA isolated from polysomal fractions (light and heavy) and total RNA using the KAPA RNA HyperPrep Kits with RiboErase protocol for Total RNASeq. The library was then sequenced using Illumina NS500 Single-End 75bp (SE75), which generated 20-35 million reads per sample. For

analysis of RNA-seq data, we removed adapters and low-quality bases by Trimmomatic (v0.38) (*61*) using default parameters. We then aligned clean reads to the mm10 mouse reference genome by HISAT2(v2.1.0) (*62*) and converted these aligned bam files into bigwig format using RSeQC (v2.6.5) (*63*) and wigToBigWig from UCSC (*64*). Cufflinks (v2.2.1) (*65*) was used to assess differentially expressed genes (DEGs) (GENCODE vM18 as the genes reference annotation file) between groups [*q* (*p*-value corrected for false discovery rate, FDR) < 0.05 and fold change > 1.5). Default thresholds of Cufflinks were used to identify DEGs. In order to improve the robustness of transcript abundance estimates, we also used "-M" parameter of Cufflinks to mask rRNA regions (build mm10) retrieved from UCSC Table Browser. Only protein-coding genes (defined in GENCODE vM18 GTF file) whose significant differential expression status were labeled "yes" by Cufflinks were used in subsequent analyses. DEGs in light and heavy polysomes are combined and expressed as DEGs at the translational level. Because of low sequence depth, one of the heavy-polysome replicates in the Ts65Dn-*Pkr*$^{-/-}$ group was excluded from the analysis. For DEGs identified only in light or heavy polysomes, we used the expression values (RPKM) from the corresponding group (Fig. 3E). However, for genes that were found expressed in both light and heavy polysomes, we only used the RPKM value from the light polysomes to avoid combining different RPKM values. KEGG pathway enrichment analysis for genes down-regulated at only the translational level in Ts65Dn mice compared to WT was performed on the DAVID 6.8 website (*66*). In order to obtain the gene expression value matrix for all samples (including the low sequence depth), we used two R packages, Rsubread and edgeR, to count the reads number and convert the count number to RPKM value. Multi-mapping reads were also counted. A multi-mapping

read will carry a count of 1/x, instead of 1, where x is the total number of alignments reported for the same read. We then used package pheatmap of R to generate the heatmap based on this RPKM matrix.

Surface Sensing of Translation (SUnSET). Protein synthesis was measured using SUnSET, a non-radioactive labeling method to monitor protein synthesis, as previously described (*67*). Briefly, hippocampal slices were cut (300 μm) with a McIlwain Tissue Chopper (Mickle, UK) and incubated for 1 hour at room temperature in oxygenated (95% O_2, 5% CO_2) ACSF followed by incubation at 32°C for 1 hour in oxygenated (95% O_2, 5% CO_2) ACSF prior to treatment as we previously described (*68*). Puromycin (10 μg/μl, dissolved in oxygenated ACSF) was bath applied to the slices for 20 min followed by a wash with untreated oxygenated ACSF. The slices were then snap-frozen on dry ice and stored at -80 C until use. Frozen slices were lysed in homogenization buffer (in mM: 40 Tris HCl, pH 8.0, 150 NaCl, 25 β-glycerophosphate, 50 NaF, 2 Na_3VO_3, 1X protease inhibitor cocktail, 10% glycerol, 1% Triton X-100). Puromycin incorporation was detected by Western blot using the 12D10 antibody to puromycin (Catalog # MABE343, 1:5000, EMD Millipore Corp, Darmstadt, Germany) as we previously described (*60*). The density of the resulting bands was quantified using ImageJ and statistical significance assessed by Student's *t*-test.

Statistical analyses. Data are presented as means ± SEM. Statistics were based on two-tailed Student's *t*-test or Mann-Whitney Rank Sum test for two-group comparisons. One-way ANOVA followed by Bonferroni *post hoc* analysis was performed for multiple

comparisons, unless otherwise indicated. $P < 0.05$ was considered significant (*$P < 0.05$, **$P < 0.01$, ***$P < 0.001$, ****$P < 0.0001$).

A

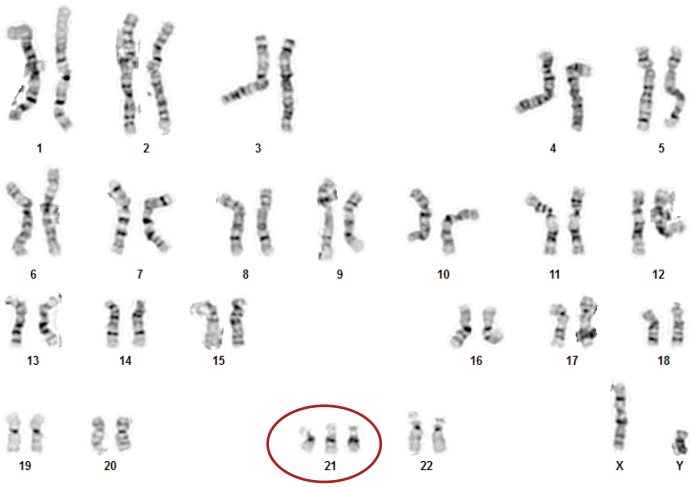

B

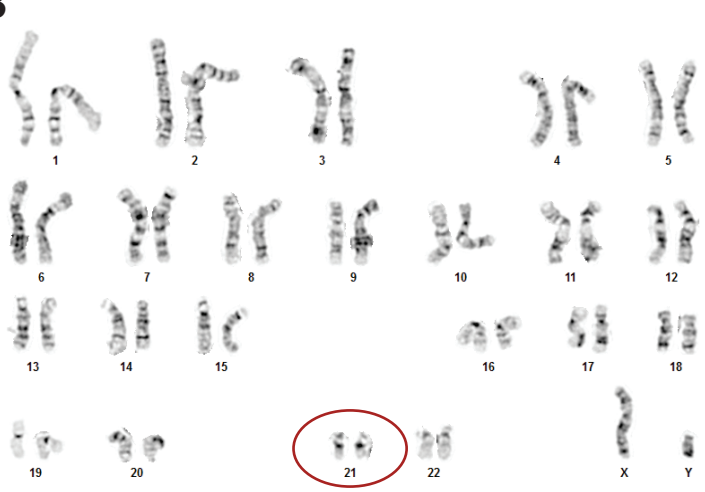

C

D3S1358	17	18						
TH01	7	9			7	9		
D21S11	30	31.2						
D18S51	12	13						
Penta_E	13	16						
D5S818	9	12			9	12		
D13S317	11	13			11	13		
D7S820	8				8			
D16S539	10	13			10	13		
CSF1PO	12				12			
Penta_D	8	9						
Amelogenin	X	Y			X	Y		
vWA	16	18			16	18		
D8S1179	12							
TPOX	8				8			
FGA	20	24						
D19S433	13	14						
D2S1338	22	25						
Number of shared alleles between query sample and database profile:								15
Total number of alleles in the database profile:								15
Percent match between the submitted sample and the database profile:								100

Fig. S1. Zhu et al.

Fig. S1. Identification of a CH21-trisomic iPSC clone and its isogenic control.

(**A-B**) Karyotype analysis shows that the DS iPSC clone was trisomic (**A**) and the isogenic control (**B**), from the same individual with DS, was euploid. (**C**) The authenticity of the euploid isogenic clone was confirmed by short-tandem repeats (STRs) profiling, which found 100% match to the original DS fibroblast CCL-54^{TM} line.

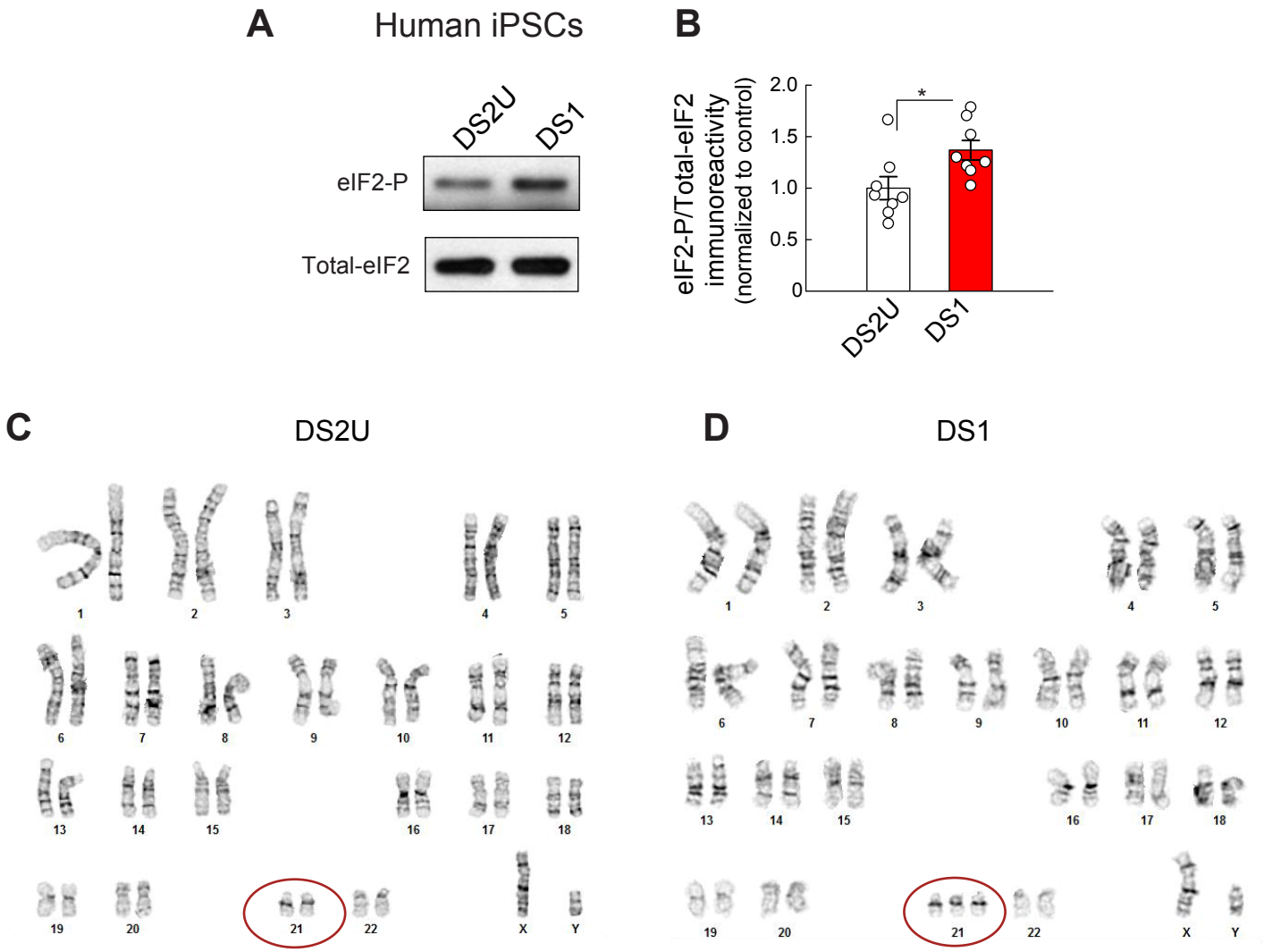

Fig. S2. Zhu et al.

Fig. S2. The ISR is activated in human iPSCs from an individual with a mosaic trisomy 21. Representative Western blot (**A**) and quantification (**B**) of eIF2-P levels in the CH21-trisomic iPSC line (DS1) and its respective isogenic control (DS2U). Both lines were previously reported (Weick et al. *PNAS*, 2013) and were derived from the same individual with mosaic DS. (**C-D**) Karyotype analysis shows that the DS1 iPSC line was CH21-trisomic (**D**) and the isogenic control iPSC line DS2U (**C**) from the same individual with DS, was euploid. Experiment was replicated in 8-wells per genotype (n = 8 per group, t_{14} = 0.59, $P < 0.05$). Data are mean ± s.e.m. *$P < 0.05$.

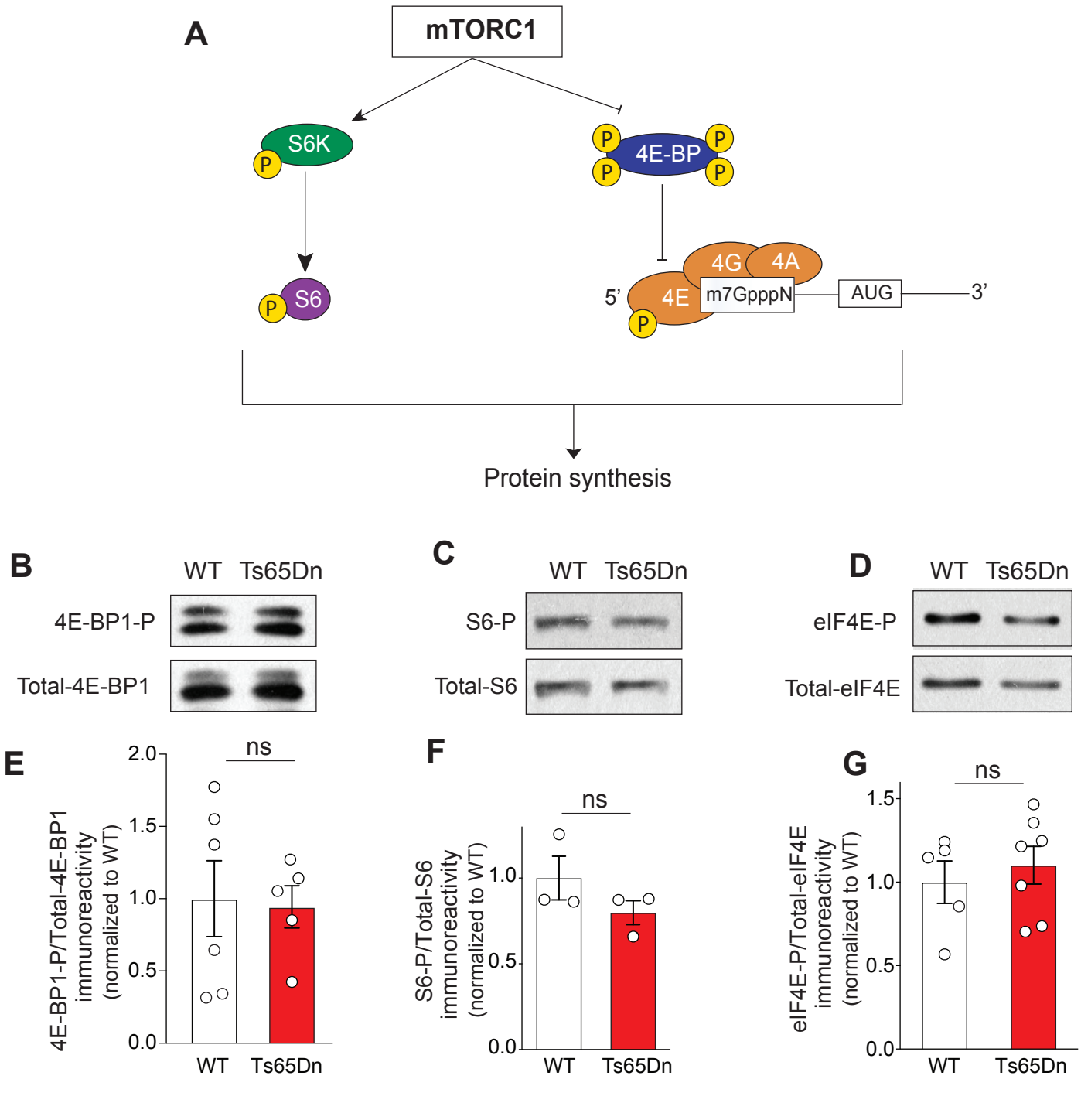

Fig. S3. Zhu et al.

Fig. S3. mTORC1 and eIF4E activity are not altered in the hippocampus of Ts65Dn mice. (**A**) Schematic of mTORC1-mediated translation signaling pathway. (**B-G**) Representative Western blots and quantification of 4E-BP1-P (**B**, **E**; n = 5-6 per group, t_9=0.18, P = 0.86), S6-P (**C**, **F**; n = 3 per group t_4 = 1.39, P = 0.24) and eIF4E-P (**D**, n = 5-7 per group, t_{10} = 0.59, P = 0.57) levels in the hippocampus of WT and Ts65Dn mice. Data are mean ± s.e.m.

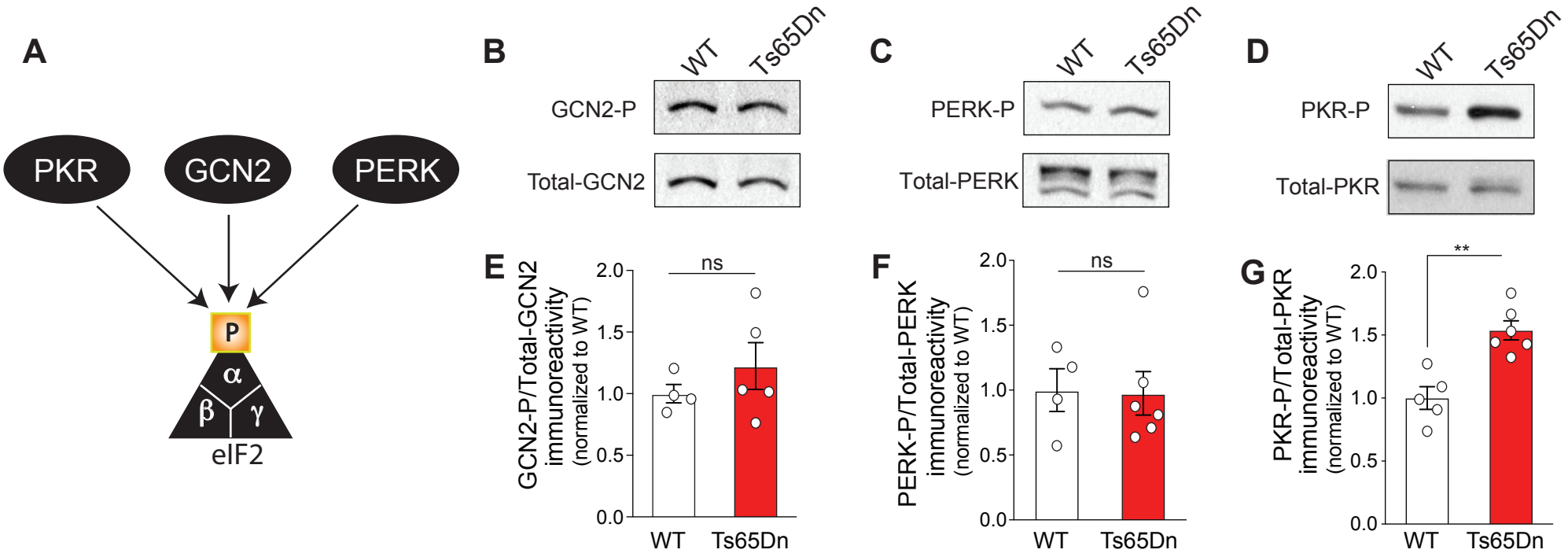

Fig. S4. Zhu et al.

Fig. S4. The PKR branch of the ISR is activated in the hippocampus of Ts65Dn mice. (**A**) Schematic of a simplified ISR signaling pathway. Representative Western blots and quantification of GCN2-P (**B**, **E**; n = 4-5 per group, t_7 = 1.00, P = 0.35), PERK-P (**C**, **F**; n = 4-6 per group, t_8 = 0.10, P = 0.92) and PKR-P (**D**, **G**; n = 5-6 per group, t_9 = 4.62) levels in the hippocampus of WT and Ts65Dn mice. Data are mean ± s.e.m. $^{**}P < 0.01$.

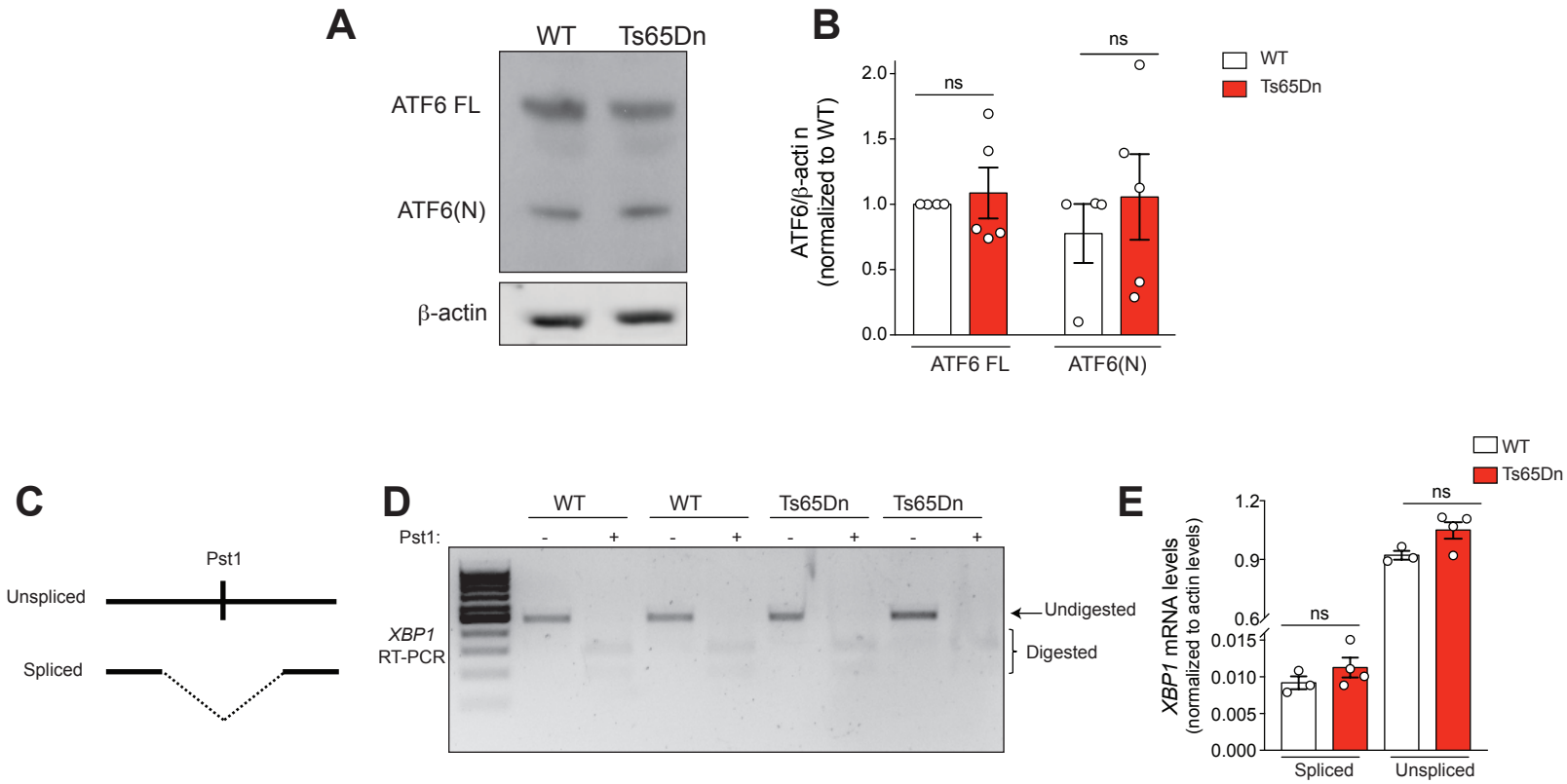

Fig. S5. Zhu et al.

Fig. S5. The Ire-1 and ATF6 branches of the UPR are not altered in the hippocampus of Ts65Dn mice. (**A-B**) Representative Western blots (**A**) and quantification (**B**) of full length (ATF6 FL) and cleaved ATF6 (ATF6(N) [n = 4-5 per group, t= 0.26, P > 0.999 for ATF6 FL and t = 0.83, P > 0.999 for ATF6(N)] levels in the hippocampus of WT and Ts65Dn mice. (**C**) Schematic representation of *XBP1* splicing assay. RT-PCR was performed to amplify the region of *XBP1* mRNA containing the IRE1 splice site. When the UPR is inactive and *XBP1* mRNA is not spliced, a Pst1 restriction enzyme site is present in the RT-PCR product. When the UPR is active, the Pst1 site is spliced out. (**D**) RT-PCR was performed on mRNA extracted from WT and Ts65Dn hippocampus. An aliquot of the PCR products was digested with Pst1 and run alongside the undigested PCR products. (**E**) RT-qPCR was performed on RNA extracted from WT and Ts65Dn mice with primers that specifically recognize spliced vs. unspliced *XBP1* mRNA (n = 3-4 per group, t = 0.05, P > 0.999 for spliced and t = 3.26, P = 0.057 for unspliced; Two-way ANOVA). Data are mean ± s.e.m.

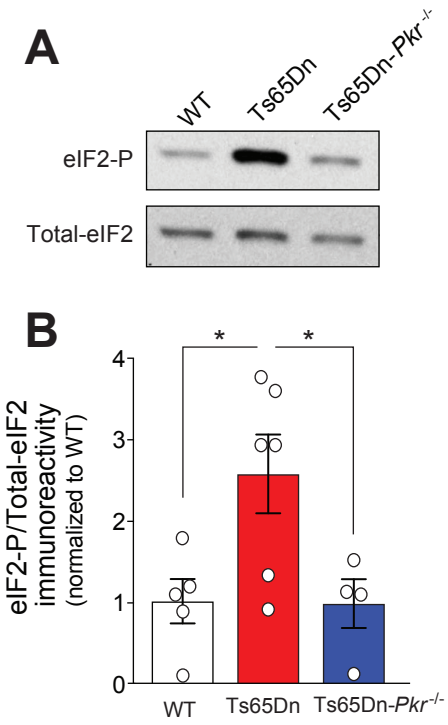

Fig. S6. Zhu et al.

Fig. S6. Genetic inhibition of the PKR branch of the ISR reduces eIF2-P levels in the cortex of Ts65Dn mice. Representative Western blots (**A**) and quantification (**B**) of eIF2-P levels in cortex from WT (n = 5), Ts65Dn (n = 6), and Ts65Dn-*Pkr*$^{-/-}$ mice (n = 4) ($F_{2,12}$ = 5.60). Data are mean ± s.e.m. *P < 0.05.

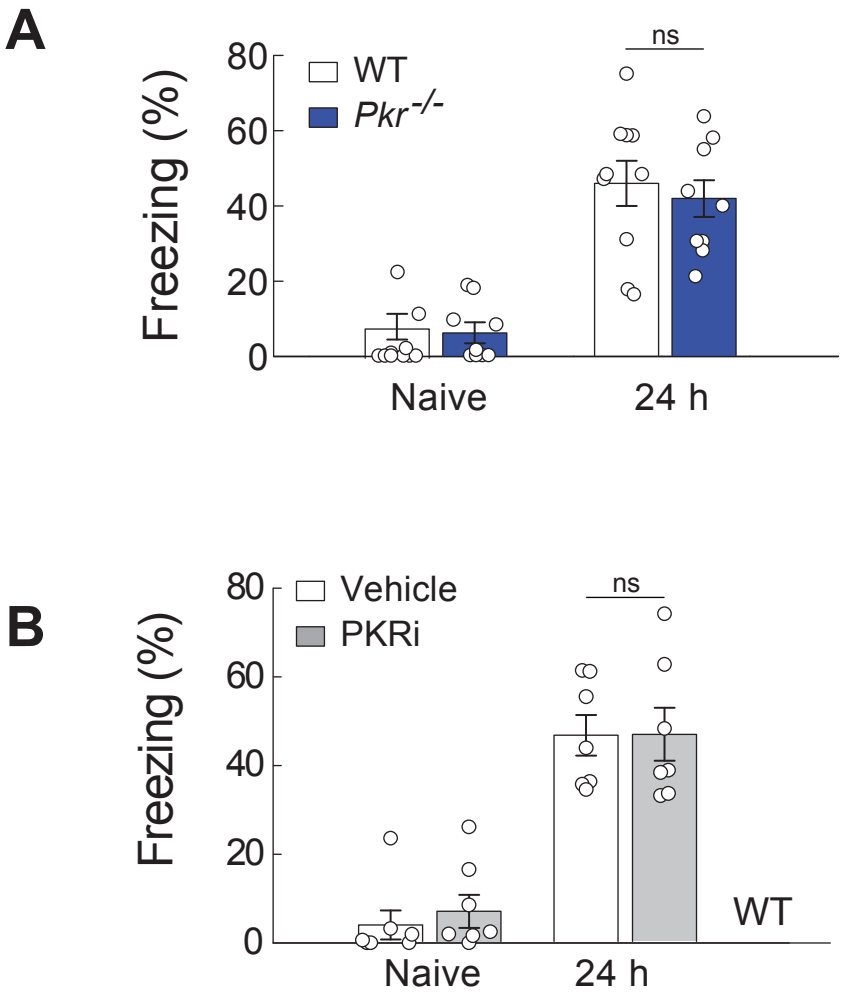

Fig. S7. Zhu et al.

Fig. S7. Genetic or pharmacological inhibition of PKR has no effect on long-term memory in WT mice. (**A-B**) Freezing behavior before training (naïve) and 24 hours after training in WT, *Pkr*$^{-/-}$ mice (**A**, n = 9-10 per group, t_{17} = 0.61, P = 0.552), and vehicle-treated and PKRi-treated WT mice (**B**, n = 7 per group, t_{12} = 0.52, P = 1.00). Mice were trained using a conventional training protocol (two foot-shocks at 0.7 mA for 2 sec). Data are mean ± s.e.m.

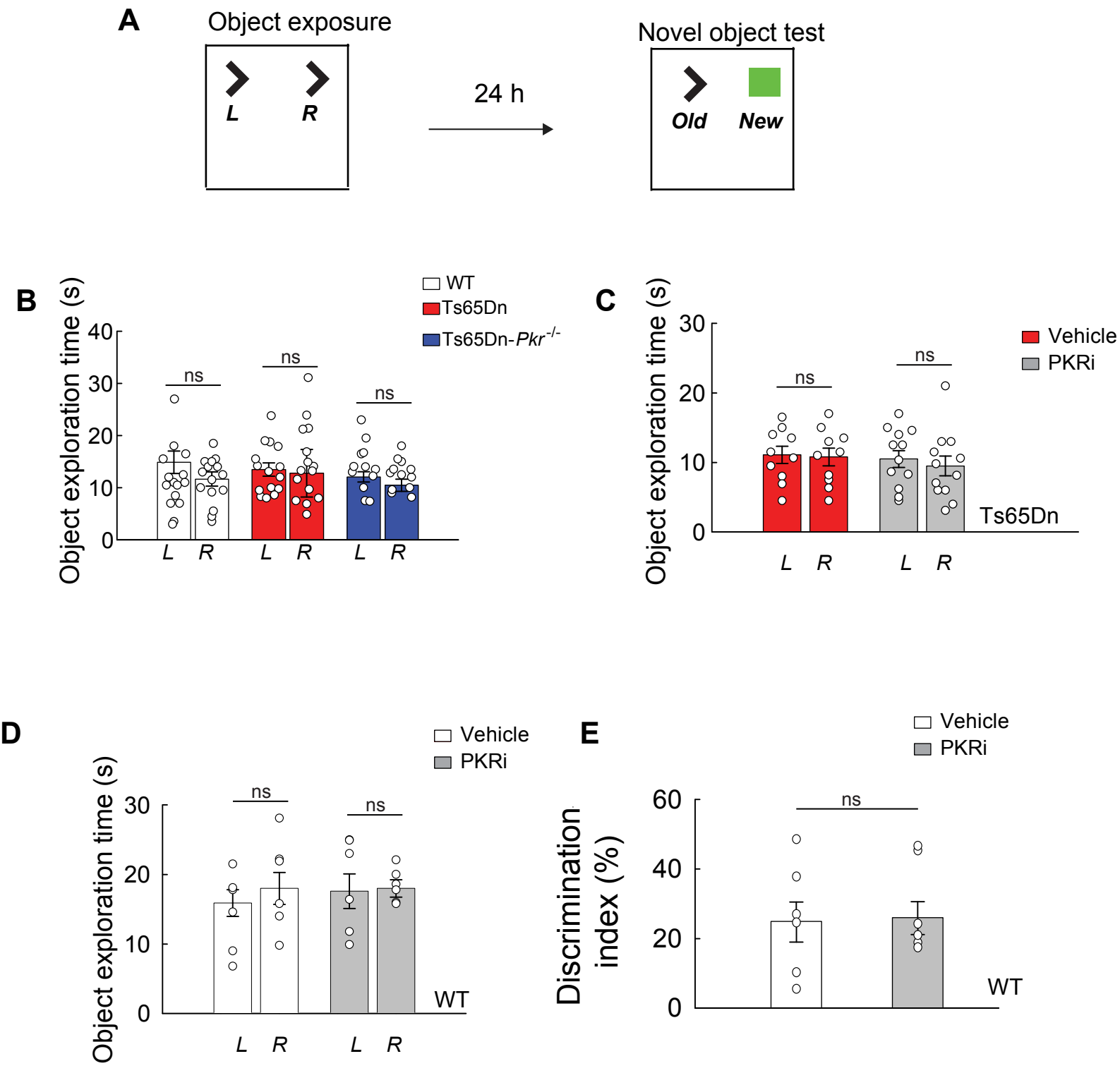

Fig. S8. Zhu et al.

Fig. S8. Neither genetic nor pharmacological inhibition of PKR affects object exploration time in Ts65Dn mice and PKRi has no effect on long-term object recognition memory in WT mice. (**A**) Schematic of the novel object recognition paradigm. (**B**) Time exploring the identical right (R) and left (L) objects: WT (n = 15, t_{28} = 0.06, P = 0.94), Ts65Dn (n = 15, t_{28} = 0.47, P = 0.64) and Ts65Dn-*Pkr*$^{-/-}$ mice (n = 12, t_{22} = 0.94, P = 0.36). (**C**) Time exploring the identical right (R) and left (L) objects: vehicle-treated (n = 10, t_{18}= 0.14, P = 0.88) and PKRi-treated Ts65Dn mice (n = 12, t_{22} = 0.68, P = 0.49). (**D**) Time exploring the identical right (R) and left (L) objects: vehicle-treated (n = 6, t_{10} = 1.12, P = 0.28) and PKRi-treated WT mice (n = 6, t_{10} = 41.0, P = 0.81, Mann-Whitney U test). (**E**) Novel object discrimination index 24 hours post-training in vehicle-treated (n = 6) and PKRi-treated WT mice (n = 6, t_{10} = 0.46, P = 0.65). Data are mean ± s.e.m.

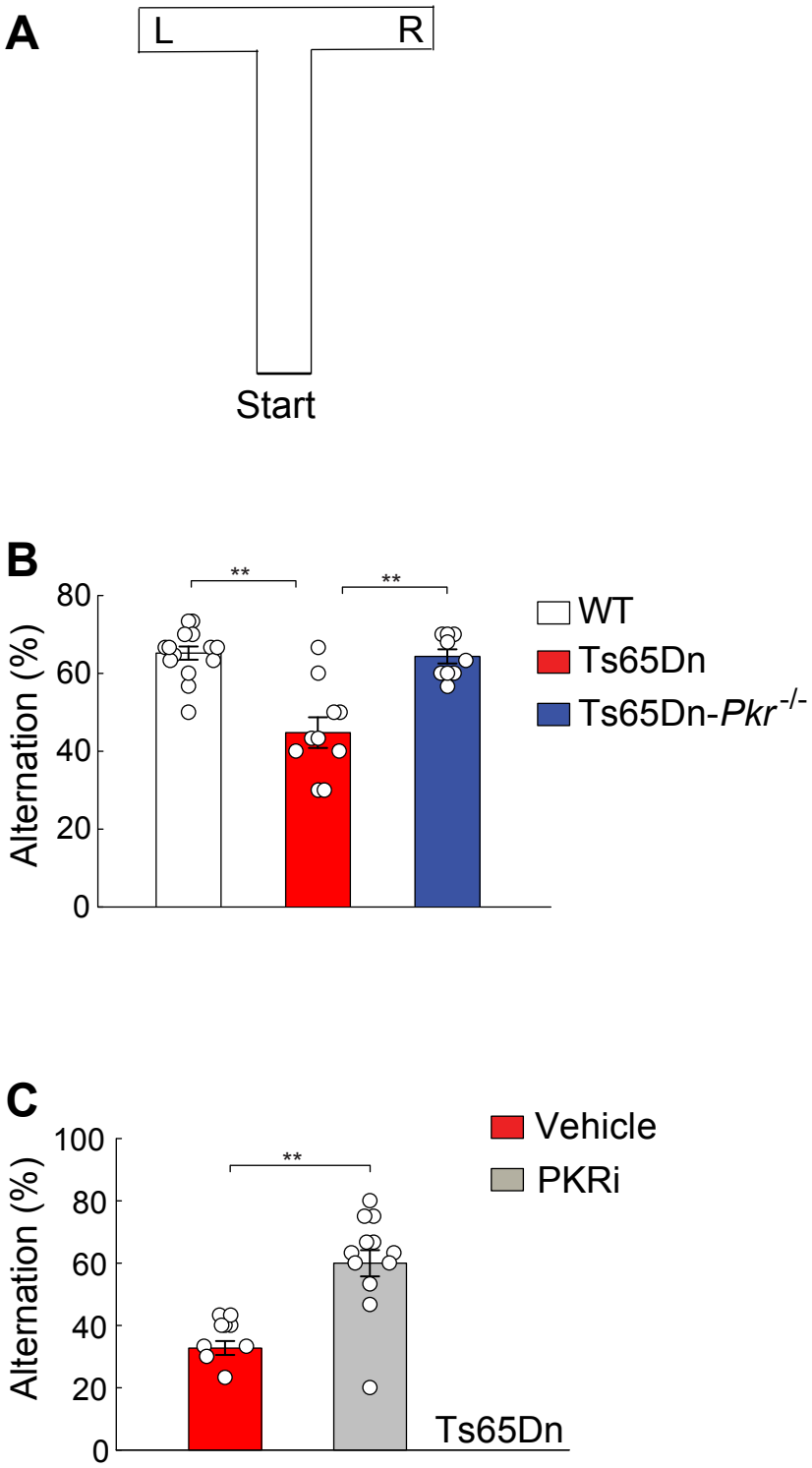

Fig. S9. Zhu et al.

Fig. S9. Genetic or pharmacological inhibition of PKR rescues abnormal spontaneous T-maze alternation in Ts65Dn mice. (**A**) Schematic of the spontaneous T-maze. (**B**) Alternation scores (%) in the spontaneous alternation task in WT (*n* = 14), Ts65Dn (*n* = 10), and Ts65Dn-*Pkr*$^{-/-}$ mice (*n* = 9, $F_{2,30}$ = 19.73). (**C**) Alternation scores (%) in the spontaneous alternation task in vehicle-treated (n = 9) and PKRi-treated (*n* = 12) Ts65Dn mice (*t* = 52.00, Mann-Whitney U test). Data are mean ± s.e.m. ***P* < 0.01

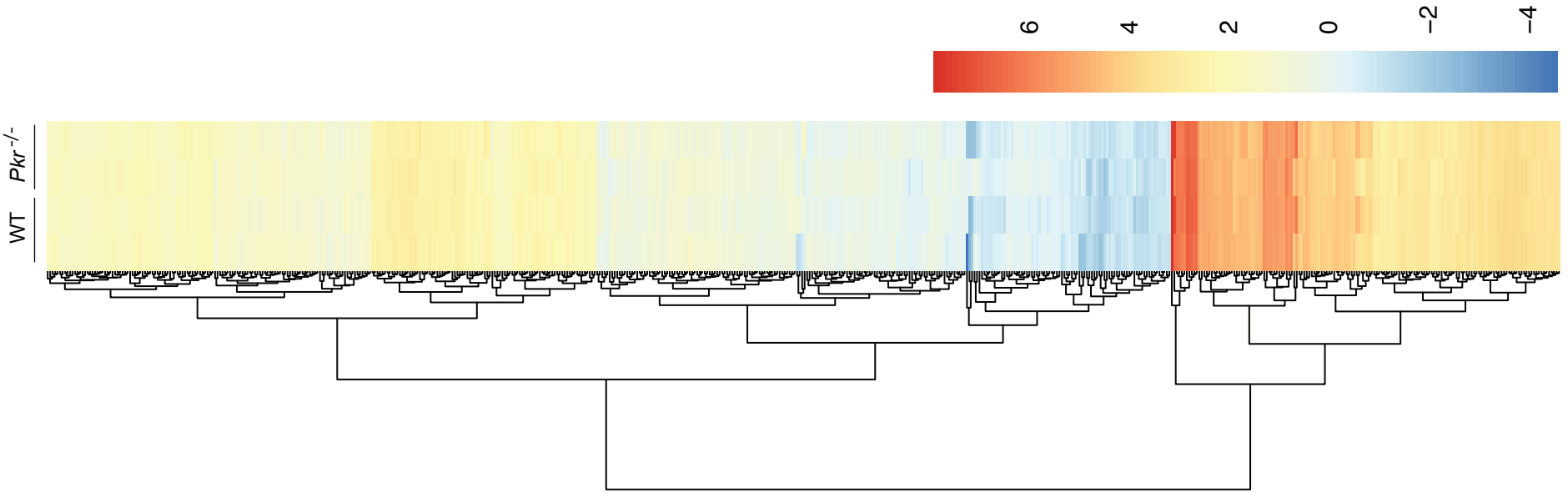

Fig. 10. Zhu et al.

Fig. S10. Similar polysome profiling in WT and PKR-deficient mice. Heat map showing that the mRNAs whose translation is altered in the brain of Ts65Dn mice are not different between WT and *Pkr*$^{-/-}$ mice.

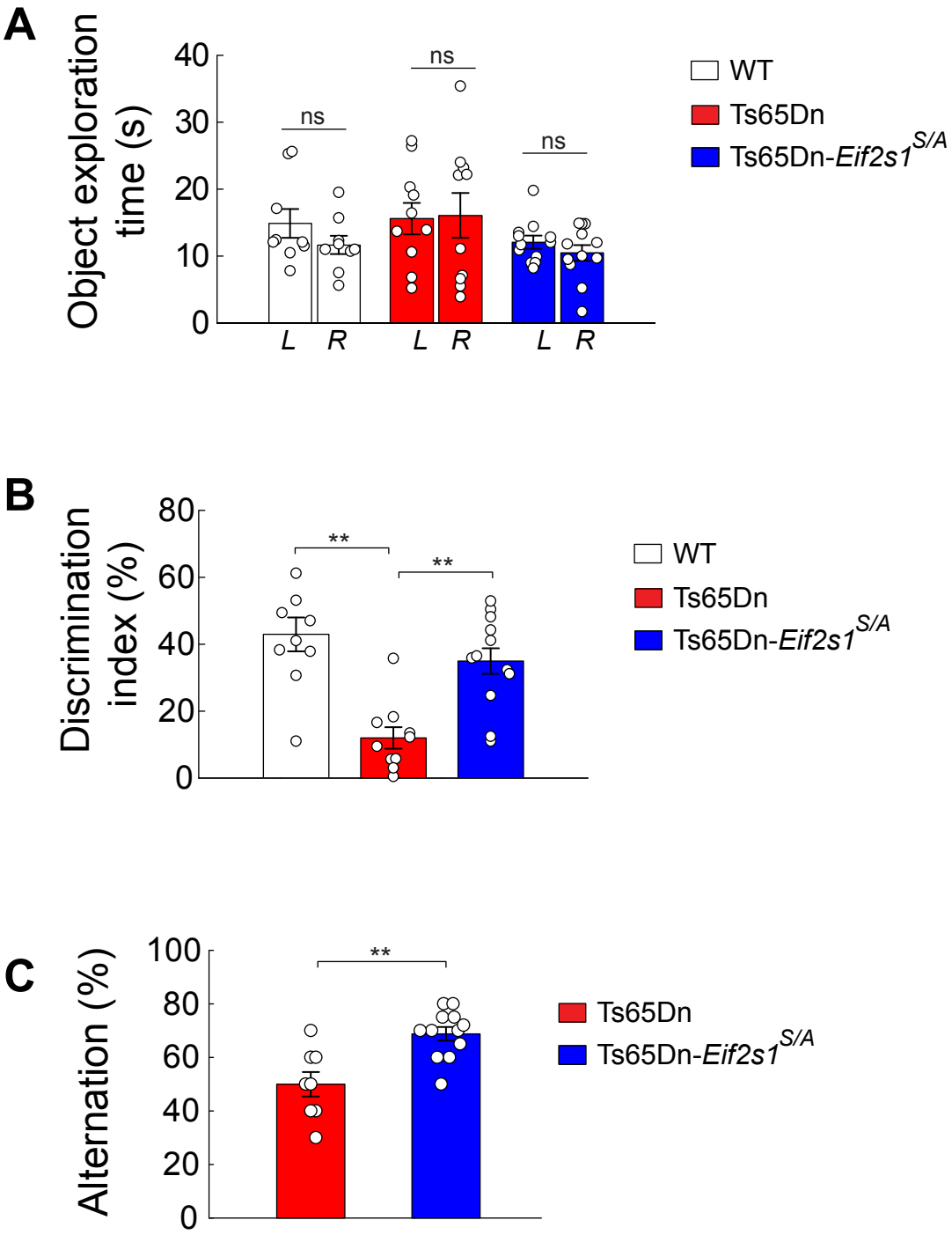

Fig. S11. Zhu et al.

Fig. S11. Genetic inhibition of eIF2-P levels improves long-term object recognition memory and spontaneous alternation in Ts65Dn mice. (**A**) Time exploring the identical right (R) and left (L) objects: WT (n = 9, t_{16} = 1.28, P = 0.22), Ts65Dn mice (n = 10, t_{18} = 0.03, P = 0.97) and Ts65Dn-*Eif2s1*$^{S/A}$ mice (n = 12, t_{22} = 1.01, P = 0.32) (**B**) Novel object discrimination index 24 hours post-training in WT (n = 9), Ts65Dn mice (n = 10) and Ts65Dn-*Eif2s1*$^{S/A}$ mice (n = 12, $F_{2,28}$ = 13.79). (**C**) Alternation scores (%) in the spontaneous alternation task in Ts65Dn mice (n = 8), and Ts65Dn-*Eif2s1*$^{S/A}$ mice (n = 12, t_{18} = 3.80). Data are mean ± s.e.m. **P < 0.01.

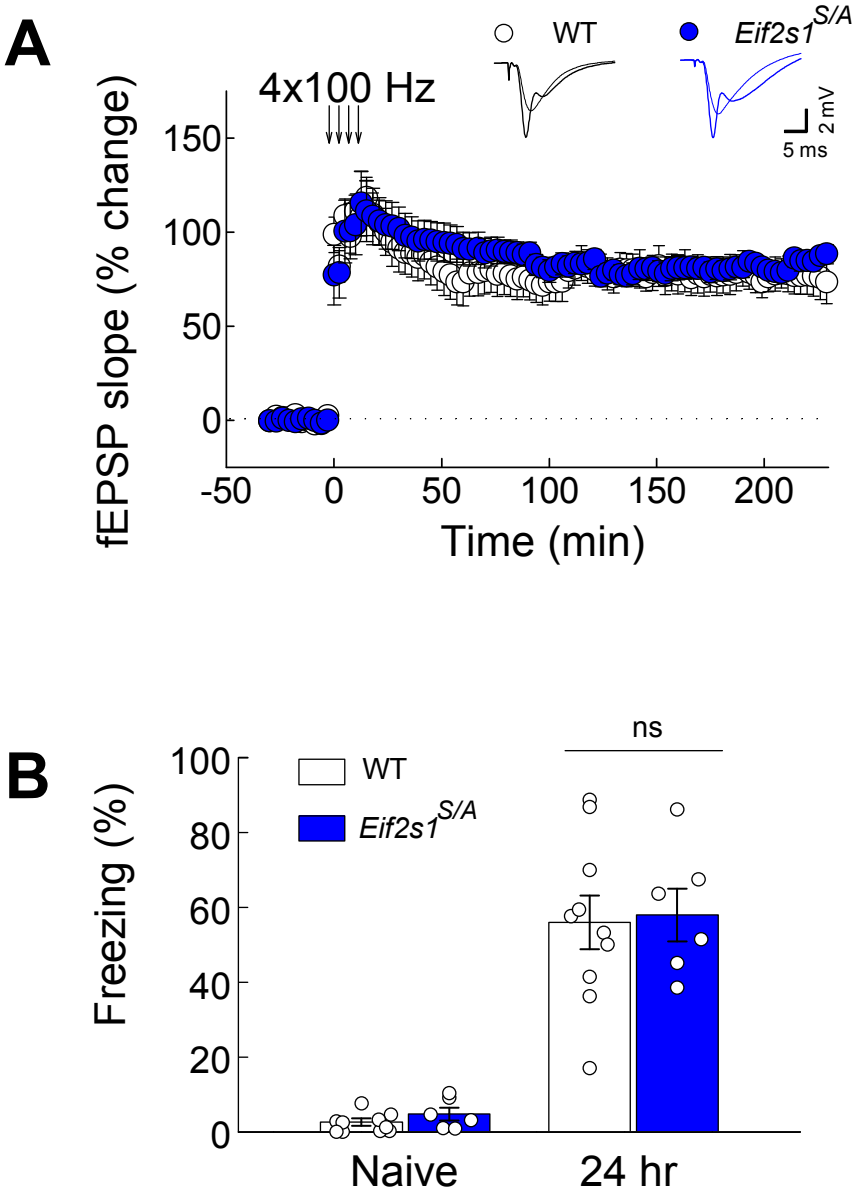

Fig. S12. Zhu et al.

Fig. S12. L-LTP and long-term memory are normal in mice with reduced eIF2-P (*Eif2s1*$^{S/A}$ mice). (A) L-LTP induced by 4 trains of high frequency stimulation (HFS, 4 x 100 Hz) in slices from WT (n = 11) and *Eif2s1*$^{S/A}$ mice (n = 8, t_{17} = 1.42, P = 0.17). (**B**) Freezing behavior before training (naïve) and 24 hours after training in WT and *Eif2s1*$^{S/A}$ littermates (n = 6-10, t_{14} = 1.42, P = 0.8). Mice were trained using a conventional training protocol (two foot-shocks at 0.7 mA for 2 sec). Data are mean ± s.e.m.

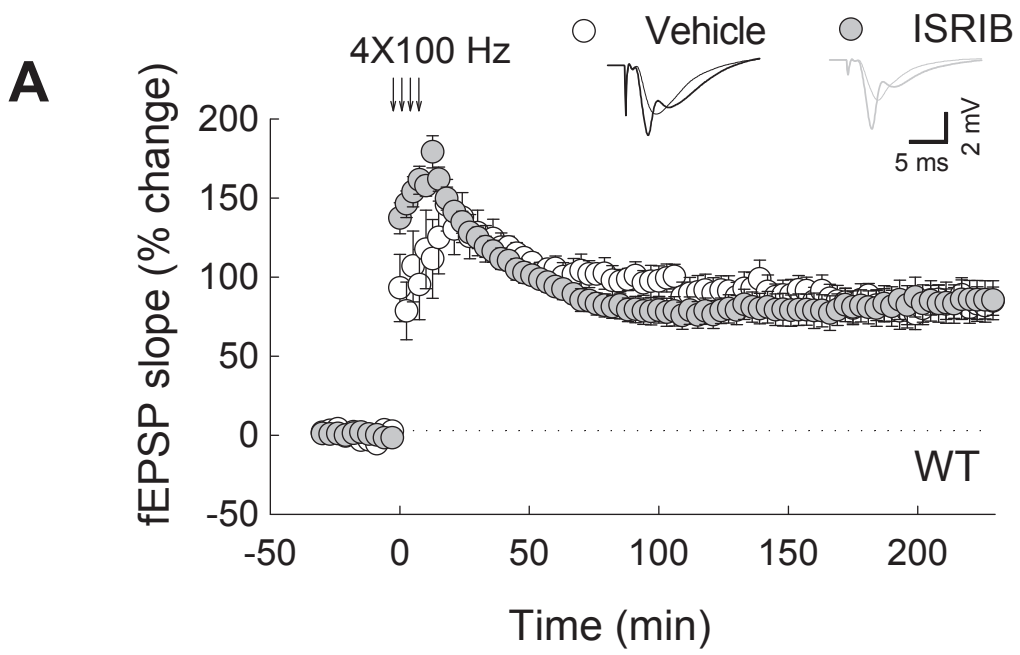

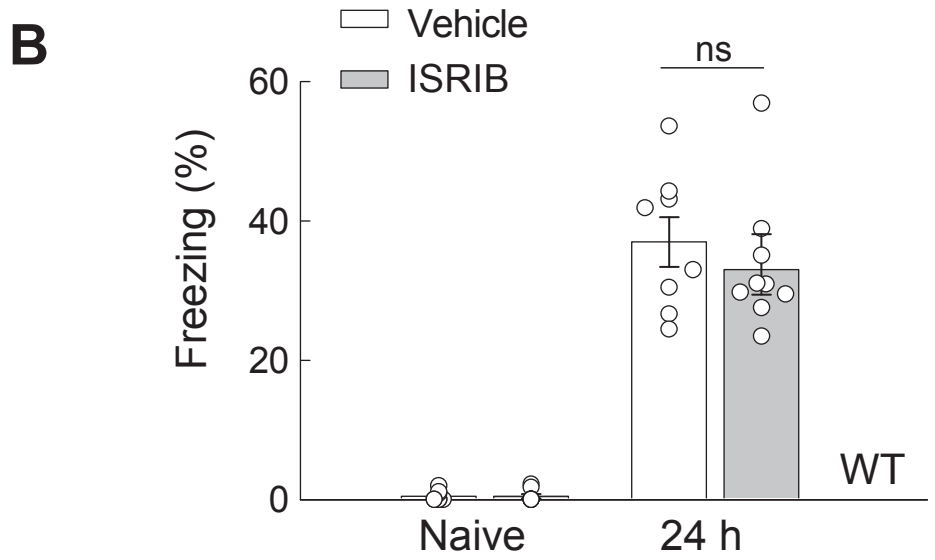

Fig. S13. Zhu et al.

Fig. S13. Treatment with ISRIB had no effect on L-LTP and long-term memory in WT mice. (**A**) L-LTP induced by 4 trains of high frequency stimulation (HFS, 4 x 100 Hz) in vehicle-treated (n = 9) and ISRIB-treated WT mice (n = 9, t_{16} = 0.51, P = 0.62). (**B**) Freezing behavior before (naïve) and 24 hours post-training in vehicle-treated (n = 8) and ISRIB-treated WT mice (n = 8, t_{14} = 1.1, P = 0.27). Data are mean ± s.e.m.

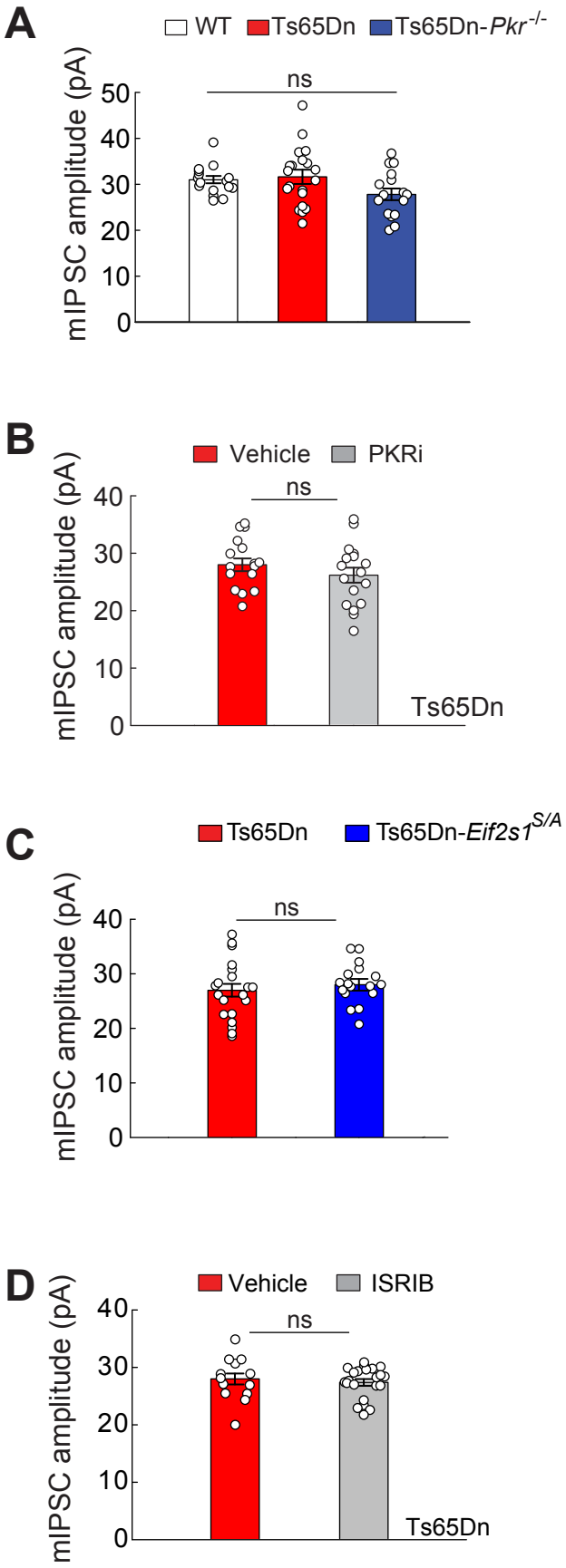

Fig. S14. Zhu et al.

Fig. S14. The amplitude of miniature inhibitory synaptic currents (mIPSCs) is unaltered in CA1 neurons from Ts65Dn mice. (**A**) Summary data show mIPSC amplitude in CA1 neurons from WT (n = 16), Ts65Dn (n = 20) and Ts65Dn-*Pkr*$^{-/-}$ mice (n = 16; H = 0.12, P = 0.12, One-way ANOVA on Ranks). (**B**) Summary data show mIPSC amplitude in CA1 neurons from vehicle-treated (n = 16) and PKRi-treated (n = 17) Ts65Dn mice (t_{31} = 1.23, P = 0.23). (**C**) Summary data show mIPSC amplitude in Ts65Dn (n = 20) and Ts65Dn-*Eif2s1*$^{S/A}$ mice (n = 17, t_{35} = 0.66, P = 0.51). **D**) Summary data show mIPSCs amplitude in vehicle-treated (n = 13) and ISRIB-treated Ts65Dn mice (n = 22, t_{33} = 0.61, P = 0.54). Data are mean ± s.e.m.

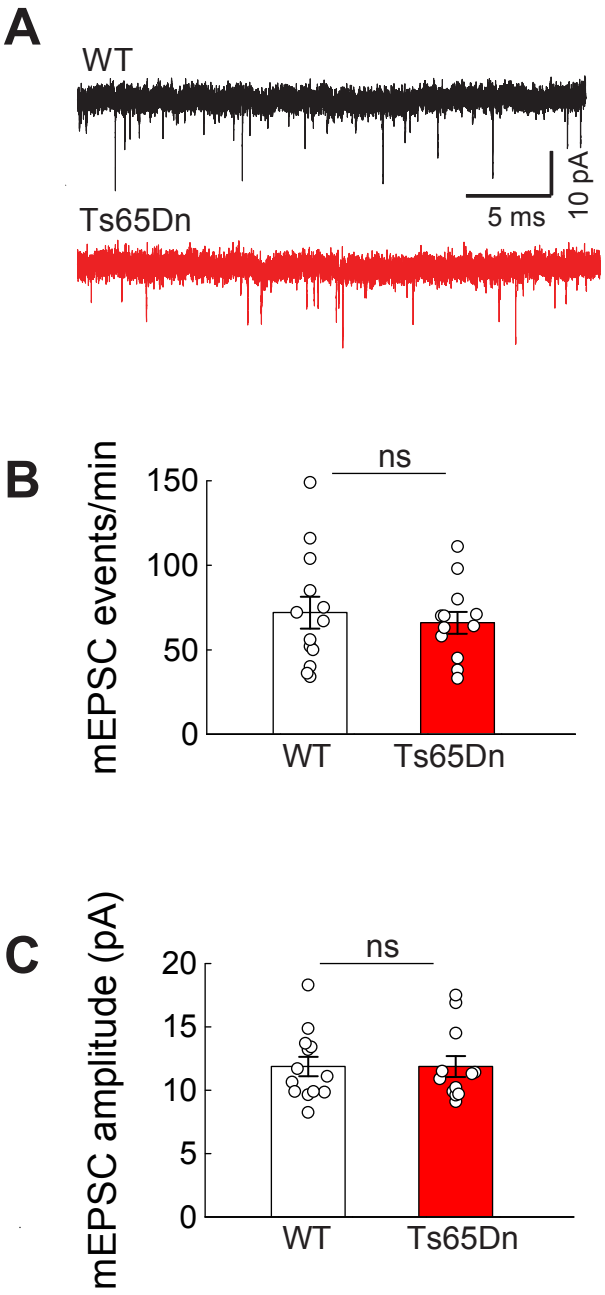

Fig. S15. Zhu et al.

Fig. S15. Excitatory synaptic transmission is unaltered in CA1 neurons from Ts65Dn mice (**A-C**) Sample traces (**A**) and summary show frequency (**B**, $t_{23} = 0.45$, $P = 0.66$) and amplitude (**C**, $t = 153$, $P = 0.89$, Mann-Whitney U test) of miniature excitatory postsynaptic currents (mESPCs) in CA1 neurons from WT ($n = 13$) and Ts65Dn mice ($n = 12$). Data are mean ± s.e.m.

Table S1

DS human tissue donor information

UMB#	Genotype	Age	Sex	Race	Post mortem interval (hours)
5762	Unaffected control	39 years 137 days	Female	Caucasian	19
5005	Down syndrome	39 years 59 days	Female	Caucasian	12
4369	Unaffected control	2 years 265 days	Female	Caucasian	14
5301	Down syndrome	3 years 212 days	Female	Caucasian	11
5871	Unaffected control	2 years 28 days	Male	Caucasian	Unknown
2135	Down syndrome	1 year 353 days	Male	Caucasian	12
5900	Unaffected control	0 years 0 days	Female	Caucasian	23
4457	Down syndrome	0 years 185 days	Female	Caucasian	32
4373	Unaffected control	0 years 100 days	Female	Caucasian	13
1282	Down syndrome	0 years 186 days	Female	Caucasian	28
6169	Unaffected control	25 years 100 days	Male	Unknown	12
5341	Down syndrome	25 years 311 days	Male	Black or African-American	16
1206	Unaffected control	57 years 134 days	Male	Caucasian	16
6135	Down syndrome	55 years 293 days	Male	Caucasian	12
5753	Unaffected control	28 years 222 days	Male	Caucasian	28
5713	Down syndrome	25 years 147 days	Male	Caucasian	22
5985	Unaffected control	55 years 227 days	Male	Caucasian	23
5439	Down syndrome	57 years 254 days	Male	Caucasian	3
6100	Unaffected control	0 years 187 days	Female	Black or African-American	32
5987	Down syndrome	0 years 65 days	Female	Black or African-American	28
5282	Unaffected control	2 years 306 days	Male	Unknown	16
5826	Down syndrome	2 years 56 days	Male	Unknown	18

Table S2

Gene ID	Gene name	log2(fold change) Ts65Dn vs WT	*P* -value	*q*- value	Up- or Down-regulated in Ts65Dn	Rescued, Up- or Down-regulated in Ts65Dn;PKR-/-
ENSMUSG00000000792.2	Slc5a5	1.26359	5.00E-05	0.00298639	Up	Rescued
ENSMUSG00000001119.7	Col6a1	-0.98814	5.00E-05	0.00298639	Down	Rescued
ENSMUSG00000001444.2	Tbx21	2.98242	5.00E-05	0.00298639	Up	Rescued
ENSMUSG00000003411.10	Rab3b	0.915858	5.00E-05	0.00298639	Up	Rescued
ENSMUSG00000003657.9	Calb2	1.01247	5.00E-05	0.00298639	Up	Down
ENSMUSG00000003929.10	Zfp81	-1.13472	5.00E-05	0.00298639	Down	Rescued
ENSMUSG00000004637.15	Wwox	-1.65005	5.00E-05	0.00298639	Down	Rescued
ENSMUSG00000004885.5	Crabp2	1.09362	5.00E-05	0.00298639	Up	Rescued
ENSMUSG00000005540.10	Fcer2a	-2.01764	5.00E-05	0.00298639	Down	Rescued
ENSMUSG00000007682.6	Dio2	-1.12694	5.00E-05	0.00298639	Down	Rescued
ENSMUSG00000014956.15	Ppp1cb	-1.25408	5.00E-05	0.00298639	Down	Rescued
ENSMUSG00000015806.12	Qdpr	0.822304	5.00E-05	0.00298639	Up	Down
ENSMUSG00000017677.11	Wsb1	-0.998422	5.00E-05	0.00298639	Down	Up
ENSMUSG00000018727.19	Cpsf4l	-2.04495	5.00E-05	0.00298639	Down	Rescued
ENSMUSG00000019878.8	Hsf2	-1.04734	5.00E-05	0.00298639	Down	Rescued
ENSMUSG00000021098.14	Six6os1	-1.76461	5.00E-05	0.00298639	Down	Rescued
ENSMUSG00000021713.9	Ppwd1	-1.23074	5.00E-05	0.00298639	Down	Rescued
ENSMUSG00000022016.16	Akap11	-0.791382	5.00E-05	0.00298639	Down	Rescued
ENSMUSG00000022119.15	Rbm26	-0.840628	5.00E-05	0.00298639	Down	Rescued
ENSMUSG00000022193.7	Psmb5	0.72882	5.00E-05	0.00298639	Up	Down
ENSMUSG00000022235.15	Cmbl	1.33967	5.00E-05	0.00298639	Up	Rescued
ENSMUSG00000022658.10	Tagln3	0.9421	5.00E-05	0.00298639	Up	Rescued
ENSMUSG00000022672.8	Prkdc	-0.890176	5.00E-05	0.00298639	Down	Rescued
ENSMUSG00000022982.10	Sod1	1.13125	5.00E-05	0.00298639	Up	Rescued
ENSMUSG00000024290.8	Rock1	-0.962921	5.00E-05	0.00298639	Down	Rescued
ENSMUSG00000024293.15	Esco1	-1.90898	5.00E-05	0.00298639	Down	Rescued
ENSMUSG00000024404.6	Riok3	-0.828684	5.00E-05	0.00298639	Down	Rescued
ENSMUSG00000024511.15	Rab27b	-0.877541	5.00E-05	0.00298639	Down	Rescued
ENSMUSG00000024570.6	Rbfa	0.966048	5.00E-05	0.00298639	Up	Rescued
ENSMUSG00000024670.16	Cd6	-1.62281	5.00E-05	0.00298639	Down	Rescued
ENSMUSG00000025068.7	Gsto1	0.898654	5.00E-05	0.00298639	Up	Rescued
ENSMUSG00000025083.18	Afap1l2	4.45027	5.00E-05	0.00298639	Up	Rescued
ENSMUSG00000025175.12	Fn3k	0.868351	5.00E-05	0.00298639	Up	Rescued
ENSMUSG00000026034.17	Clk1	-1.23962	5.00E-05	0.00298639	Down	Rescued
ENSMUSG00000026355.11	Mcm6	2.13917	5.00E-05	0.00298639	Up	Rescued
ENSMUSG00000027363.15	Usp8	-0.778933	5.00E-05	0.00298639	Down	Rescued
ENSMUSG00000027447.6	Cst3	1.18947	5.00E-05	0.00298639	Up	Rescued
ENSMUSG00000027581.12	Stmn3	0.788781	5.00E-05	0.00298639	Up	Rescued
ENSMUSG00000027712.13	Anxa5	-1.14516	5.00E-05	0.00298639	Down	Rescued
ENSMUSG00000028256.16	Odf2l	-1.39284	5.00E-05	0.00298639	Down	Rescued
ENSMUSG00000028341.9	Nr4a3	-1.35156	5.00E-05	0.00298639	Down	Down
ENSMUSG00000028670.14	Lypla2	0.864241	5.00E-05	0.00298639	Up	Rescued
ENSMUSG00000028756.12	Pink1	0.801485	5.00E-05	0.00298639	Up	Rescued

ENSMUSG00000028964.14	Park7	0.73187	5.00E-05	0.00298639	Up	Down
ENSMUSG00000029169.11	Dhx15	-0.900311	5.00E-05	0.00298639	Down	Rescued
ENSMUSG00000029202.12	Pds5a	-1.17339	5.00E-05	0.00298639	Down	Rescued
ENSMUSG00000029712.14	Actl6b	0.871934	5.00E-05	0.00298639	Up	Rescued
ENSMUSG00000029781.7	Fkbp9	1.13981	5.00E-05	0.00298639	Up	Rescued
ENSMUSG00000029823.16	Luc7l2	-1.00155	5.00E-05	0.00298639	Down	Rescued
ENSMUSG00000029875.5	Ccdc184	1.04216	5.00E-05	0.00298639	Up	Rescued
ENSMUSG00000030225.11	Dera	-2.0097	5.00E-05	0.00298639	Down	Rescued
ENSMUSG00000030307.8	Slc6a11	0.932067	5.00E-05	0.00298639	Up	Rescued
ENSMUSG00000030652.11	Coq7	0.926164	5.00E-05	0.00298639	Up	Down
ENSMUSG00000031445.5	Proz	-1.17434	5.00E-05	0.00298639	Down	Rescued
ENSMUSG00000031712.10	Il15	#NAME?	5.00E-05	0.00298639	Up	Rescued
ENSMUSG00000032128.15	Robo3	-1.92741	5.00E-05	0.00298639	Down	Rescued
ENSMUSG00000032446.14	Eomes	1.63707	5.00E-05	0.00298639	Up	Rescued
ENSMUSG00000032925.16	Itgbl1	-1.07204	5.00E-05	0.00298639	Down	Rescued
ENSMUSG00000032959.12	Pebp1	0.949576	5.00E-05	0.00298639	Up	Down
ENSMUSG00000033036.9	AC164004.4	#NAME?	5.00E-05	0.00298639	Up	Rescued
ENSMUSG00000033981.14	Gria2	-0.798946	5.00E-05	0.00298639	Down	Rescued
ENSMUSG00000034009.14	Rxfp1	-1.15291	5.00E-05	0.00298639	Down	Rescued
ENSMUSG00000034021.15	Pds5b	-0.878031	5.00E-05	0.00298639	Down	Rescued
ENSMUSG00000034265.8	Zdhhc14	0.89449	5.00E-05	0.00298639	Up	Up
ENSMUSG00000034551.12	Hdx	-1.6923	5.00E-05	0.00298639	Down	Rescued
ENSMUSG00000034640.9	Tiparp	-1.61689	5.00E-05	0.00298639	Down	Down
ENSMUSG00000034681.16	Rnps1	0.726424	5.00E-05	0.00298639	Up	Rescued
ENSMUSG00000035133.9	Arhgap5	-1.01096	5.00E-05	0.00298639	Down	Rescued
ENSMUSG00000035202.8	Lars2	1.34513	5.00E-05	0.00298639	Up	Down
ENSMUSG00000035429.13	Ptprh	2.79182	5.00E-05	0.00298639	Up	Rescued
ENSMUSG00000035868.8	Zfp983	-2.01709	5.00E-05	0.00298639	Down	Rescued
ENSMUSG00000035967.15	Ddx26b	-1.12726	5.00E-05	0.00298639	Down	Rescued
ENSMUSG00000036097.7	Slf2	-0.861008	5.00E-05	0.00298639	Down	Rescued
ENSMUSG00000036181.2	Hist1h1c	1.0926	5.00E-05	0.00298639	Up	Down
ENSMUSG00000036469.16	1-Mar	-0.83142	5.00E-05	0.00298639	Down	Rescued
ENSMUSG00000036887.5	C1qa	1.47556	5.00E-05	0.00298639	Up	Rescued
ENSMUSG00000036916.13	Zfp280c	-1.47151	5.00E-05	0.00298639	Down	Rescued
ENSMUSG00000037166.5	Ppp1r14a	1.02256	5.00E-05	0.00298639	Up	Rescued
ENSMUSG00000037266.18	Rsrp1	-0.992466	5.00E-05	0.00298639	Down	Rescued
ENSMUSG00000037627.16	Rgs22	-3.23615	5.00E-05	0.00298639	Down	Rescued
ENSMUSG00000038370.6	Pcp4l1	0.872394	5.00E-05	0.00298639	Up	Rescued
ENSMUSG00000038855.10	Itpkb	0.913897	5.00E-05	0.00298639	Up	Rescued
ENSMUSG00000039539.13	Sgcz	-1.13418	5.00E-05	0.00298639	Down	Rescued
ENSMUSG00000039634.12	Zfp189	-1.33146	5.00E-05	0.00298639	Down	Down
ENSMUSG00000039735.15	Fnbp1l	-0.938381	5.00E-05	0.00298639	Down	Rescued
ENSMUSG00000039753.16	Fbxl5	-0.882835	5.00E-05	0.00298639	Down	Rescued
ENSMUSG00000040123.17	Zmym5	-0.954815	5.00E-05	0.00298639	Down	Rescued
ENSMUSG00000040258.6	Nxph4	1.14864	5.00E-05	0.00298639	Up	Rescued
ENSMUSG00000040321.3	Zfp770	-0.788117	5.00E-05	0.00298639	Down	Rescued
ENSMUSG00000040511.14	Pvr	-1.51864	5.00E-05	0.00298639	Down	Rescued
ENSMUSG00000040565.7	Btaf1	-0.834797	5.00E-05	0.00298639	Down	Rescued

ENSMUSG00000040740.7	Slc25a34	1.38686	5.00E-05	0.00298639	Up	Rescued
ENSMUSG00000042256.4	Ptchd4	-0.906744	5.00E-05	0.00298639	Down	Rescued
ENSMUSG00000042670.5	Immp1l	-1.06868	5.00E-05	0.00298639	Down	Down
ENSMUSG00000043424.10	Eif3j2	-1.53049	5.00E-05	0.00298639	Down	Rescued
ENSMUSG00000044349.15	Snhg11	-1.30919	5.00E-05	0.00298639	Down	Rescued
ENSMUSG00000044676.10	Zfp612	-0.81242	5.00E-05	0.00298639	Down	Rescued
ENSMUSG00000046138.15	RP24-408B13.1	-0.80175	5.00E-05	0.00298639	Down	Rescued
ENSMUSG00000046160.6	Olig1	1.00978	5.00E-05	0.00298639	Up	Down
ENSMUSG00000046402.10	Rbp1	1.26894	5.00E-05	0.00298639	Up	Rescued
ENSMUSG00000048222.3	Mfap1b	-1.09211	5.00E-05	0.00298639	Down	Down
ENSMUSG00000048285.9	Frmd6	-1.29357	5.00E-05	0.00298639	Down	Rescued
ENSMUSG00000049539.3	Hist1h1a	1.12716	5.00E-05	0.00298639	Up	Rescued
ENSMUSG00000051617.3	Krt9	0.978625	5.00E-05	0.00298639	Up	Rescued
ENSMUSG00000052676.16	Zmat1	-1.07601	5.00E-05	0.00298639	Down	Rescued
ENSMUSG00000052861.13	Dnah6	-1.20195	5.00E-05	0.00298639	Down	Rescued
ENSMUSG00000055202.10	Zfp811	-1.49595	5.00E-05	0.00298639	Down	Rescued
ENSMUSG00000058064.5	Gm10036	-2.04722	5.00E-05	0.00298639	Down	Down
ENSMUSG00000058773.2	Hist1h1b	1.33164	5.00E-05	0.00298639	Up	Rescued
ENSMUSG00000060224.3	Pyroxd2	-2.11493	5.00E-05	0.00298639	Down	Down
ENSMUSG00000060803.5	Gstp1	0.800398	5.00E-05	0.00298639	Up	Rescued
ENSMUSG00000063535.7	Zfp773	-1.59699	5.00E-05	0.00298639	Down	Rescued
ENSMUSG00000064179.13	Tnnt1	1.22472	5.00E-05	0.00298639	Up	Rescued
ENSMUSG00000064341.1	mt-Nd1	-1.75986	5.00E-05	0.00298639	Down	Up
ENSMUSG00000064345.1	mt-Nd2	-1.91025	5.00E-05	0.00298639	Down	Up
ENSMUSG00000064351.1	mt-Co1	-1.38715	5.00E-05	0.00298639	Down	Up
ENSMUSG00000064363.1	mt-Nd4	-1.67834	5.00E-05	0.00298639	Down	Up
ENSMUSG00000064367.1	mt-Nd5	-1.29512	5.00E-05	0.00298639	Down	Up
ENSMUSG00000064370.1	mt-Cytb	-1.75487	5.00E-05	0.00298639	Down	Up
ENSMUSG00000067928.6	Zfp760	-1.51582	5.00E-05	0.00298639	Down	Rescued
ENSMUSG00000067931.5	Zfp948	-1.33724	5.00E-05	0.00298639	Down	Rescued
ENSMUSG00000068523.12	Gng5	1.10266	5.00E-05	0.00298639	Up	Up
ENSMUSG00000068748.7	Ptprz1	-0.898523	5.00E-05	0.00298639	Down	Rescued
ENSMUSG00000069049.11	Eif2s3y	-1.47188	5.00E-05	0.00298639	Down	Rescued
ENSMUSG00000069309.2	Hist1h2an	#NAME?	5.00E-05	0.00298639	Up	Rescued
ENSMUSG00000070803.6	Cited4	1.17064	5.00E-05	0.00298639	Up	Rescued
ENSMUSG00000071073.4	Lrrc73	0.802965	5.00E-05	0.00298639	Up	Rescued
ENSMUSG00000074505.5	Fat3	-0.789768	5.00E-05	0.00298639	Down	Rescued
ENSMUSG00000078435.5	RP24-406I15.2	-1.73392	5.00E-05	0.00298639	Down	Rescued
ENSMUSG00000078866.10	RP23-67E6.5	-1.7641	5.00E-05	0.00298639	Down	Rescued
ENSMUSG00000079065.3	RP23-314A12.1	-1.39383	5.00E-05	0.00298639	Down	Rescued
ENSMUSG00000087075.2	RP23-41J14.2	1.10931	5.00E-05	0.00298639	Up	Down
ENSMUSG00000090622.1	RP23-281E24.2	-2.19773	5.00E-05	0.00298639	Down	Rescued
ENSMUSG00000090862.3	Rps13	0.805572	5.00E-05	0.00298639	Up	Down
ENSMUSG00000092607.9	Scnm1	1.2747	5.00E-05	0.00298639	Up	Rescued
ENSMUSG00000095567.7	Noc2l	1.1201	5.00E-05	0.00298639	Up	Rescued
ENSMUSG00000096883.2	Shisa8	1.52941	5.00E-05	0.00298639	Up	Rescued
ENSMUSG00000096910.1	Zfp955b	-1.53109	5.00E-05	0.00298639	Down	Rescued
ENSMUSG00000110185.1	Igip	-0.831958	5.00E-05	0.00298639	Down	Rescued

ENSMUSG00000114279.1	Hist1h2bm	2.32053	5.00E-05	0.00298639	Up	Rescued
ENSMUSG00000001383.8	Zmat2	-0.676109	5.00E-05	0.00413376	Down	Rescued
ENSMUSG00000002365.10	Snx9	0.925744	5.00E-05	0.00413376	Up	Rescued
ENSMUSG00000007877.2	Tcap	-1.44671	5.00E-05	0.00413376	Down	Rescued
ENSMUSG00000009185.2	Ccl8	#NAME?	5.00E-05	0.00413376	Up	Rescued
ENSMUSG00000020255.8	RP24-227O16.1	-0.764809	5.00E-05	0.00413376	Down	Rescued
ENSMUSG00000020459.14	Mtif2	-1.36506	5.00E-05	0.00413376	Down	Rescued
ENSMUSG00000021136.13	Smoc1	1.00924	5.00E-05	0.00413376	Up	Rescued
ENSMUSG00000022205.15	Sub1	-0.886893	5.00E-05	0.00413376	Down	Rescued
ENSMUSG00000022762.18	Ncam2	-1.09059	5.00E-05	0.00413376	Down	Rescued
ENSMUSG00000023031.8	Cela1	3.35731	5.00E-05	0.00413376	Up	Rescued
ENSMUSG00000023224.12	Serping1	1.48227	5.00E-05	0.00413376	Up	Up
ENSMUSG00000024610.14	Cd74	1.38196	5.00E-05	0.00413376	Up	Rescued
ENSMUSG00000025278.9	Flnb	3.87393	5.00E-05	0.00413376	Up	Rescued
ENSMUSG00000025867.8	Cplx2	-0.755761	5.00E-05	0.00413376	Down	Rescued
ENSMUSG00000026678.10	Rgs5	-0.915822	5.00E-05	0.00413376	Down	Rescued
ENSMUSG00000027162.7	Lin7c	-1.01999	5.00E-05	0.00413376	Down	Rescued
ENSMUSG00000027597.15	Ahcy	0.845411	5.00E-05	0.00413376	Up	Rescued
ENSMUSG00000027875.12	Hmgcs2	1.36858	5.00E-05	0.00413376	Up	Rescued
ENSMUSG00000030935.15	Acsm3	#VALUE!	5.00E-05	0.00413376	Down	Rescued
ENSMUSG00000032231.14	Anxa2	0.986395	5.00E-05	0.00413376	Up	Rescued
ENSMUSG00000033192.5	Lpcat2	1.3796	5.00E-05	0.00413376	Up	Rescued
ENSMUSG00000033770.13	Clcnka	#VALUE!	5.00E-05	0.00413376	Down	Rescued
ENSMUSG00000034729.16	Mrps10	-0.997393	5.00E-05	0.00413376	Down	Rescued
ENSMUSG00000036438.12	Calm2	-0.804658	5.00E-05	0.00413376	Down	Rescued
ENSMUSG00000036594.14	H2-Aa	2.37599	5.00E-05	0.00413376	Up	Rescued
ENSMUSG00000036908.16	Unc93b1	1.20818	5.00E-05	0.00413376	Up	Up
ENSMUSG00000038255.6	Neurod2	-0.709876	5.00E-05	0.00413376	Down	Rescued
ENSMUSG00000038550.10	Ciart	-0.903252	5.00E-05	0.00413376	Down	Down
ENSMUSG00000039007.10	Cpq	1.49549	5.00E-05	0.00413376	Up	Rescued
ENSMUSG00000039221.10	Rpl22l1	-1.19083	5.00E-05	0.00413376	Down	Rescued
ENSMUSG00000039323.18	Igfbp2	0.889919	5.00E-05	0.00413376	Up	Rescued
ENSMUSG00000039801.7	AC158971.1	-2.07534	5.00E-05	0.00413376	Down	Rescued
ENSMUSG00000040128.9	Pnrc1	0.762287	5.00E-05	0.00413376	Up	Rescued
ENSMUSG00000040935.12	Padi6	#NAME?	5.00E-05	0.00413376	Up	Rescued
ENSMUSG00000044533.15	Rps2	-1.51922	5.00E-05	0.00413376	Down	Down
ENSMUSG00000050211.14	Pla2g4e	-0.984052	5.00E-05	0.00413376	Down	Rescued
ENSMUSG00000053070.5	RP23-349N15.3	-1.3355	5.00E-05	0.00413376	Down	Rescued
ENSMUSG00000053475.5	Tnfaip6	1.12635	5.00E-05	0.00413376	Up	Rescued
ENSMUSG00000054428.12	Atpif1	-0.729807	5.00E-05	0.00413376	Down	Rescued
ENSMUSG00000057163.3	Prss2	#NAME?	5.00E-05	0.00413376	Up	Rescued
ENSMUSG00000061086.12	Myl4	-1.19084	5.00E-05	0.00413376	Down	Rescued
ENSMUSG00000063698.9	Sfxn4	1.65811	5.00E-05	0.00413376	Up	Rescued
ENSMUSG00000066107.6	RP23-434B7.2	-1.99151	5.00E-05	0.00413376	Down	Rescued
ENSMUSG00000069516.8	Lyz2	2.09639	5.00E-05	0.00413376	Up	Up
ENSMUSG00000073079.6	Srp54a	-1.36797	5.00E-05	0.00413376	Down	Rescued
ENSMUSG00000079012.11	Serpina3m	#VALUE!	5.00E-05	0.00413376	Down	Rescued
ENSMUSG00000090093.8	RP23-330D3.6	5.73901	5.00E-05	0.00413376	Up	Rescued

ENSMUSG00000093931.2	Amy2a3	#NAME?	5.00E-05	0.00413376	Up	Rescued
ENSMUSG00000112449.1	Srp54b	4.25324	5.00E-05	0.00413376	Up	Rescued
ENSMUSG00000000838.17	Fmr1	-0.927091	0.0001	0.00533164	Down	Rescued
ENSMUSG00000008140.17	Emc10	0.750334	0.0001	0.00533164	Up	Rescued
ENSMUSG00000017009.3	Sdc4	0.810426	0.0001	0.00533164	Up	Rescued
ENSMUSG00000020620.14	Abca8b	-0.938131	0.0001	0.00533164	Down	Rescued
ENSMUSG00000020732.13	Rab37	1.32795	0.0001	0.00533164	Up	Rescued
ENSMUSG00000020848.7	Doc2b	0.697578	0.0001	0.00533164	Up	Rescued
ENSMUSG00000024193.7	Phf1	0.675499	0.0001	0.00533164	Up	Rescued
ENSMUSG00000026730.12	Pter	-0.883801	0.0001	0.00533164	Down	Rescued
ENSMUSG00000028214.13	Gem	-1.696	0.0001	0.00533164	Down	Down
ENSMUSG00000030075.10	Cntn3	-0.82616	0.0001	0.00533164	Down	Rescued
ENSMUSG00000030309.16	Caprin2	-1.67102	0.0001	0.00533164	Down	Rescued
ENSMUSG00000030536.10	Iqgap1	-1.66505	0.0001	0.00533164	Down	Rescued
ENSMUSG00000033991.9	Ttc37	-1.45378	0.0001	0.00533164	Down	Rescued
ENSMUSG00000038535.17	Zfp280d	-1.18839	0.0001	0.00533164	Down	Rescued
ENSMUSG00000042834.14	Nrep	-0.70448	0.0001	0.00533164	Down	Down
ENSMUSG00000044519.8	Zfp488	-1.00108	0.0001	0.00533164	Down	Rescued
ENSMUSG00000049164.6	Zfp518a	-1.14943	0.0001	0.00533164	Down	Rescued
ENSMUSG00000056201.7	Cfl1	0.813036	0.0001	0.00533164	Up	Down
ENSMUSG00000061665.6	Cd2ap	-1.02093	0.0001	0.00533164	Down	Rescued
ENSMUSG00000086022.1	Rad51ap2	-2.0408	0.0001	0.00533164	Down	Rescued
ENSMUSG00000017144.8	Rnd3	-1.27309	0.00015	0.00735351	Down	Down
ENSMUSG00000018293.4	Pfn1	0.677197	0.00015	0.00735351	Up	Down
ENSMUSG00000020436.17	Gabrg2	-0.806579	0.00015	0.00735351	Down	Rescued
ENSMUSG00000021712.15	Trim23	-0.738264	0.00015	0.00735351	Down	Rescued
ENSMUSG00000023882.15	Zfp54	-2.56085	0.00015	0.00735351	Down	Rescued
ENSMUSG00000025228.4	Actr1a	0.696921	0.00015	0.00735351	Up	Rescued
ENSMUSG00000027201.16	Myef2	-0.823422	0.00015	0.00735351	Down	Rescued
ENSMUSG00000030759.16	Far1	-0.993465	0.00015	0.00735351	Down	Rescued
ENSMUSG00000032285.15	Dnaja4	1.01346	0.00015	0.00735351	Up	Rescued
ENSMUSG00000034227.7	Foxj1	1.09034	0.00015	0.00735351	Up	Rescued
ENSMUSG00000040459.11	Arglu1	-0.742293	0.00015	0.00735351	Down	Rescued
ENSMUSG00000040681.15	Hmgn1	0.701853	0.00015	0.00735351	Up	Rescued
ENSMUSG00000041801.5	Phlda3	0.70176	0.00015	0.00735351	Up	Rescued
ENSMUSG00000049288.4	Lix1l	0.839148	0.00015	0.00735351	Up	Rescued
ENSMUSG00000053825.15	Ppfia2	-0.698583	0.00015	0.00735351	Down	Rescued
ENSMUSG00000067608.4	Pcna-ps2	-1.55182	0.00015	0.00735351	Down	Rescued
ENSMUSG00000071655.11	Ubxn1	0.662531	0.00015	0.00735351	Up	Down
ENSMUSG00000020460.15	Rps27a	-0.832728	0.0001	0.00786812	Down	Rescued
ENSMUSG00000023074.11	Mospd1	-1.20276	0.0001	0.00786812	Down	Rescued
ENSMUSG00000026234.12	Ncl	-0.703577	0.0001	0.00786812	Down	Down
ENSMUSG00000075602.10	Ly6a	3.45902	0.0001	0.00786812	Up	Rescued
ENSMUSG00000010538.14	Tsacc	-1.36863	0.0002	0.00903062	Down	Down
ENSMUSG00000013662.5	Atad1	-0.754921	0.0002	0.00903062	Down	Rescued
ENSMUSG00000022358.7	Fbxo32	-0.803165	0.0002	0.00903062	Down	Rescued
ENSMUSG00000024217.9	Snrpc	0.796919	0.0002	0.00903062	Up	Down
ENSMUSG00000024785.6	Rcl1	0.767016	0.0002	0.00903062	Up	Rescued

ENSMUSG00000024870.5	Rab1b	0.647036	0.0002	0.00903062	Up	Down
ENSMUSG00000025492.6	Ifitm3	0.978212	0.0002	0.00903062	Up	Rescued
ENSMUSG00000030079.15	Ruvbl1	0.939302	0.0002	0.00903062	Up	Rescued
ENSMUSG00000034525.7	Ice1	-0.726657	0.0002	0.00903062	Down	Rescued
ENSMUSG00000037416.13	Dmxl1	-0.78835	0.0002	0.00903062	Down	Rescued
ENSMUSG00000041238.15	Rbbp8	-1.07168	0.0002	0.00903062	Down	Rescued
ENSMUSG00000041685.16	Fcho2	-0.995185	0.0002	0.00903062	Down	Rescued
ENSMUSG00000042271.13	Nxt2	-1.00193	0.0002	0.00903062	Down	Rescued
ENSMUSG00000048388.3	Fam171b	-0.675569	0.0002	0.00903062	Down	Rescued
ENSMUSG00000052397.8	Ezr	1.00385	0.0002	0.00903062	Up	Up
ENSMUSG00000060594.6	Layn	2.46601	0.0002	0.00903062	Up	Rescued
ENSMUSG00000062931.15	Zfp938	-0.842997	0.0002	0.00903062	Down	Rescued
ENSMUSG00000063804.8	Lin28b	-1.18817	0.0002	0.00903062	Down	Rescued
ENSMUSG00000079317.10	Trappc2	-1.07854	0.0002	0.00903062	Down	Down
ENSMUSG00000100967.1	RP23-180L12.5	-1.02537	0.0002	0.00903062	Down	Rescued
ENSMUSG00000112160.1	RP24-406I15.3	-1.76841	0.0002	0.00903062	Down	Rescued
ENSMUSG00000001627.12	Ifrd1	-0.903095	0.00025	0.0107239	Down	Rescued
ENSMUSG00000004748.5	Mtfp1	0.652291	0.00025	0.0107239	Up	Rescued
ENSMUSG00000011837.4	Snapc2	0.990624	0.00025	0.0107239	Up	Rescued
ENSMUSG00000014603.2	Alx3	1.41475	0.00025	0.0107239	Up	Rescued
ENSMUSG00000024317.14	Rnf138	-0.899807	0.00025	0.0107239	Down	Rescued
ENSMUSG00000025898.6	Cwf19l2	-1.00959	0.00025	0.0107239	Down	Rescued
ENSMUSG00000026656.15	Fcgr2b	-1.53813	0.00025	0.0107239	Down	Rescued
ENSMUSG00000027495.4	Fam210b	0.720206	0.00025	0.0107239	Up	Rescued
ENSMUSG00000030929.17	Eri2	-1.6194	0.00025	0.0107239	Down	Rescued
ENSMUSG00000032849.14	Abcc4	-1.62588	0.00025	0.0107239	Down	Rescued
ENSMUSG00000034560.6	RP23-233B6.2	-0.870328	0.00025	0.0107239	Down	Rescued
ENSMUSG00000037593.11	RP23-185A18.11	-1.41877	0.00025	0.0107239	Down	Rescued
ENSMUSG00000037833.14	Sh2d4b	-1.41827	0.00025	0.0107239	Down	Rescued
ENSMUSG00000044254.6	Pcsk9	1.14381	0.00025	0.0107239	Up	Up
ENSMUSG00000046351.11	Zfp322a	-1.04089	0.00025	0.0107239	Down	Rescued
ENSMUSG00000046470.5	Sox18	1.12009	0.00025	0.0107239	Up	Rescued
ENSMUSG00000023089.12	Ndufa5	-0.811123	0.00015	0.0111048	Down	Rescued
ENSMUSG00000041935.10	RP23-372O9.2	-1.19123	0.00015	0.0111048	Down	Rescued
ENSMUSG00000044018.3	Mrpl50	-0.788737	0.00015	0.0111048	Down	Rescued
ENSMUSG00000046008.7	Pnlip	4.5071	0.00015	0.0111048	Up	Rescued
ENSMUSG00000073471.3	Rsph3a	1.8202	0.00015	0.0111048	Up	Rescued
ENSMUSG00000015656.17	Hspa8	1.01214	0.0003	0.012203	Up	Rescued
ENSMUSG00000020275.9	Rel	-0.958676	0.0003	0.012203	Down	Rescued
ENSMUSG00000022858.16	Tra2b	-0.921797	0.0003	0.012203	Down	Rescued
ENSMUSG00000030660.9	Pik3c2a	-1.02936	0.0003	0.012203	Down	Rescued
ENSMUSG00000033382.14	Trappc8	-0.9795	0.0003	0.012203	Down	Rescued
ENSMUSG00000033439.12	Trmt13	-2.0238	0.0003	0.012203	Down	Rescued
ENSMUSG00000033735.9	Spr	0.815988	0.0003	0.012203	Up	Rescued
ENSMUSG00000036902.11	Neto2	-0.782823	0.0003	0.012203	Down	Rescued
ENSMUSG00000037857.16	Nufip2	-0.726122	0.0003	0.012203	Down	Rescued
ENSMUSG00000039680.10	Mrps6	1.03013	0.0003	0.012203	Up	Rescued
ENSMUSG00000040648.14	Ppip5k2	-0.880972	0.0003	0.012203	Down	Rescued

ENSMUSG00000040706.4	Agmat	-1.08083	0.0003	0.012203	Down	Rescued
ENSMUSG00000041837.4	Pdcd7	0.744993	0.0003	0.012203	Up	Rescued
ENSMUSG00000043241.14	Upf2	-0.780613	0.0003	0.012203	Down	Rescued
ENSMUSG00000047844.3	Bex4	0.821667	0.0003	0.012203	Up	Down
ENSMUSG00000054178.1	Gm9938	-0.946944	0.0003	0.012203	Down	Rescued
ENSMUSG00000056592.14	Zfp658	-0.942166	0.0003	0.012203	Down	Rescued
ENSMUSG00000056673.14	Kdm5d	-0.811517	0.0003	0.012203	Down	Down
ENSMUSG00000059970.7	Hspa2	0.790537	0.0003	0.012203	Up	Rescued
ENSMUSG00000078853.8	Igtp	2.10172	0.0003	0.012203	Up	Rescued
ENSMUSG00000078862.10	RP24-87L14.1	-1.16468	0.0003	0.012203	Down	Rescued
ENSMUSG00000079108.6	Srp54c	-0.944357	0.0003	0.012203	Down	Rescued
ENSMUSG00000004044.9	Ptrf	0.829187	0.0002	0.0135725	Up	Rescued
ENSMUSG00000019737.14	Syne4	-1.98017	0.0002	0.0135725	Down	Rescued
ENSMUSG00000024142.14	Mlst8	0.676842	0.0002	0.0135725	Up	Rescued
ENSMUSG00000026424.8	Gpr37l1	0.708886	0.0002	0.0135725	Up	Rescued
ENSMUSG00000046312.4	RP23-100C7.2	0.785998	0.0002	0.0135725	Up	Rescued
ENSMUSG00000051048.17	P4ha3	1.91291	0.0002	0.0135725	Up	Up
ENSMUSG00000008200.14	Fnbp4	-1.29249	0.00035	0.0137337	Down	Rescued
ENSMUSG00000011263.16	Exoc3l2	-1.45036	0.00035	0.0137337	Down	Rescued
ENSMUSG00000020385.16	Clk4	-0.991758	0.00035	0.0137337	Down	Rescued
ENSMUSG00000022540.16	Rogdi	0.668294	0.00035	0.0137337	Up	Rescued
ENSMUSG00000023809.10	Rps6ka2	1.00041	0.00035	0.0137337	Up	Up
ENSMUSG00000025019.15	Lcor	-0.725554	0.00035	0.0137337	Down	Rescued
ENSMUSG00000028572.13	Hook1	-1.25838	0.00035	0.0137337	Down	Rescued
ENSMUSG00000029422.15	Rsrc2	-0.899065	0.00035	0.0137337	Down	Rescued
ENSMUSG00000036572.16	Upf3b	-0.834036	0.00035	0.0137337	Down	Rescued
ENSMUSG00000039233.12	Tbce	-1.09206	0.00035	0.0137337	Down	Rescued
ENSMUSG00000041607.16	Mbp	0.733715	0.00035	0.0137337	Up	Down
ENSMUSG00000042109.8	Csdc2	0.678679	0.00035	0.0137337	Up	Down
ENSMUSG00000063810.7	Alms1	-1.13818	0.00035	0.0137337	Down	Rescued
ENSMUSG00000109588.1	Lnp1	2.07554	0.00035	0.0137337	Up	Rescued
ENSMUSG00000004207.14	Psap	0.705273	0.0004	0.0150992	Up	Up
ENSMUSG00000004665.10	Cnn2	1.23084	0.0004	0.0150992	Up	Rescued
ENSMUSG00000022337.7	Emc2	-0.676363	0.0004	0.0150992	Down	Rescued
ENSMUSG00000022947.8	Cbr3	0.790755	0.0004	0.0150992	Up	Rescued
ENSMUSG00000025791.18	Pgm2	0.756379	0.0004	0.0150992	Up	Rescued
ENSMUSG00000031659.13	Adcy7	-1.20329	0.0004	0.0150992	Down	Rescued
ENSMUSG00000031698.14	Mylk3	2.23258	0.0004	0.0150992	Up	Rescued
ENSMUSG00000043964.14	Orai3	-0.755766	0.0004	0.0150992	Down	Rescued
ENSMUSG00000051483.9	Cbr1	0.734507	0.0004	0.0150992	Up	Rescued
ENSMUSG00000058355.8	Abce1	-0.733604	0.0004	0.0150992	Down	Rescued
ENSMUSG00000061371.7	Zfp873	-1.14666	0.0004	0.0150992	Down	Rescued
ENSMUSG00000068617.5	Efcab1	-0.98477	0.0004	0.0150992	Down	Rescued
ENSMUSG00000110105.1	RP24-77E13.10	4.40623	0.0004	0.0150992	Up	Rescued
ENSMUSG00000001473.6	Tubb6	1.05012	0.00025	0.015782	Up	Rescued
ENSMUSG00000020432.12	Tcn2	0.885122	0.00025	0.015782	Up	Rescued
ENSMUSG00000022674.15	Ube2v2	-1.10352	0.00025	0.015782	Down	Rescued
ENSMUSG00000023992.14	Trem2	1.42059	0.00025	0.015782	Up	Rescued

ENSMUSG00000026308.8	Klhl30	1.48145	0.00025	0.015782	Up	Rescued
ENSMUSG00000029304.14	Spp1	1.39525	0.00025	0.015782	Up	Rescued
ENSMUSG00000037152.11	Ndufc1	-1.15039	0.00025	0.015782	Down	Rescued
ENSMUSG00000074892.9	B3galt5	0.975232	0.00025	0.015782	Up	Rescued
ENSMUSG00000003198.10	Zfp959	-1.54742	0.00045	0.0163963	Down	Rescued
ENSMUSG00000024045.5	Akap8	-0.683415	0.00045	0.0163963	Down	Rescued
ENSMUSG00000028223.8	Decr1	0.86184	0.00045	0.0163963	Up	Rescued
ENSMUSG00000046994.9	Mars2	-0.713233	0.00045	0.0163963	Down	Rescued
ENSMUSG00000047485.6	Klhl34	-0.715258	0.00045	0.0163963	Down	Rescued
ENSMUSG00000058748.9	Zfp958	-1.26662	0.00045	0.0163963	Down	Rescued
ENSMUSG00000069300.3	Hist1h2bj	1.20839	0.00045	0.0163963	Up	Rescued
ENSMUSG00000078117.2	Gm16485	-0.77539	0.00045	0.0163963	Down	Rescued
ENSMUSG00000094441.1	Zfp955a	-1.18379	0.00045	0.0163963	Down	Rescued
ENSMUSG00000004655.5	Aqp1	3.48245	0.0003	0.0179636	Up	Rescued
ENSMUSG00000008822.15	Acyp1	-0.804276	0.0003	0.0179636	Down	Rescued
ENSMUSG00000020473.13	Aebp1	0.902517	0.0003	0.0179636	Up	Rescued
ENSMUSG00000026021.15	Sumo1	-1.00261	0.0003	0.0179636	Down	Rescued
ENSMUSG00000042712.10	Tceal9	-0.756243	0.0003	0.0179636	Down	Rescued
ENSMUSG00000003541.6	Ier3	0.807772	0.0005	0.0180095	Up	Rescued
ENSMUSG00000027881.14	Prpf38b	-1.03909	0.0005	0.0180095	Down	Rescued
ENSMUSG00000029014.14	Dnajc2	-0.846379	0.0005	0.0180095	Down	Rescued
ENSMUSG00000064288.4	Hist1h4k	0.730686	0.0005	0.0180095	Up	Rescued
ENSMUSG00000027313.3	Chac1	0.833963	0.00055	0.019367	Up	Rescued
ENSMUSG00000032212.10	Sltm	-0.823381	0.00055	0.019367	Down	Rescued
ENSMUSG00000035270.15	Impg2	-3.4357	0.00055	0.019367	Down	Rescued
ENSMUSG00000041153.9	Osgin2	-0.987659	0.00055	0.019367	Down	Rescued
ENSMUSG00000042672.15	Dcst1	-0.84495	0.00055	0.019367	Down	Rescued
ENSMUSG00000051627.3	Hist1h1e	0.721142	0.00055	0.019367	Up	Down
ENSMUSG00000057894.10	Zfp329	-0.836416	0.00055	0.019367	Down	Rescued
ENSMUSG00000113061.1	RP23-371K8.1	-2.09432	0.00055	0.019367	Down	Down
ENSMUSG00000017550.14	Atad5	-1.39361	0.00035	0.0202144	Down	Rescued
ENSMUSG00000025290.17	Rps24	-0.82761	0.00035	0.0202144	Down	Rescued
ENSMUSG00000053898.12	Ech1	0.824836	0.00035	0.0202144	Up	Rescued
ENSMUSG00000014496.8	Ankrd28	-0.961482	0.0006	0.0205898	Down	Rescued
ENSMUSG00000027550.14	Lrrcc1	-1.22203	0.0006	0.0205898	Down	Rescued
ENSMUSG00000029086.15	Prom1	-1.68518	0.0006	0.0205898	Down	Rescued
ENSMUSG00000029676.15	Pot1a	-1.091	0.0006	0.0205898	Down	Rescued
ENSMUSG00000040212.12	Emp3	1.44689	0.0006	0.0205898	Up	Rescued
ENSMUSG00000051285.17	Pcmtd1	-0.83612	0.0006	0.0205898	Down	Rescued
ENSMUSG00000073371.3	Gm6594	-2.78058	0.0006	0.0205898	Down	Rescued
ENSMUSG00000091636.1	Akain1	0.810101	0.0006	0.0205898	Up	Rescued
ENSMUSG00000018042.18	Cyb5r3	0.669521	0.00065	0.0216751	Up	Rescued
ENSMUSG00000021706.14	Zfyve16	-1.37187	0.00065	0.0216751	Down	Rescued
ENSMUSG00000027397.14	Slc20a1	-0.857474	0.00065	0.0216751	Down	Rescued
ENSMUSG00000027935.14	Rab13	1.04924	0.00065	0.0216751	Up	Rescued
ENSMUSG00000034007.10	Scaper	-0.777121	0.00065	0.0216751	Down	Rescued
ENSMUSG00000036733.16	Rbm42	0.64177	0.00065	0.0216751	Up	Rescued
ENSMUSG00000036905.8	C1qb	0.847949	0.00065	0.0216751	Up	Rescued

ENSMUSG00000037475.15	Thoc2	-1.40264	0.00065	0.0216751	Down	Rescued
ENSMUSG00000041268.17	Dmxl2	-0.797954	0.00065	0.0216751	Down	Rescued
ENSMUSG00000062077.14	Trim54	-1.30047	0.00065	0.0216751	Down	Rescued
ENSMUSG00000069308.7	Hist1h2bp	-1.30487	0.00065	0.0216751	Down	Rescued
ENSMUSG00000090129.10	Olfr287	4.10032	0.00065	0.0216751	Up	Rescued
ENSMUSG00000026238.14	Ptma	-0.770074	0.0004	0.0220841	Down	Rescued
ENSMUSG00000030108.14	Slc6a13	1.05738	0.0004	0.0220841	Up	Rescued
ENSMUSG00000036856.4	Wnt4	-0.886864	0.0004	0.0220841	Down	Rescued
ENSMUSG00000039246.8	Lyplal1	-1.13649	0.0004	0.0220841	Down	Rescued
ENSMUSG00000052681.8	Rap1b	-0.75148	0.0004	0.0220841	Down	Rescued
ENSMUSG00000063011.6	Msln	1.66449	0.0004	0.0220841	Up	Rescued
ENSMUSG00000069045.11	Ddx3y	-0.697502	0.0004	0.0220841	Down	Rescued
ENSMUSG00000018199.9	Trove2	-0.740872	0.0007	0.0230171	Down	Rescued
ENSMUSG00000030757.13	Zkscan2	-1.20017	0.0007	0.0230171	Down	Rescued
ENSMUSG00000050029.7	Rap2c	-0.673883	0.0007	0.0230171	Down	Rescued
ENSMUSG00000079003.2	Samd1	0.704437	0.0007	0.0230171	Up	Rescued
ENSMUSG00000020362.13	Cnot6	-0.764125	0.00075	0.0240331	Down	Rescued
ENSMUSG00000027366.12	Sppl2a	-0.763328	0.00075	0.0240331	Down	Rescued
ENSMUSG00000028779.16	Pef1	0.6236	0.00075	0.0240331	Up	Rescued
ENSMUSG00000031327.10	Chic1	-0.628632	0.00075	0.0240331	Down	Rescued
ENSMUSG00000037608.16	Bclaf1	-0.84798	0.00075	0.0240331	Down	Rescued
ENSMUSG00000043410.16	Hfm1	-2.0671	0.00075	0.0240331	Down	Rescued
ENSMUSG00000051951.5	Xkr4	-0.692068	0.00075	0.0240331	Down	Rescued
ENSMUSG00000062995.12	Ica1	0.958778	0.00075	0.0240331	Up	Rescued
ENSMUSG00000064354.1	mt-Co2	-2.56109	0.00075	0.0240331	Down	Rescued
ENSMUSG00000070695.4	Cntnap5a	-0.625484	0.00075	0.0240331	Down	Rescued
ENSMUSG00000095217.1	Hist1h2bn	1.42916	0.00075	0.0240331	Up	Rescued
ENSMUSG00000031226.13	Pbdc1	-0.993927	0.00045	0.0245122	Down	Rescued
ENSMUSG00000036390.8	Gadd45a	-1.14648	0.00045	0.0245122	Down	Rescued
ENSMUSG00000062929.8	Cfl2	-0.833209	0.00045	0.0245122	Down	Rescued
ENSMUSG00000021065.16	Fut8	-0.658599	0.0008	0.0250817	Down	Rescued
ENSMUSG00000024793.14	Tnfrsf25	-3.3438	0.0008	0.0250817	Down	Rescued
ENSMUSG00000025588.4	Nat1	-1.79466	0.0008	0.0250817	Down	Rescued
ENSMUSG00000028080.16	Lrba	-0.683874	0.0008	0.0250817	Down	Rescued
ENSMUSG00000034891.13	Sncb	0.757024	0.0008	0.0250817	Up	Rescued
ENSMUSG00000036860.14	Mrpl55	0.738055	0.0008	0.0250817	Up	Down
ENSMUSG00000038784.13	Cnot4	-0.693937	0.0008	0.0250817	Down	Rescued
ENSMUSG00000044229.9	Nxpe4	-0.860917	0.0008	0.0250817	Down	Rescued
ENSMUSG00000021936.14	Mapk8	-0.736888	0.00085	0.0260015	Down	Rescued
ENSMUSG00000024614.6	Tmx3	-0.723485	0.00085	0.0260015	Down	Rescued
ENSMUSG00000027086.16	Fastkd1	-0.73927	0.00085	0.0260015	Down	Rescued
ENSMUSG00000028832.11	Stmn1	0.821289	0.00085	0.0260015	Up	Down
ENSMUSG00000030357.10	Fkbp4	0.789521	0.00085	0.0260015	Up	Rescued
ENSMUSG00000036790.5	Slitrk2	-0.719732	0.00085	0.0260015	Down	Rescued
ENSMUSG00000041079.12	Rwdd2b	0.758846	0.00085	0.0260015	Up	Rescued
ENSMUSG00000041548.4	Hspb8	0.928112	0.00085	0.0260015	Up	Rescued
ENSMUSG00000052726.15	Kcnt2	-0.776957	0.00085	0.0260015	Down	Rescued
ENSMUSG00000053398.11	Phgdh	1.37609	0.00085	0.0260015	Up	Rescued

ENSMUSG00000064061.13	Dzip3	-0.926387	0.00085	0.0260015	Down	Rescued
ENSMUSG00000096916.7	Zfp850	-1.10542	0.00085	0.0260015	Down	Rescued
ENSMUSG00000021619.6	Atg10	-0.774328	0.0009	0.0270057	Down	Down
ENSMUSG00000034848.17	Ttc21b	-0.882499	0.0009	0.0270057	Down	Rescued
ENSMUSG00000037465.10	Klf10	-1.05141	0.0009	0.0270057	Down	Rescued
ENSMUSG00000038418.7	Egr1	-0.595364	0.0009	0.0270057	Down	Down
ENSMUSG00000058503.11	Fam133b	-0.770342	0.0009	0.0270057	Down	Rescued
ENSMUSG00000060227.15	Casc4	-0.764919	0.0009	0.0270057	Down	Rescued
ENSMUSG00000036896.5	C1qc	0.781356	0.00095	0.0281923	Up	Rescued
ENSMUSG00000042599.8	Kdm7a	-0.666703	0.00095	0.0281923	Down	Rescued
ENSMUSG00000062456.3	Rpl9-ps6	-1.15866	0.00095	0.0281923	Down	Down
ENSMUSG00000063021.3	Hist1h2ak	0.894767	0.00095	0.0281923	Up	Rescued
ENSMUSG00000091811.2	Inafm1	0.648927	0.00095	0.0281923	Up	Rescued
ENSMUSG00000027889.17	Ampd2	0.603885	0.00055	0.0288034	Up	Rescued
ENSMUSG00000030672.12	Mylpf	-3.80356	0.00055	0.0288034	Down	Rescued
ENSMUSG00000056216.9	Cebpg	-0.889526	0.00055	0.0288034	Down	Rescued
ENSMUSG00000057561.9	Eif1a	-0.728498	0.00055	0.0288034	Down	Rescued
ENSMUSG00000057604.9	Lmcd1	0.865045	0.00055	0.0288034	Up	Rescued
ENSMUSG00000098132.1	Rassf10	-1.31718	0.00055	0.0288034	Down	Rescued
ENSMUSG00000020153.14	Ndufs7	0.589742	0.001	0.0293075	Up	Down
ENSMUSG00000031197.11	Vbp1	-0.702634	0.001	0.0293075	Down	Rescued
ENSMUSG00000031337.16	Mtm1	-1.06644	0.001	0.0293075	Down	Rescued
ENSMUSG00000035964.8	Tmem59l	0.663609	0.001	0.0293075	Up	Rescued
ENSMUSG00000037355.14	Uvssa	-0.844933	0.001	0.0293075	Down	Rescued
ENSMUSG00000037977.6	RP23-115A1.5	0.840538	0.001	0.0293075	Up	Rescued
ENSMUSG00000059474.13	Mbtd1	-1.09496	0.001	0.0293075	Down	Rescued
ENSMUSG00000004892.13	Bcan	0.622881	0.0006	0.0301611	Up	Rescued
ENSMUSG00000019773.7	Fbxo5	-2.80976	0.0006	0.0301611	Down	Rescued
ENSMUSG00000019837.8	Gtf3c6	-1.19116	0.0006	0.0301611	Down	Rescued
ENSMUSG00000023043.7	Krt18	3.00051	0.0006	0.0301611	Up	Rescued
ENSMUSG00000025017.9	Pik3ap1	1.02307	0.0006	0.0301611	Up	Rescued
ENSMUSG00000026502.13	Desi2	-0.979212	0.0006	0.0301611	Down	Rescued
ENSMUSG00000031848.15	Lsm4	-0.890414	0.0006	0.0301611	Down	Rescued
ENSMUSG00000057841.5	Rpl32	-0.785884	0.0006	0.0301611	Down	Rescued
ENSMUSG00000069874.7	Irgm2	1.90074	0.0006	0.0301611	Up	Rescued
ENSMUSG00000021327.19	Zkscan3	-0.842877	0.00105	0.0303952	Down	Rescued
ENSMUSG00000021569.10	Trip13	-2.25882	0.00105	0.0303952	Down	Down
ENSMUSG00000024383.8	Map3k2	-0.634948	0.00105	0.0303952	Down	Rescued
ENSMUSG00000041058.15	Wwp1	-0.654249	0.00105	0.0303952	Down	Rescued
ENSMUSG00000067071.8	Hes6	0.672708	0.00105	0.0303952	Up	Rescued
ENSMUSG00000070047.14	Fat1	-0.964963	0.00105	0.0303952	Down	Rescued
ENSMUSG00000000530.16	Acvrl1	2.37087	0.0011	0.0311733	Up	Rescued
ENSMUSG00000001128.7	Cfp	-1.03258	0.0011	0.0311733	Down	Rescued
ENSMUSG00000002718.14	Cse1l	-0.864707	0.0011	0.0311733	Down	Rescued
ENSMUSG00000025199.16	Chuk	-1.05794	0.0011	0.0311733	Down	Rescued
ENSMUSG00000029238.11	Clock	-0.687187	0.0011	0.0311733	Down	Rescued
ENSMUSG00000030647.8	Ndufc2	0.622656	0.0011	0.0311733	Up	Down
ENSMUSG00000033488.11	AC161108.3	1.21283	0.0011	0.0311733	Up	Rescued

ENSMUSG00000034341.17	Wbp2	0.624569	0.0011	0.0311733	Up	Rescued
ENSMUSG00000039194.16	Rlbp1	1.12041	0.0011	0.0311733	Up	Rescued
ENSMUSG00000053181.1	RP24-270A10.2	1.67213	0.0011	0.0311733	Up	Rescued
ENSMUSG00000063953.3	Amd2	-1.22169	0.0011	0.0311733	Down	Rescued
ENSMUSG00000068882.13	Ssb	-0.920228	0.0011	0.0311733	Down	Rescued
ENSMUSG00000001827.12	Folr1	-2.60982	0.00065	0.0320805	Down	Rescued
ENSMUSG00000038507.6	Parp12	0.847545	0.00065	0.0320805	Up	Rescued
ENSMUSG00000036192.15	Rorb	-0.722439	0.00115	0.0322993	Down	Rescued
ENSMUSG00000043411.15	Usp48	-0.878233	0.00115	0.0322993	Down	Rescued
ENSMUSG00000063065.13	Mapk3	0.788528	0.00115	0.0322993	Up	Rescued
ENSMUSG00000063364.10	RP23-91K11.3	-1.14521	0.00115	0.0322993	Down	Rescued
ENSMUSG00000000983.13	Wfdc18	1.93955	0.0012	0.0333561	Up	Rescued
ENSMUSG00000019841.15	Rev3l	-1.183	0.0012	0.0333561	Down	Rescued
ENSMUSG00000020514.8	Mrpl22	0.722818	0.0012	0.0333561	Up	Rescued
ENSMUSG00000041377.12	Ninj2	1.68113	0.0012	0.0333561	Up	Rescued
ENSMUSG00000044966.4	Fbxo48	-1.34849	0.0012	0.0333561	Down	Rescued
ENSMUSG00000053560.4	Ier2	-0.801117	0.0012	0.0333561	Down	Down
ENSMUSG00000010797.6	Wnt2	1.20374	0.0007	0.033631	Up	Rescued
ENSMUSG00000023953.8	Polh	0.908237	0.0007	0.033631	Up	Rescued
ENSMUSG00000024352.11	Spata24	-1.47985	0.0007	0.033631	Down	Rescued
ENSMUSG00000034639.7	Setmar	-0.986316	0.0007	0.033631	Down	Rescued
ENSMUSG00000045288.10	Ush1g	1.33719	0.0007	0.033631	Up	Rescued
ENSMUSG00000032582.14	Rbm6	-0.925698	0.00125	0.034492	Down	Rescued
ENSMUSG00000041702.7	Btbd7	-0.663993	0.00125	0.034492	Down	Rescued
ENSMUSG00000068011.4	Mkrn2os	-1.27159	0.00125	0.034492	Down	Rescued
ENSMUSG00000094724.8	Rnaset2b	1.30145	0.00125	0.034492	Up	Rescued
ENSMUSG00000015733.13	Capza2	-0.796075	0.00075	0.0353042	Down	Rescued
ENSMUSG00000022322.8	Shcbp1	-1.8068	0.00075	0.0353042	Down	Rescued
ENSMUSG00000028270.12	Gbp2	1.93919	0.00075	0.0353042	Up	Rescued
ENSMUSG00000030417.15	Pdcd5	-1.36506	0.00075	0.0353042	Down	Down
ENSMUSG00000031410.14	Nxf7	-1.59372	0.00075	0.0353042	Down	Rescued
ENSMUSG00000020952.10	Scfd1	-0.822892	0.0013	0.0354058	Down	Rescued
ENSMUSG00000024007.14	Ppil1	0.70316	0.0013	0.0354058	Up	Rescued
ENSMUSG00000028771.13	Ptpn12	-1.06774	0.0013	0.0354058	Down	Rescued
ENSMUSG00000029468.17	P2rx7	-1.51499	0.0013	0.0354058	Down	Rescued
ENSMUSG00000030905.5	Crym	0.607588	0.0013	0.0354058	Up	Rescued
ENSMUSG00000032264.9	Zw10	-0.872583	0.0013	0.0354058	Down	Rescued
ENSMUSG00000039967.14	Zfp292	-0.656127	0.0013	0.0354058	Down	Rescued
ENSMUSG00000054519.8	Zfp867	-0.776177	0.0013	0.0354058	Down	Rescued
ENSMUSG00000021709.14	Erbb2ip	-0.624166	0.00135	0.0359378	Down	Rescued
ENSMUSG00000025525.12	Apool	-0.990174	0.00135	0.0359378	Down	Rescued
ENSMUSG00000028150.14	Rorc	1.48673	0.00135	0.0359378	Up	Rescued
ENSMUSG00000028478.18	Clta	0.562431	0.00135	0.0359378	Up	Rescued
ENSMUSG00000037808.13	Fam76b	-1.31382	0.00135	0.0359378	Down	Rescued
ENSMUSG00000038242.12	Aox4	-2.43293	0.00135	0.0359378	Down	Rescued
ENSMUSG00000053985.10	Zfp14	-0.830054	0.00135	0.0359378	Down	Rescued
ENSMUSG00000057411.8	Fam173a	0.608723	0.00135	0.0359378	Up	Rescued
ENSMUSG00000058093.13	Zfp729b	-1.75812	0.00135	0.0359378	Down	Rescued

ENSMUSG00000060427.15	Zfp868	-1.15132	0.00135	0.0359378	Down	Rescued
ENSMUSG00000067424.12	Zfp563	-0.979838	0.00135	0.0359378	Down	Rescued
ENSMUSG00000075486.10	Commd6	-0.802351	0.00135	0.0359378	Down	Rescued
ENSMUSG00000003477.5	Inmt	2.99147	0.0008	0.0364975	Up	Rescued
ENSMUSG00000005233.16	Spc25	-2.11376	0.0008	0.0364975	Down	Rescued
ENSMUSG00000008384.8	Sertad1	-0.685555	0.0008	0.0364975	Down	Down
ENSMUSG00000018593.13	Sparc	0.869434	0.0008	0.0364975	Up	Up
ENSMUSG00000020919.11	Stat5b	0.621017	0.0008	0.0364975	Up	Rescued
ENSMUSG00000052566.8	Hook2	0.808401	0.0008	0.0364975	Up	Rescued
ENSMUSG00000071267.11	Zfp942	-1.3288	0.0008	0.0364975	Down	Rescued
ENSMUSG00000026516.8	Nvl	-1.081	0.0014	0.0370078	Down	Rescued
ENSMUSG00000027770.5	Dhx36	-0.653441	0.0014	0.0370078	Down	Rescued
ENSMUSG00000052565.7	Hist1h1d	0.60475	0.0014	0.0370078	Up	Down
ENSMUSG00000068479.5	Mfap1a	-0.785226	0.0014	0.0370078	Down	Rescued
ENSMUSG00000029484.12	Anxa3	1.44348	0.00085	0.0376194	Up	Rescued
ENSMUSG00000075232.5	Amd1	-0.82067	0.00085	0.0376194	Down	Rescued
ENSMUSG00000001260.10	Gabrg1	-0.843778	0.00145	0.037748	Down	Rescued
ENSMUSG00000026187.8	Xrcc5	-0.674351	0.00145	0.037748	Down	Rescued
ENSMUSG00000027829.15	Ccnl1	-1.29341	0.00145	0.037748	Down	Rescued
ENSMUSG00000028813.2	RP23-183D18.1	1.03024	0.00145	0.037748	Up	Rescued
ENSMUSG00000029208.16	Guf1	-0.998403	0.00145	0.037748	Down	Rescued
ENSMUSG00000031139.15	Mcf2	-0.928355	0.00145	0.037748	Down	Rescued
ENSMUSG00000031389.17	Arhgap4	-2.55873	0.00145	0.037748	Down	Rescued
ENSMUSG00000040044.11	Orc3	-0.860838	0.00145	0.037748	Down	Rescued
ENSMUSG00000049538.14	Adamts16	-1.04809	0.00145	0.037748	Down	Rescued
ENSMUSG00000022861.17	Dgkg	0.593879	0.0015	0.0386235	Up	Rescued
ENSMUSG00000024146.9	Cript	-0.623526	0.0015	0.0386235	Down	Rescued
ENSMUSG00000050668.9	Gpatch11	-0.61616	0.0015	0.0386235	Down	Rescued
ENSMUSG00000056071.12	S100a9	3.21112	0.0015	0.0386235	Up	Rescued
ENSMUSG00000059518.14	Znhit1	0.69197	0.0015	0.0386235	Up	Rescued
ENSMUSG00000076441.9	Ass1	0.65639	0.0015	0.0386235	Up	Rescued
ENSMUSG00000021177.16	Tdp1	0.995572	0.0009	0.0387786	Up	Rescued
ENSMUSG00000021719.9	Rgs7bp	-0.557704	0.0009	0.0387786	Down	Rescued
ENSMUSG00000023913.17	Pla2g7	0.846733	0.0009	0.0387786	Up	Rescued
ENSMUSG00000030137.8	Tuba8	0.656162	0.0009	0.0387786	Up	Rescued
ENSMUSG00000060284.7	Sp7	1.01008	0.0009	0.0387786	Up	Rescued
ENSMUSG00000074968.11	Ano3	-0.738046	0.0009	0.0387786	Down	Rescued
ENSMUSG00000022951.16	Rcan1	1.07097	0.00155	0.0391629	Up	Rescued
ENSMUSG00000023484.14	Prph	-1.43316	0.00155	0.0391629	Down	Rescued
ENSMUSG00000024006.16	Stk38	-1.01319	0.00155	0.0391629	Down	Rescued
ENSMUSG00000048482.14	Bdnf	-0.701181	0.00155	0.0391629	Down	Rescued
ENSMUSG00000049932.3	H2afx	0.571002	0.00155	0.0391629	Up	Down
ENSMUSG00000058927.5	Gm10053	-1.2049	0.00155	0.0391629	Down	Down
ENSMUSG00000020766.4	Galk1	0.743098	0.0016	0.0397871	Up	Rescued
ENSMUSG00000021384.14	Susd3	2.24049	0.0016	0.0397871	Up	Up
ENSMUSG00000034160.13	Ogt	-0.719275	0.0016	0.0397871	Down	Rescued
ENSMUSG00000037058.14	Paip2	-0.605042	0.0016	0.0397871	Down	Down
ENSMUSG00000050549.8	RP23-173N16.6	0.962025	0.0016	0.0397871	Up	Rescued

ENSMUSG00000056267.14	Cep70	-1.31853	0.0016	0.0397871	Down	Rescued
ENSMUSG00000073565.4	Prr16	-0.717613	0.0016	0.0397871	Down	Rescued
ENSMUSG00000016206.6	H2-M3	1.47613	0.00095	0.039981	Up	Rescued
ENSMUSG00000032215.15	Rsl24d1	-0.69174	0.00095	0.039981	Down	Rescued
ENSMUSG00000042043.6	Tbca	-0.734785	0.00095	0.039981	Down	Rescued
ENSMUSG00000031431.13	Tsc22d3	0.595879	0.00165	0.0408153	Up	Down
ENSMUSG00000047797.14	Gjb1	0.704981	0.00165	0.0408153	Up	Rescued
ENSMUSG00000048602.8	Morc2b	-0.946607	0.00165	0.0408153	Down	Rescued
ENSMUSG00000060512.7	RP23-192C21.1	1.25963	0.00165	0.0408153	Up	Rescued
ENSMUSG00000018648.15	Dusp14	-0.599401	0.001	0.0410252	Down	Rescued
ENSMUSG00000042363.14	Lgalsl	-0.739289	0.001	0.0410252	Down	Rescued
ENSMUSG00000043061.10	Tmem18	-0.880807	0.001	0.0410252	Down	Rescued
ENSMUSG00000028610.16	Dmrtb1	1.43043	0.0017	0.0416699	Up	Rescued
ENSMUSG00000032688.8	Malt1	-1.17882	0.0017	0.0416699	Down	Rescued
ENSMUSG00000039361.11	Picalm	-0.813203	0.0017	0.0416699	Down	Rescued
ENSMUSG00000048647.9	Exd1	-1.90633	0.0017	0.0416699	Down	Rescued
ENSMUSG00000070583.1	Fv1	-0.836588	0.0017	0.0416699	Down	Rescued
ENSMUSG00000022323.11	Hrsp12	-1.23591	0.00105	0.0423301	Down	Rescued
ENSMUSG00000047821.16	Trim16	2.27626	0.00105	0.0423301	Up	Rescued
ENSMUSG00000051154.11	Commd3	-0.67402	0.00105	0.0423301	Down	Rescued
ENSMUSG00000004895.9	Prcc	0.586278	0.00175	0.0423455	Up	Rescued
ENSMUSG00000024411.9	Aqp4	-0.655314	0.00175	0.0423455	Down	Rescued
ENSMUSG00000026994.9	Galnt3	-2.5494	0.00175	0.0423455	Down	Rescued
ENSMUSG00000027474.12	Ccm2l	1.97743	0.00175	0.0423455	Up	Rescued
ENSMUSG00000034297.14	Med13	-0.683481	0.00175	0.0423455	Down	Rescued
ENSMUSG00000043190.14	Rfesd	-0.769319	0.00175	0.0423455	Down	Rescued
ENSMUSG00000047213.14	Ythdf3	-0.598909	0.00175	0.0423455	Down	Rescued
ENSMUSG00000057409.6	Zfp53	-0.999949	0.00175	0.0423455	Down	Rescued
ENSMUSG00000094475.7	RP23-294G7.1	#VALUE!	0.00175	0.0423455	Down	Down
ENSMUSG00000025591.6	Tma16	-0.846226	0.0018	0.0428414	Down	Rescued
ENSMUSG00000057497.8	Fam136a	-0.605231	0.0018	0.0428414	Down	Down
ENSMUSG00000071337.11	Tia1	-0.942762	0.0018	0.0428414	Down	Rescued
ENSMUSG00000074457.10	S100a16	0.591394	0.0018	0.0428414	Up	Rescued
ENSMUSG00000078578.9	Ube2d3	0.86848	0.0018	0.0428414	Up	Rescued
ENSMUSG00000078779.4	Zfp59	-1.02363	0.0018	0.0428414	Down	Rescued
ENSMUSG00000078870.9	RP23-360A2.8	-0.787013	0.0018	0.0428414	Down	Down
ENSMUSG00000000600.15	Krit1	-0.768549	0.00185	0.0434831	Down	Rescued
ENSMUSG00000019102.10	Aldh3a1	-1.24703	0.00185	0.0434831	Down	Rescued
ENSMUSG00000020520.14	Galnt10	0.750112	0.00185	0.0434831	Up	Rescued
ENSMUSG00000028444.17	Cntfr	0.686836	0.00185	0.0434831	Up	Rescued
ENSMUSG00000031672.8	Got2	0.718104	0.00185	0.0434831	Up	Rescued
ENSMUSG00000057182.14	Scn3a	-0.946695	0.00185	0.0434831	Down	Rescued
ENSMUSG00000034993.7	Vat1	0.637932	0.0011	0.043911	Up	Rescued
ENSMUSG00000024843.15	Chka	-1.15055	0.0019	0.0443271	Down	Rescued
ENSMUSG00000038274.12	Fau	0.597192	0.0019	0.0443271	Up	Down
ENSMUSG00000050855.16	Zfp940	-2.06014	0.0019	0.0443271	Down	Rescued
ENSMUSG00000064368.1	mt-Nd6	-1.4656	0.0019	0.0443271	Down	Up
ENSMUSG00000023873.12	RP23-67C3.2	1.80072	0.00115	0.0451327	Up	Rescued

ENSMUSG00000044881.7	Coa4	-1.33589	0.00115	0.0451327	Down	Rescued
ENSMUSG00000057858.7	Fam204a	-0.756714	0.00115	0.0451327	Down	Rescued
ENSMUSG00000030235.17	Slco1c1	-0.779404	0.00195	0.0452697	Down	Rescued
ENSMUSG00000032673.5	Prorsd1	-1.00975	0.00195	0.0452697	Down	Rescued
ENSMUSG00000035413.8	Tmem98	0.753473	0.00195	0.0452697	Up	Rescued
ENSMUSG00000034206.15	Polq	-1.32195	0.002	0.0460904	Down	Rescued
ENSMUSG00000051403.9	Ppp1r37	0.634769	0.002	0.0460904	Up	Rescued
ENSMUSG00000055044.12	Pdlim1	1.01992	0.002	0.0460904	Up	Rescued
ENSMUSG00000056537.11	Rlim	-0.59313	0.002	0.0460904	Down	Rescued
ENSMUSG00000059708.12	Akap17b	-0.729664	0.002	0.0460904	Down	Rescued
ENSMUSG00000063838.6	Cdc42ep5	1.17425	0.002	0.0460904	Up	Rescued
ENSMUSG00000023868.16	Pde10a	0.718198	0.0012	0.0465343	Up	Rescued
ENSMUSG00000037447.16	Arid5a	-1.15575	0.0012	0.0465343	Down	Rescued
ENSMUSG00000015090.13	Ptgds	0.615419	0.00205	0.0466165	Up	Rescued
ENSMUSG00000028576.12	Ift74	-0.749237	0.00205	0.0466165	Down	Rescued
ENSMUSG00000038446.8	Cdc40	-0.651935	0.00205	0.0466165	Down	Rescued
ENSMUSG00000039831.16	Arhgap29	-0.796542	0.00205	0.0466165	Down	Rescued
ENSMUSG00000049625.6	Tifab	0.999837	0.00205	0.0466165	Up	Rescued
ENSMUSG00000091511.2	Vmn2r87	-1.47207	0.00205	0.0466165	Down	Rescued
ENSMUSG00000027599.9	Armc1	-0.545795	0.0021	0.0474108	Down	Down
ENSMUSG00000027620.16	Rbm39	-0.805734	0.0021	0.0474108	Down	Rescued
ENSMUSG00000060475.12	Wtap	-1.06382	0.0021	0.0474108	Down	Rescued
ENSMUSG00000005892.4	Trh	0.954513	0.00215	0.0479658	Up	Rescued
ENSMUSG00000027130.15	Slc12a6	-0.899054	0.00215	0.0479658	Down	Rescued
ENSMUSG00000029070.9	Mxra8	-1.24829	0.00215	0.0479658	Down	Rescued
ENSMUSG00000030512.13	Snrpa1	-0.795559	0.00215	0.0479658	Down	Rescued
ENSMUSG00000032254.10	Kif23	-1.79001	0.00215	0.0479658	Down	Rescued
ENSMUSG00000033392.16	Clasp2	-0.594594	0.00215	0.0479658	Down	Rescued
ENSMUSG00000036437.6	Npy1r	-0.686297	0.00215	0.0479658	Down	Rescued
ENSMUSG00000042104.18	Uggt2	-1.34931	0.00215	0.0479658	Down	Rescued
ENSMUSG00000049791.4	Fzd4	-0.8156	0.00215	0.0479658	Down	Rescued
ENSMUSG00000032359.14	Ctsh	1.17525	0.00125	0.0482435	Up	Rescued
ENSMUSG00000033111.16	RP24-315N18.1	-1.40713	0.00125	0.0482435	Down	Rescued
ENSMUSG00000026205.8	Slc23a3	-1.32353	0.0022	0.0488504	Down	Rescued
ENSMUSG00000054453.11	Sytl5	-0.840329	0.0022	0.0488504	Down	Rescued
ENSMUSG00000059713.12	Rcan3	0.808563	0.0022	0.0488504	Up	Rescued
ENSMUSG00000001158.13	Snrnp27	-0.666634	0.0013	0.0493545	Down	Rescued
ENSMUSG00000024479.3	Mal2	-0.624738	0.0013	0.0493545	Down	Rescued
ENSMUSG00000025571.13	Tnrc6c	-0.704826	0.0013	0.0493545	Down	Rescued
ENSMUSG00000050944.14	Efcab5	-2.86293	0.0013	0.0493545	Down	Rescued
ENSMUSG00000023892.8	Zfp51	-1.11106	0.00225	0.0496104	Down	Rescued
ENSMUSG00000026042.16	Col5a2	-2.9273	0.00225	0.0496104	Down	Rescued
ENSMUSG00000026349.14	Ccnt2	-0.80626	0.00225	0.0496104	Down	Rescued